2015

Nucleolar Stress Due to Depletion of Nopp140 in Drosophila melanogaster

Allison James
Louisiana State University and Agricultural and Mechanical College, ajame18@lsu.edu

NUCLEOLAR STRESS DUE TO DEPLETION OF NOPP140 IN *DROSOPHILA MELANOGASTER*

A Dissertation

Submitted to the Graduate Faculty of the
Louisiana State University and
Agricultural and Mechanical College
in partial fulfillment of the
requirements for the degree of
Doctor of Philosophy

in

The Department of Biological Sciences

by
Allison A. James
B.S., Louisiana State University, 2011
December 2015

ACKNOWLEDGEMENTS

I would first like to thank my family for their constant support through college and graduate school. I would also like to thank Dr. Pat DiMario for introducing me to the world of research six years ago, for being an inspiring mentor, and importantly your constant guidance and encouragement. Thanks to my committee members, Dr. Steve Hand, Dr. Craig Hart, Dr. David Donze, and Dr. Juana Moreno for your direction and help throughout graduate school, and to Dr. Hollie Dale-Donze and Ying Xiao at the LSU Socolofsky Microscopy Center for your help and expertise. To my lab mates past and present, Yubo Wang, Himanshu Raje, Sonu Baral, Dr. Raphyel Rosby, and Dr. Fang He, thank you for your assistance with my experiments, your knowledge, and your friendship. Additionally, I would like to thank several undergraduate researchers in our lab for their contribution to my research: Renford Cindass, Dana Mayer, Stephanie Terhoeve, Courney Mumphrey, Rainey Gerald, David Odenheimer, and Scott Gaignard.

TABLE OF CONTENTS

LIST OF FIGURES

ABSTRACT

Nucleolar stress results when ribosome biogenesis is disrupted. An excellent example is the human Treacher Collins syndrome in which the loss of the nucleolar chaperone, Treacle, leads to p53-dependent apoptosis in embryonic neural crest cells, and ultimately to craniofacial birth defects. We show that depletion of the related nucleolar and Cajal body phospho-protein, Nopp140, in *Drosophila melanogaster* led to nucleolar stress and eventual lethality when multiple tissues were depleted of Nopp140 by RNAi. We used TEM, immuno-blot analysis, and metabolic protein labeling to show the loss of ribosomes. Targeted loss of Nopp140 only in larval wing discs caused apoptosis, which eventually led to defects in the adult wings. These defects were not rescued by a *p53* gene deletion, as the craniofacial defects were in the murine model of TCS, thus suggesting that apoptosis caused by nucleolar stress in *Drosophila* is induced by a p53-independent mechanism. Loss of Nopp140 in larval polyploid midgut cells induced premature autophagy as marked by the accumulation of mCherry-ATG8a into autophagic vesicles. We also found elevated phenoloxidase A3 levels in whole larval lysates and within the hemolymph of Nopp140-depleted larvae, coincident with the appearance of melanotic tumors. The occurrence of apoptosis, autophagy, and phenoloxidase A3 release to the hemolymph upon nucleolar stress correlated well with the activation of JNK in Nopp140-depleted larvae.

Nopp140 is considered a ribosome assembly factor, but its precise functions remain unknown. To approach this problem, we deleted the *Nopp140*

gene in *Drosophila* using FLP-FRT recombination. Genomic PCR, RT-PCR, and immunofluorescence microscopy confirmed the loss of *Nopp140*, its mRNA, and protein products. *Nopp140-/-* larvae arrested in the second instar stage and died within 8 days. While nucleoli appeared intact in *Nopp140-/-* cells, the C/D snoRNP methyl-transferase, fibrillarin, redistributed to the nucleoplasm in variable amounts; RT-PCRs showed that 2'-*O*-methylation of rRNA in *Nopp140-/-* cells was reduced. Ultra structural analysis showed that *Nopp140-/-* cells were deficient in cytoplasmic ribosomes, but instead contained abnormal electron dense cytoplasmic granules. Furthermore, metabolic labeling showed a significant drop in protein translation. We believe the phenotypes described here define novel intracellular ribosomopathies.

CHAPTER 1. LITERATURE REVIEW*

1.1 Introduction

Advances over the past two decades have revealed multiple functions for the eukaryotic nucleolus (Pederson 1998; Boisvert et al. 2007). Beyond its primary function in ribosome biosynthesis, the nucleolus initiates assembly of the signal recognition particle and processes several other small RNAs such as tRNAs, the telomerase RNA, the U6 snRNA, and the RNase P RNA. Regulatory proteins that participate in genome maintenance, telomere replication, and cell cycle progression associate dynamically with nucleoli. The nucleolus also acts as a principal stress sensor within mammalian cells by regulating murine double minute 2 (MDM2), the E3 ubiquitin ligase that negatively regulates p53, a critical tumor suppressor protein in mammalian cells (Olson 2004). In doing so, the nucleolus regulates mammalian cell cycle progression, senescence, and apoptosis. Obviously, these cell states have profound impacts on cell growth and organism development.

"Nucleolar stress" is the term now used to describe failures in ribosome biogenesis or function that ultimately lead to disruptions in cell homeostasis. Over the last 10 years we have seen a veritable explosion of papers describing nucleolar stress. Several recent reviews collectively cover nucleolar stress (Hein et al. 2013; Drygin et al. 2013; Vlatković et al. 2013; Grummt 2013; Montanaro et

*This chapter previously appeared as James A, Wang Y, Raje H, Rosby R, DiMario P (2014) Nucleolar stress with and without p53. *Nucleus*. 5:402 - 426; PMID: 25093852. http://dx.doi.org/10.4161/nucl.32235. It is reprinted by permission of Landes Bioscience – see the permission letter for proper acknowledgement phrase in Appendix A of this thesis.

al. 2013; Parlato and Kreiner 2013; Quin et al. 2014; Golomb et al. 2014; Tsai and Pederson 2014). While nucleolar stress leading to p53-dependent cell cycle arrest has captured our full attention, several recent reports describe nucleolar stress inducing p53-independent response pathways that also lead to cell cycle arrest or apoptosis. Since >50% of human cancers lack functional p53, understanding these p53-independent pathways could potentially reveal additional cancer therapies that utilize induced nucleolar stress. Our aim here is to compare and contrast p53-dependent and p53-independent nucleolar stress pathways in metazoan systems.

1.2 Overview of Nucleolar Biology

Comprehensive reviews on nucleolar biology have been provided by Busch and Smetana (1970), Jordan and Cullis (1982), Hadjiolov (1985), and Olson (2004, 2011). We know from the pioneering work of Perry (1961, 1962), Edström et al. (1961), and Warner and Soeiro (1967) that nucleoli are responsible for ribosome biogenesis (Figure 1.1), and from the work of Brown and Gurdon (1964), Ritossa et al. (1965, 1966) and Birnstiel et al. (1966) that chromosomal nucleolar organizers first described by Heitz (1933) and McClintock (1934) contain tandemly repeated genes that encode pre-ribosomal RNA. Indeed, our best direct visualization of gene transcription comes from the electron microscopic spreads of rRNA genes (Miller and Beatty 1969). Detailed mechanistic models now describe the tandem rDNA transcription units, recruitment of RNA polymerase I (Pol I) to rDNA promoters by various transcription factors, and cell cycle-dependent regulation of Pol I transcription

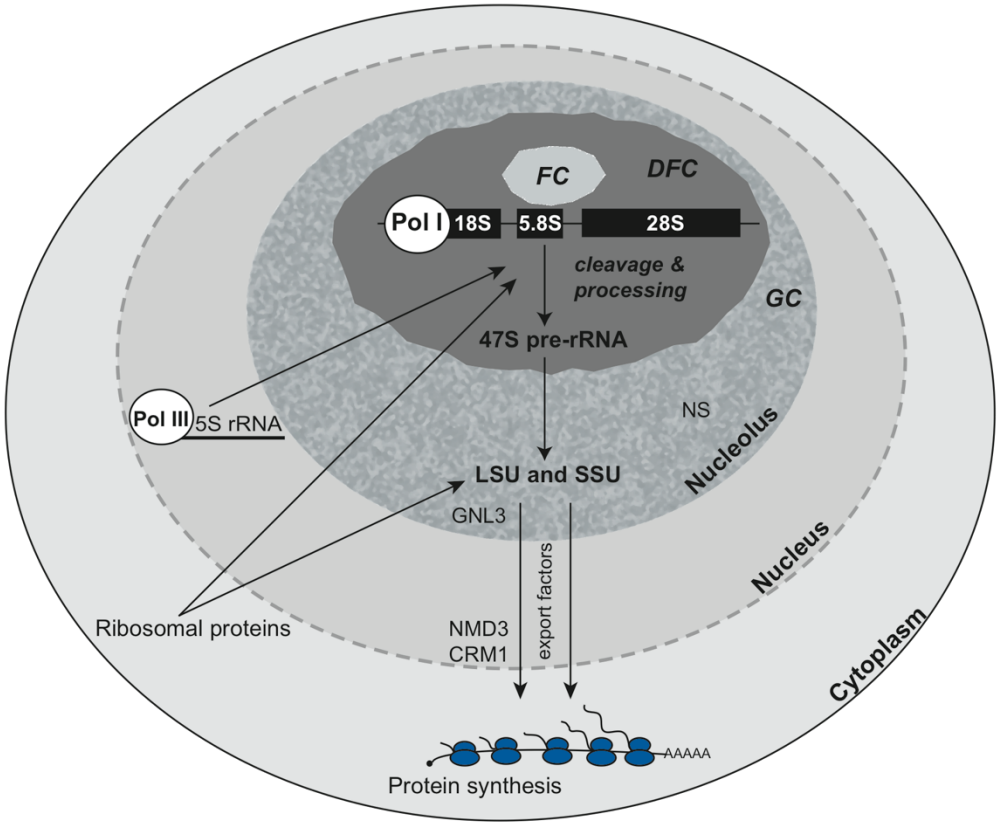

FIGURE 1.1. Overview of Ribosome Biogenesis in Mammalian Cells. Ribosome biogenesis in eukaryotic cells occurs in the nucleolus, a nuclear compartment that displays the fibrillar center (FC), the dense fibrillar component (DFC), and the granular component (GC) at the ultra structural level. Transcription of pre-rRNA (47S in mammals) by RNA polymerase I (Pol I) is generally thought to occur at the boarders of the FC and DFC on tandem gene repeats emanating as radial loops from more condensed rDNA within the FCs. The 5S rRNA is transcribed by RNA Pol III in all eukaryotes; in yeast the 5S genes reside within the nucleolus within intergenic sequences that lie between the larger tandem rDNA gene repeats, but in metazoans, the 5S genes reside as tandem repeats outside the nucleolus. Processing and cleavage of the 47S pre-rRNA occurs in the DFC as ribosomal proteins synthesized in the cytoplasm enter the nucleolus and assemble with the 18S rRNA to form the small ribosomal subunit (SSU) and with the 5.8S, 28S, and 5S rRNAs to form the large ribosomal subunit (LSU). Large and small ribosomal subunits continue to assemble and mature as they enter the GC that contains GTPases (e.g. GNL3) that likely function in subunit maturation or nucleolar release. The GC is drawn here as a heterogeneous nucleolar compartment consisting of RNA-containing and RNA-deficient zones. Another GTPase, Nucleostemin (NS), resides in the RNA-deficient zones of the GC (Politz et al. 2005). Rather than participating in ribosome biogenesis directly, NS functions in maintaining stem cell homeostasis and in responding to nucleolar stress (Tsai 2011). Export of the ribosomal subunits is finally mediated by nuclear export factors, NMD3 and CRM1.

which indirectly regulates nucleolar disassembly during prophase and re-assembly (nucleologenesis) beginning in telophase (Voit and Grummt 2011; Hernandez-Verdun 2011).

By transmission electron microscopy, typical nucleoli contain three morphologically distinct sub-compartments (Figure 1.1): the fibrillar center (FC), the dense fibrillar component (DFC), and the peripheral granular component (GC). Transcription of pre-rRNA occurs on the boarders between the FC and DFC, while pre-rRNA processing and initial ribosome subunit assembly occur largely within the DFC. In mammals, Pol I transcription produces a 47S pre-rRNA transcript (35S in yeast) which is cleaved (processed) to generate 18S, 5.8S, and 28S rRNAs. Genes encoding the 5S rRNA are transcribed by Pol III; in metazoans the 5S genes are tandem repeats lying outside the nucleolus. In yeast, the 5S genes reside within intergenic regions that separate individual nucleolar rDNA transcription units (French et al. 2008).

1.3 Nucleolar Stress Effectors

Several ribosome assembly factors maintain their greatest steady-state concentrations within nucleoli under normal growth conditions, but assume altered functions to act as effectors under nucleolar stress conditions. In this section we introduce these factors by describing their normal nucleolar functions. In the next section we describe their altered roles during nucleolar stress. Besides these nucleolar assembly factors, the ribosomal proteins themselves act as stress effectors when they fail to assemble into small and large ribosomal subunits (in this case referred to as ribosomal stress).

1.3.1 Pol I transcription of pre-rRNA

The Pol I machinery has been well described in yeast and vertebrate systems (Moss and Stefanovsky 2002; Grummt 2003; Goodfellow and Zomerdijk 2012). For instance, the productive Pol I transcription initiation complex in mouse includes the upstream binding factor UBF, the multi-protein complex TIF-IB (called selectivity factor SL-1 in humans), TIF-IA, the Pol I complex itself, and several other factors that regulate Pol I transcription, in particular SIRT7 that deacetylates the Pol I subunit PAF53 under normal non-stress conditions to ensure occupancy of Pol I with the rDNA (Chen et al. 2013). UBF dimers bind the core promoter element that spans the transcription start site; they also bind the upstream control element (UCE) to perform several roles (Grob et al. 2011). Once bound, UBF participates in opening the promoter region and in recruiting TIF-IB and Pol I complexes to the promoter core. UBF may also participate in the release of Pol I from the promoter at transcription initiation and in transcription elongation as UBF also decorates the length of the rDNA transcription units (O'Sullivan et al. 2002).

Of the Pol I transcription factors, TIF-IA is likely the central homeostatic factor in activating Pol I transcription. Under normal growth conditions, TIF-IA is critical in establishing productive Pol I transcription initiation complexes, due in part to its growth factor-dependent phosphorylation by ERK, or by its nutrient-dependent mTOR signaling and activation (Zhao et al. 2003; Mayer et al. 2004). However, upon oxidative stress (H_2O_2) or ribotoxic stress with anisomycin, activated c-Jun amino terminal kinase 2 (JNK2) phosphorylates Thr_{200} in

mammalian TIF-IA, and this not only abrogates TIF-IA's interactions with both Pol I and TIF-IB, but also redistributes TIF-IA to the nucleoplasm. Thus, pre-initiation complex assembly fails under these particular conditions leading to nucleolar stress (Mayer et al. 2005; Mayer and Grummt 2005).

1.3.2 Pre-rRNA processing

Pre-rRNA processing and ribosome assembly occur within complex yet highly coordinated reactions and interactions within the 90S processome of the nucleolar DFC (Staley and Woolford 2009). In general, we know the major pre-rRNA processing events: box C/D and box H/ACA small nucleolar ribonucleoprotein particles (snoRNPs) catalyze nucleotide-specific 2'-*O*-ribose methylation and pseudouridylation, respectively (Bleichert and Baserga 2007). Concomitantly, pre-rRNA undergoes endo-nucleolytic cleavage reactions to generate mature 18S, 5.8S, and 28S rRNAs as nascent ribosomal proteins arrive from the cytoplasm to assemble with these rRNAs (Figure 1.1).

Approximately 250 non-ribosomal nucleolar proteins act as ribosome assembly factors; specifically, they function as nucleases, helicases or chaperones to mediate the many processing and assembly events. Many of these nucleolar proteins are conserved throughout eukaryotes. For instance, fibrillarin is the well conserved methyl-transferase associated with box C/D snoRNPs, while dyskerin (Cbf5 in yeast) is the pseudouridylase within box H/ACA snoRNPs. While fibrillarin and dyskerin appear to be limited to their sole tasks, nucleophosmin and nucleolin are multi-functional DFC proteins. Nucleophosmin 1 (NPM1, also called B23, numatrin in mammals, or NO38 in

amphibians) binds nucleic acids, displays RNase activity, and participates in cleaving the second internal transcribed spacer within pre-rRNA, clearly making it a ribosome assembly factor. When over-expressed, NPM1 binds p53, suggesting a role in modulating p53's abundance and function (see detailed discussion below).

Nucleolin contains four RNA recognition motifs (RRMs) followed by a carboxyl tail rich in Arg-Gly-Gly tri-peptide motifs. These RNA-binding motifs allow nucleolin to bind defined stem-loop structures within the pre-rRNA, perhaps acting as a chaperone for proper RNA folding in ribosome assembly (Ginisty et al. 1999). Nucleolin, however, also contains an amino terminal domain consisting of alternating acidic and basic motifs. The acidic motifs are rich in phospho-serine, while the basic domains resemble the tails of histone H1, especially with its multiple CDK1/Cyclin B phosphorylation sites. Studies indicate that nucleolin associates with nucleolar chromatin and participates in Pol I transcription, perhaps linking Pol I transcription with pre-rRNA processing in a regulatory feedback mechanism (Roger et al. 2003; Rickards et al. 2007; Schneider 2012). Similar to NPM1, nucleolin interacts with several proteins (Cong et al. 2011), including p53 (Daniely et al. 2002). Takagi et al. (2005) showed that when over-expressed, nucleolin binds the 5' UTR of the *p53* transcript to suppress its translation; conversely, down-regulation of nucleolin promotes p53 expression.

1.3.3 Ribosome assembly

During the course of ribosome assembly, equimolar amounts of ribosomal proteins are translated in the cytoplasm and imported into the nucleus. The 18S

rRNA assembles with 33 proteins to form the small 40S ribosomal subunit (SSU in Figure 1.1), while the 5.8S, 28S, and Pol III-transcribed 5S rRNAs assemble with 50 proteins to form the large 60S ribosomal subunit (LSU in Figure 1.1). Ribosomal proteins comprising the small subunit are designated RpS1, RpS2, etc., while large subunit proteins are designated RpL1, RpL2, etc. Important for discussions on nucleolar stress are RpS3, RpS7, RpL5, RpL11, RpL23, and RpL26.

Immature 40S and 60S subunits emerge from the DFC to occupy specified sub-compartments within the GCs (Politz et al. 2005; see Figure 1.1 and below). Subunit export to the cytoplasm is mediated by the adaptor protein NMD3 and the export factor CRM1 (Bai et al. 2013). We continue to discern how the ribosomal subunits achieve functional maturation within the cytoplasm (Zemp and Kutay 2007; Panse and Johnson 2010; Sengupta et al. 2010; Lo and Lu 2010). Cryo-EM and crystallographic structures of eukaryotic ribosomes provide opportunities to fully comprehend not only ribosome function during translation initiation, elongation, and termination, but emerging inter-relationships between ribosome biogenesis/function and cell homeostasis; that is, how cell homeostasis is lost when individual ribosomal proteins are mutated or deleted (the ribosomopathies) (Armache et al. 2010a; Armache et al 2010b; Ben-Shem et al 2011; Klinge et al 2011; Rabl et al. 2011; Wilson and Doudna 2012; Klinge et al 2012). As discussed below, these investigations should allow us to select strategically nucleolar or ribosomal targets for novel anti-cancer therapeutics.

1.4 p53 Dependent Nucleolar Stress

In their landmark paper, Rubbi and Milner (2003) employed UV irradiation to induce DNA damage to disrupt nucleoli, which in turn resulted in p53 activation and cell cycle arrest. Links between double-strand chromosomal breaks, activation of ataxia telangiectasia, mutated (ATM), and the transient block of Pol I initiation complex assembly and in transcription elongation were subsequently established (Kruhlak et al. 2007; Boulon et al. 2010). Rubbi and Milner (2003) could bypass the UV-induced stimulation of nucleolar stress by injecting an antibody against Upstream Binding Factor (UBF), the Pol I transcription/nucleolar chromatin factor. Thus, by blocking Pol I transcription selectively, they were able to induce nucleolar disruption leading to p53 activation, but now without DNA damage. They concluded that the nucleolus is a major stress sensor that when disrupted, initiates p53-dependent cell cycle arrest. The principal mechanism that links nucleolar disruption with p53 activation and mammalian cell cycle arrest utilizes MDM2 (murine/human double minute 2), the ubiquitin E3 ligase that negatively regulates p53 by marking it for ubiquitin-mediated proteasomal degradation (Brooks and Gu 2006; see Figure 1.2, A).

1.4.1 Nucleolar factors that block MDM2

Upon nucleolar stress, several ribosome assembly factors that normally enrich within nucleoli redistribute to the nucleoplasm, while ribosomal proteins entering the nucleus (nucleoplasm) are incapable of assembling into ribosomes. Several of these assembly factors and ribosomal proteins bind to and block MDM2 activity resulting in p53 stabilization. Even the 5S ribosomal RNA is now

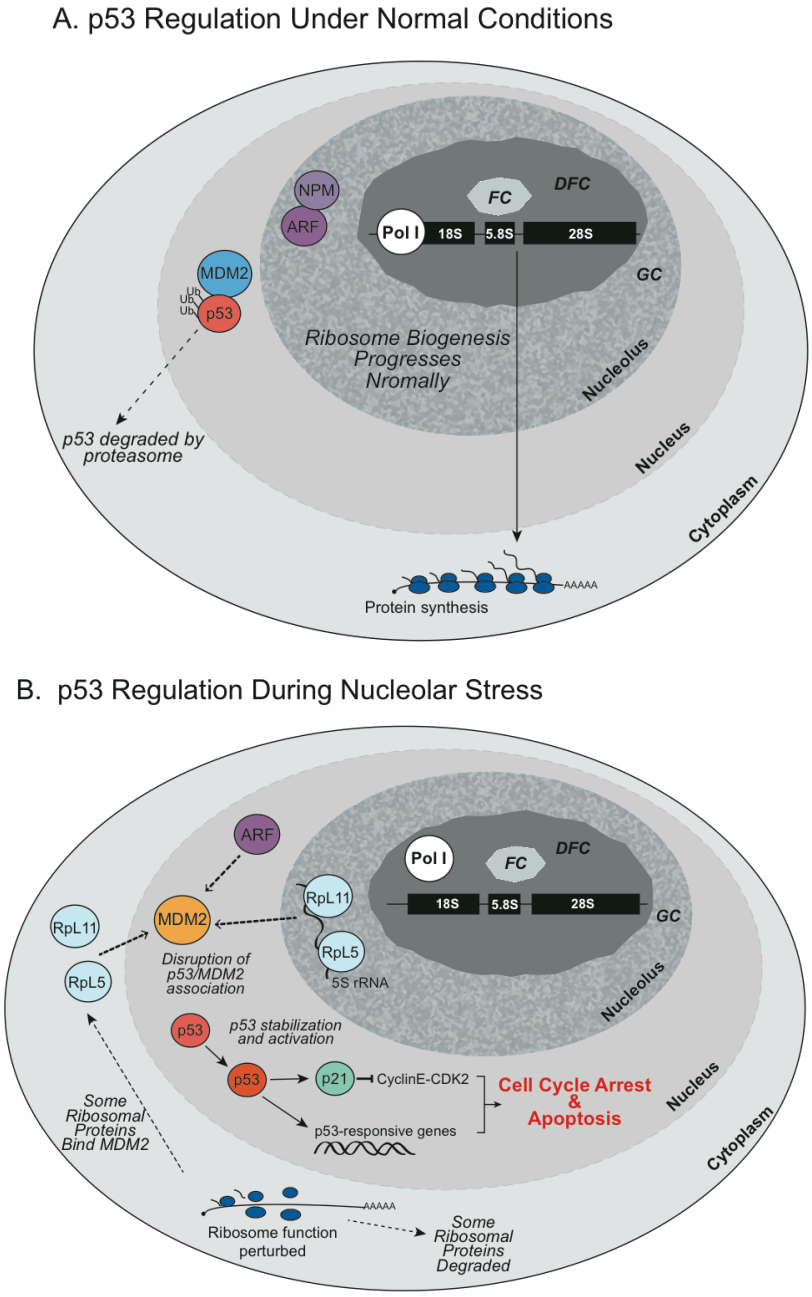

FIGURE 1.2. Regulation of p53 During Normal and Nucleolar Stress Conditions in Mammalian Cells. (A) During normal, non-stressed conditions, the E3 ubiquitin ligase, MDM2, associates with p53, promoting p53's degradation (Brooks and Gu 2006). Nucleophosmin (NPM) and Arf are located in the nucleolus (Brady et al., 2004). (B) During nucleolar stress, normal ribosome biogenesis and function are perturbed. The association between MDM2 and p53 is disrupted; additional proteins such as ribosomal proteins (RpL5, RpL11) with the 5S rRNA (Sloan et al. 2013; Donati et al., 2013) and Arf can associate with MDM2 (Llanos et al. 2001). p53 is stabilized and activates the cell cycle inhibitor *p21* and other p53-responsive genes. These events lead to cell cycle arrest and apoptosis.

known to help trigger the activation of p53 by inactivating MDM2 (Figure 1.2). Figure 1.3 shows where various factors bind MDM2 to inhibit its activity; the amino terminal domain of MDM2 binds p53, preventing p53 from inducing transcription of downstream effector genes (e.g. *p21*). The carboxy RING finger domain of MDM2 is the E3 ligase responsible for ubiquitination of p53, marking it for proteasomal destruction. The central acidic domain of MDM2 contains a C4 zinc finger, and it likely folds such that the amino terminal domain of MDM2 with its bound p53 now lies in close juxtaposition with the carboxy E3 ligase. Preventing the central domain of MDM2 from folding would likely interfere with MDM2-mediated p53 degradation.

Arf (alternative reading frame protein, $p19^{Arf}$ in mouse, $p14^{Arf}$ in humans) is a tumor suppressor protein expressed from the *p16*^{INK4a} gene locus that also expresses $p16^{INK4a}$, a cyclin-dependent kinase (CDK) inhibitor. The locus expresses both proteins by alternative utilization of exons and reading frames (Quelle et al. 1996). Arf normally localizes to nucleoli in non-stressed cells, most likely due to its interaction with nucleophosmin (see below). While exogenous Arf can sequester MDM2 to nucleoli (Figure 1.2, B), subsequent studies indicate that nucleolar stress induces the release of Arf to the nucleoplasm where it binds and inhibits MDM2 (Weber et al. 1999; Llanos et al. 2001), thus allowing p53 to accumulate and block cell cycle progression (Figure 1.2). When released from nucleoli, Arf binds the central acidic region of MDM2 to inhibit its ubiquitination of p53 (Argentini et al. 2001; Zhang et al. 2003; Kawai et al. 2003; Meulmeester et al. 2003; Sherr 2006).

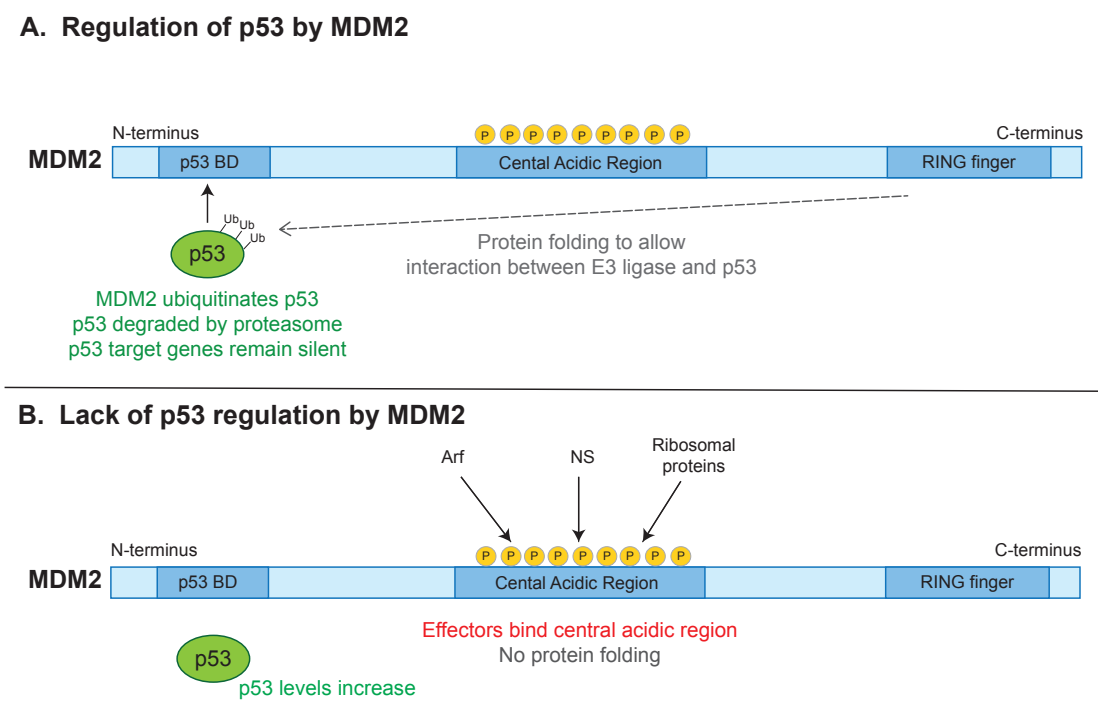

FIGURE 1.3. MDM2 and p53 Regulation. MDM2 has three main functional domains: a N-terminal p53-binding domain, a central acidic region, and a carboxy RING finger which has E3 ubiquitin ligase activity (Kawai et al. 2003). (A) MDM2 folds such that the carboxy RING finger domain interacts with p53 bound at MDM2's N-terminus. p53 is then ubiquitinated and targeted for degradation (Brooks and Gu 2006; Argentini et al. 2001). (B) Protein folding is prevented when certain proteins such as ARF, Nucleostemin (NS), or other ribosomal proteins bind to the phosphorylated central domain of MDM2. This results in stabilization and accumulation of p53 levels (Zhang and Lu 2009; Chen et al. 2007).

NPM1 is an abundant nucleolar protein with multiple, complex roles. As mentioned above, it acts as a nucleolar endoribonuclease required for ITS2 cleavage in pre-rRNA processing (Savkur and Olson 1998), and it functions as a key regulator in nucleolar control of cell homeostasis. For example, NPM1 shuttles between the nucleolus and the nucleoplasm, and in so doing it may regulate transcription by interacting with factors such as Myc, NFκB, YY1, p53, and others. NPM1 is a histone chaperone that helps maintain genome stability by

participating in DNA double-strand break repair, blocks apoptosis when over-expressed, and participates in centrosome duplication at prophase and mitotic spindle pole formation at metaphase (Colombo et al. 2011; Yip et al. 2011). NPM1 is also a critical regulator in the nucleolar stress response. Specifically, NPM1 interacts with the amino terminus of Arf; one interpretation suggests that up-regulation of Arf sequesters NPM1 to the nucleolus thus blocking NPM1's shuttling to the nucleoplasm (Brady et al. 2004), the result being an inhibition of NPM1's function and cell cycle arrest. MDM2 also binds the amino terminus of Arf antagonizing the interaction between Arf and NPM1, and thereby reversing the inhibitory effects of Arf on NPM1. Itahana et al. (2003) further suggested that exogenously expressed Arf negatively regulates NPM1 by promoting the poly-ubiquitination of NPM1, leading to its destruction and a block in ribosome biogenesis.

A more recent interpretation, however, suggests that under normal growth conditions, the abundance of NPM1 exceeds that of Arf, and as a consequence, most Arf protein is bound to NPM1 within the nucleolus (Korgaonkar et al. 2005; Colombo et al. 2005). Sequestering Arf to the nucleolus would prevent its association with MDM2 in the nucleoplasm (Korgaonkar et al. 2005). The interaction with NPM1 in the nucleolus would also stabilize Arf, which rapidly degrades in the absence of NPM1.

Nucleostemin (NS) is another nucleolar regulator of p53, and it can modulate p53 indirectly by binding MDM2 (Tsai 2011). Mammalian NS consists of an amino terminal basic domain followed by a coiled-coil domain, a central

GTP-binding domain, an RNA-binding domain, and finally a carboxyl acidic domain. NS belongs to the YawG subfamily of GTPases with its central GTP-binding motifs arranged in permutated fashion (G5-G4-G1-G2-G3) rather than in the conventional G1-G2-G3-G4-G5 as found in Ras-family GTPases. NS is abundant in stem cells and cancer cells, but its abundance drops in stem cells as they enter differentiation pathways where cycle progression (proliferation) slows down (Tsai and McKay 2002). NS localizes to nucleoli with GTP bound, but it transits to the nucleoplasm with GDP bound (Tsai and McKay 2005; Meng et al. 2006). Cycling between the nucleolus and the nucleoplasm likely imparts separate functions for NS (Misteli 2005). Interestingly, mammalian NS occupies sub-compartments within the GC that are actually deficient in RNA (the lighter gray areas within the GC of Figure 1.1) (Politz et al. 2005). This suggests that the RNA-containing compartments of the GC function in ribosomal subunit maturation and release, while RNA-deficient compartments within the GC are reserved for maintaining cell homeostasis. As discussed below, mammalian NS plays a critical role in nucleolar stress response by also interacting directly with p53 (Tsai 2011).

Determining the precise function(s) of mammalian NS, however, has been challenging. Romanova et al. (2009) showed that NS forms a large complex that co-fractionates with the pre-60S subunit. The complex contains processing factors Pes1, DDX21, EBP2, and several ribosomal proteins. Prolonged depletion of NS inhibited the processing of the pre-rRNA 32S intermediate to the mature 28S rRNA, while over-expression of NS facilitated 32S processing.

However, because NS localizes to non-rRNA containing regions of the GC (Politz et al. 2005), it may not be directly involved with ribosome biosynthesis or maturation. Outside the nucleolus, NS has been reported to protect DNA at telomeres by mediating the interaction between PML-IV and SUMOylated telomeric repeat factor 1 (TRF1), which then recruits RAD51 to the telomeres (Hsu et al. 2012). Furthermore, NS may protect the genome from double-strand breaks associated with DNA replication in actively dividing stem cells by interacting with (perhaps recruiting) RAD51 to the sites of damage (Meng et al. 2013). Recently, Lin et al. (2014) argued that the *NS* gene in mammals has evolved from an ancestral gene, *GNL3,* such that now the primary role of NS is to protect the genome (*e.g.* from S-phase DNA damage) while maintaining only a minor, perhaps even indirect role in ribosome biogenesis.

Other, paralogous NS-like family members have been implicated directly in ribosome biogenesis. For example, loss of Grn1 in *S. pombe* blocks 35S pre-rRNA processing while blocking the release of RpL25a (Du et al. 2006). Similarly, loss of NST-1 in *C. elegans* reduces 18S and 26S rRNA abundance (Kudron and Reinke 2008). Rosby et al. (2009) depleted *Drosophila* NS1 (homologous to vertebrate GNL3L) (Tsai 2011) by RNAi expression, and showed an inhibition in LSU release from nucleoli leading to autophagy in terminally differentiated polyploid cells, and loss of diploid progenitor island cells in the larval intestines. Wang and DiMario (submitted) depleted *Drosophila* NS2 (homologous to human Ngp1) by RNAi expression, and also showed an inhibition of LSU release from nucleoli in polyploid midgut cells. TEM analysis of NS2-depleted midgut cells

showed enlarged granular regions of the nucleoli and mitophagy (mitochondria eclosed by selection membranes derived from rER). Additionally, loss of NS2 function induced apoptosis in diploid imaginal wing discs, which led to malformed adult wing structures (Wang and DiMario submitted).

Regulation of p53 by NS is likewise complex: both over- and under-expression of NS seems to activate p53 leading to cell cycle arrest (Lo and Lu 2010; Tsai 2011). When over-expressed and therefore abundant in the nucleoplasm, NS uses its coiled-coil domain to bind the acidic domain of MDM2. This blocks MDM2's E3 ubiquitin ligase activity, thus allowing p53 to accumulate (Figure 1.3) (Dai et al. 2008). Conversely, siRNA depletion of NS causes p53-dependent cell cycle arrest (Dai et al. 2008; Ma and Pederson 2007). In this case, ribosome production is disrupted by the loss of NS, and unassembled RpL5 and RpL11 are thought to bind MDM2 to block its ubiquitination of p53 in the same nucleolar stress mechanism already described (Dai et al. 2008). Thus, MDM2 activity is blocked either by NS itself when over-expressed, or by ribosomal proteins when ribosome production is disrupted by NS depletion.

Regulation of NS is made more complicated due to its interactions with other nucleolar and nuclear proteins. Ma and Pederson (2007) showed that NS abundance was inversely related to the abundance of Arf, a negative regulator of MDM2 (described above). They showed that NS levels fell by 50% when Arf was expressed exogenously in U2OS osteosarcoma cells, which normally lack Arf. The instability of NS was attributed to the rise in p53 levels, perhaps due to Arf blocking MDM2 activity. Conversely, NS levels rose when endogenous Arf was

depleted in HeLa cells. NS function may also be regulated by mechanisms that were not immediately obvious (*i.e.* ubiquitination), while its stability is regulated by GTP levels in mechanisms that remain largely unknown (Lo and Lu 2010). For example, Lo et al. (2012) showed that NS undergoes proteasomal degradation in the absence of GTP, but in an ubiquitin and MDM2-independent fashion.

Regulation of NS may involve nucleophosmin (NPM1). As described above, NPM1 is a multi-functional nucleolar processing/assembly factor implicated in centrosome duplication, cell proliferation, and both oncogenic and tumor-suppressor activities depending on p53 levels in particular cell types. Ma and Pederson (2008) showed that in human U2OS osteosarcoma cells, NS and NPM1 co-localize within the granular component of interphase nucleoli and to telophase pre-nucleolar bodies prior to nucleologenesis; they showed a direct interaction between NS and NPM1 by co-IP, yeast two-hybrid, and *in vivo* bimolecular fluorescence complementation.

Avitabile et al. (2011) extended these studies to neonatal rat cardiomyocytes and cardiac progenitor cells, and therefore to heart disease. They showed that NS, NPM1, and Arf redistribute to the nucleoplasm upon doxorubicin-induced cardiotoxicity, which causes nucleolar stress. Release of Arf to the nucleoplasm correlated with increased p53 activity as measured by increased *p21* gene expression and by induced DNA damage, assayed by TUNEL staining. Silencing of NPM1 in these cells caused nucleolar stress resulting in the redistribution of NS and Arf from nucleoli to the nucleoplasm, but depletion of NS did not redistribute NPM1. Interestingly, they showed a re-

expression of NS and NPM1 in border zone cardiomyocytes after pathological injury (myocardial infarction) indicating that reintroduction of NS in adult myocardial cells may be an important aspect of healing after myocardial infarction. Hariharan and Sussman (2014) review the role of the nucleolus and nucleolar proteins in cardiovascular pathophysiology, especially the nucleolus as a stress sensor in cardiac disease.

1.4.2 Ribosomal proteins

Besides nucleolar assembly factors, several ribosomal proteins are known to bind MDM2 to block its ubiquitination of p53 (Figure 1.3) (Zhang et al. 2009; Warner and McIntosh, 2009). These include RpS3 (Yadavilli et al. 2009), RpS7 (Chen et al. 2007; Zhu et al. 2009), RpL5, (Marechal et al. 1994; Dai and Lu 2004; Bursać et al. 2012), RpL11, (Zhang et al. 2003; Lohrum et al. 2003; Bhat et al. 2004; Fumagalli et al. 2009) and RpL23 (Dai et al. 2004). Upon nucleolar stress (failure in ribosome biogenesis), rather than being released from the nucleolus, these ribosomal proteins likely bind MDM2 in the nucleoplasm as they first enter the nucleus from the cytoplasm. Like Arf, these ribosomal proteins bind to the acidic central domain of MDM2. The functional significance of MDM2's central domain for normal ubiquitination of p53 is well established (Kawai et al. 2003). One hypothesis suggests that binding of ribosomal proteins and other nucleolar factors reduces the flexibility of MDM2's central domain, preventing the amino terminal domain of MDM2 with its bound p53 from folding to form a close juxtaposition with its carboxy domain that displays E3 ubiquitin ligase activity (Figure 1.3) (Zhang and Lu 2009).

Disruption of nucleoli may not be the only trigger that liberates ribosomal proteins that then block MDM2. Fumagalli et al. (2009) conditionally depleted RpS6 and thus the 40S subunit in mouse hepatocytes, but under these conditions nucleoli remained intact and biogenesis of the 60S subunit continued. Interestingly, when the 40S subunit is depleted, extra amounts of RpL11 were produced by a selective recruitment of *rpL11* mRNA to actively translating polysomes. The *rpL11* mRNA contains a translation-repressive 5' poly-pyrimidine tract (5'-TOP). This transcript and others with 5'-TOP sequences (those encoding RpS8, RpS16, RpL26) actually maintain translational activity upon loss of the 40S subunit, suggesting a de-repression of the 5'-TOP upon loss of the 40S subunit. Thus, when the 40S subunit is depleted by loss of RpS6 (or RpS7, RpS23), translation of 5'-TOP transcripts (e.g. *rpL11*) produces excess RpL11, which then blocks MDM2 to ultimately activate p53 and arrest the cell cycle. How de-repression of 5'-TOP transcripts is mediated by loss of the 40S remains an intriguing question.

While most ribosomal proteins degrade rapidly within proteasomes during nucleolar stress (Warner 1977; Lam et al. 2007; Andersen et al. 2005), RpL5 and RpL11 tend to accumulate selectively (Bursać et al. 2012). This is in contrast to other ribosomal proteins known to bind MDM2. RpL5 and RpL11 accumulate by continued *de novo* protein synthesis, and by mutual protection from proteasomal degradation. During nucleolar stress (actinomycin D-mediated inhibition of Pol I transcription), these two proteins co-localize with each other, p53, MDM2, and the promyelocytic leukemia (PML) protein within remnant nucleoli. Based upon

their co-localizations, Bursać et al. (2012) suggest the nucleoli serve as the staging site for RpL5 and RpL11 binding and inhibition of MDM2, resulting in p53 activation (Figure 1.2, B). Two subsequent reports further showed that RpL5 and RpL11 interact with the 5S rRNA to form a trimeric RNP complex that then blocks MDM2 (HDM2) (Sloan et al. 2013; Donati et al. 2013). Sloan et al. (2013) noted the accumulation of the trimeric RpL5/RpL11/5S rRNA complex within the nucleoplasm rather than in nucleoli as observed by Bursać et al. (2012), but this may be due to the different cell types used in the respective studies.

1.5 Drugs and Environmental Insults that Induce Nucleolar Stress

Nucleolar stress (often referred to as ribosomal stress) is any disruption in ribosome biogenesis. The term ribosomopathy describes phenotypes associated with non-functional ribosomes within the cytoplasm. Nucleolar stress can be induced at multiple steps within the nucleolus, from Pol I transcription initiation and elongation to early and late pre-rRNA processing (ribosome assembly), and eventually to ribosome maturation and eventual release from the GC. Perturbations in ribosome biogenesis can cause disruptions in nucleolar integrity, which releases nucleolar and ribosomal proteins to the nucleoplasm where they take on secondary functions as stress response effectors (Rubbi and Milner 2003). Here we briefly look at the various methods that have been used to block ribosome biosynthesis to induce nucleolar stress, beginning with Pol I transcription.

RNA Pol I transcription can be blocked by several drugs leading to nucleolar disruption (Hein et al. 2013; Burger et al. 2010). Early on we knew that

actinomycin D at low concentrations (<5 nM) intercalates preferentially within GC rich rDNA to block Pol I transcription elongation. Inhibition of Pol I by actinomycin D causes nucleolar segregation where the FC and DFC form a crescent shaped “cap” over a somewhat centralized GC (Hernandez-Verdun 2011). Other intercalating agents known to disrupt nucleolar transcription include mitomycin C, mitoxantrone, and doxorubicin; the latter two block topoisomerase function. The alkylating and DNA-crosslinking agents, cisplatin and oxaliplatin also block Pol I transcription effectively, as does the anti-metabolic drug, methotrexate. All these drugs have been used as chemotherapeutic agents in various cancer treatments (Hein et al. 2013; Burger et al. 2010). Depending upon the drug, nucleoli could also fragment into smaller “spots” or into “necklaces” as observed by the redistribution of nucleolar markers such as fibrillarin (Burger et al. 2010). Newer drugs currently in Phase I and II clinical trials include ellipticine which blocks Pol I transcription initiation (Andrews et al. 2013), CX-3543 which blocks Pol I elongation by disrupting nucleolin interactions with rDNA (Drygin et al. 2009), and CX-5461 which blocks Selectivity Factor-1 (SL-1) from binding rDNA promoters to thus prevent pre-initiation complex assembly (Drygin et al. 2011). Expectations in cancer therapy may be high regarding these latter two drugs as they have exceptional specificity for targeting transcription by Pol I versus Pol II and Pol III (Hein et al. 2013; Drygin et al. 2013).

While the drugs described above block Pol I transcription, other drugs target pre-rRNA processing. Camptothecin, flavopiridol, and roscovitin block early pre-rRNA processing as measured by inhibitions in 47S pre-rRNA

cleavage. MG-132, homoharringtonine, and 5-fluorouracil block later processing events as measured by loss of mature 18S and 28S despite the presence of the 32S pre-rRNA intermediate (Burger et al. 2010). While 5-fluorouracil blocks thymidylate synthetase, it also incorporates into nascent RNA which blocks subsequent pseudo-uridylation and marks these RNAs for destruction by the exosome (Burger et al. 2010).

Besides drugs, environmental insults such as heat shock, oxidative stress, hypoxia, and UV irradiation can induce nucleolar re-organization or disruption. Several reports show that heat shock disrupts nucleoli and redistributes nucleolar proteins (Welch and Suhan 1985; Liu et al. 1996). Interestingly, mRNAs can transit through the yeast nucleoli during heat shock (Liu et al. 1996). *Trypanosoma cruzi* at the epimastigote stage (the life cycle stage at which the tail is anterior to the nucleus) also accumulates mRNAs within its nucleoli during severe heat shock (Názer et al. 2012). Hypoxia and acidosis can also down-regulate rDNA transcription via the hypoxia-inducible factor (HIF) and the von Hippel-Lindau tumor suppressor protein (VHL) (Mekhail et al. 2006). UV irradiation damages genomic DNA, blocking RNA Pol II transcription, and this ultimately leads to nucleolar disruption. Hypotonic shock is also known to quickly and reversibly disrupt nucleoli (Zatsepina et al. 1997), while hypertonic shock disrupts related Cajal bodies (Cioce et al. 2006). As far as we know, however, the effects of osmotic shock on nucleolar stress pathways have not been described.

Pre-rRNA transcription by RNA polymerase I is the rate-limiting step in ribosome biogenesis (Voit and Grummt 2011); as such, it is tightly regulated by growth factor signaling and nutrient availability (*e.g.* TOR signaling). The mammalian target of rapamycin (mTOR) kinase regulates Pol I transcription by positively controlling transcription factors TIF-1A, SL-1, and UBF (Grummt 2003; Mayer and Grummt 2005). mTOR also regulates protein translation by phosphorylating 4E-BP and S6 kinase that then respectively regulate eIF4E for cap-dependent translation initiation and RpS6 which influences elongation factor 2 kinase (Xiao and Grove 2009). Starvation or treatment with rapamycin down-regulates mTOR in yeast and mammalian cells, and this leads to a significant reduction in nucleolar size and a block in rDNA transcription. Tsang et al. (2003) showed that upon inhibiting mTOR in yeast, the histone deacetylase, Rpd3-Sin3, rapidly associated with rDNA to deacetylate K5 and K12 of histone H4 in a rDNA-specific manner. Consequently, Pol I redistributed from the nucleolus and rRNA transcription was blocked. Deleting the *rpd3* gene or H4 hyper-acetylation mutants blocked these adverse effects on nucleolar structure and function caused by inhibiting mTOR.

1.6 Endogenous Mutations: The Ribosomopathies

In their comprehensive review, Narla and Ebert (2010) defined the ribosomopathies as a collection of human disorders with defined clinical phenotypes caused by impaired ribosome biogenesis and function. These disorders result from natural mutations in genes that encode ribosome assembly factors within nucleoli or the ribosomal proteins themselves. The mutations can

lead to craniofacial malformations, skin lesions, or an absence of erythroid progenitor cells in the bone marrow leading to anemia. Why only certain tissues are affected remains an intriguing question (Armistead and Triggs-Raine 2014). Here we briefly describe the ribosomopathies and the nucleolar or ribosome stress associated with each, but keep in mind that these diseases may not result simply from a defect in protein synthesis. The possibility that unassembled mutant ribosomal proteins may exert toxic effects on non-translation events has not been completely ruled out (Tsai and Pederson 2014).

1.6.1 Treacher Collins syndrome (TCS)

TCS is most frequently associated with mutations in *Tcof1*/treacle, an assembly factor within the dense fibrillar component of nucleoli. TCS presents as a collection of craniofacial malformations that arise during early development (Dixon et al. 2006; Sakai and Trainor 2009). Treacle is similar to Nopp140 in motif composition and likely function (Dixon et al. 1997; He and DiMario 2011); both proteins are considered chaperones for nucleolar snoRNPs, however, treacle (and perhaps Nopp140) may also play a vital role in recruiting UBF and Pol I to the rDNA promoter (Lin and Yeh 2009). Haplo-insufficiencies in treacle ($Tcof^{+/-}$) cause a block in 2'-*O*-ribose methylation (Gonzales et al. 2005), an overall loss of cytoplasmic ribosomes (Jones et al. 2008), and most telling, a loss of specialized embryonic neural crest cells that ostensibly have a high demand for protein synthesis and thus functional ribosomes (Dixon et al. 2006). These cells die by apoptosis prior to their normal migration into branchial arches I and II that give rise to the craniofacial structures that are adversely affected in TCS.

Interestingly, most other stem and progenitor cells in *Tcof*$^{+/-}$ embryos survive treacle insufficiencies, again indicating diverse ribosome requirements in different progenitor cell populations at defined points in embryonic development. Using a *Trp53* gene deletion in mouse or pifithrin-α, a drug that specifically blocks p53, Jones et al. (2008) blocked apoptosis in these *Tcof*$^{+/-}$ neural crest cells, thus preventing the cranial abnormalities and confirming p53-dependent nucleolar stress. While mutations in *Tcof1* have been most often associated with TCS, haplo-insufficiencies in *POLR1D* or mutations in both alleles of *POLR1C* (*POLR1D* and *POLR1C* encode subunits for both RNA Pol I and III) have also been linked to TCS (Dauwerse et al. 2011). Therefore, in terms of nucleolar stress, haplo-insufficiencies in treacle or Pol I and Pol III result in the loss of ribosome production, and this leads to p53-dependent cell cycle arrest and apoptosis principally in the neural epithelium and neural crest. Ellis (2014) discusses the dissimilar phenotypes associated with the TCS versus the hematopoietic failures observed in other ribosomopathies as described below. These phenotypic differences may result from errors in pre-rRNA transcription and early processing (*i.e.* mutations in Pol I and treacle for TCS) versus mutations in individual genes encoding the ribosomal proteins themselves.

1.6.2 Dyskeratosis congenita (DC)

DC is a human skin and hematopoietic disorder associated with mutations in the X-linked *DKC1* gene, which encodes dyskerin, the box H/ACA snoRNP enzyme responsible for pseudouridylation of targeted residues within non-coding RNAs (*e.g.* pre-rRNA, spliceosomal). Dyskerin also interacts with the human

telomerase RNA component (TER) due to the H/ACA-like domain at the RNA's 3' end of the RNA (Mitchell et al. 1999; Rashid et al. 2006) and is required for telomerase biogenesis (Thumati et al. 2013). Mutations in *DKC1* are associated with premature aging, a propensity for certain cancers (Narla and Ebert 2010), abnormalities in the skin and mucous membranes, and bone marrow defects (Thumati et al. 2013). Hoyeraal-Hreidarrson syndrome is a severe form of DC with earlier onset, additional neurological disorders, and higher morbidity (Thumati et al. 2013). At the molecular level, defects have been observed in rRNA processing and reduced telomere length (Ruggero et al. 2003; Mochizuki et al. 2004), both of which could lead to loss of bone marrow stem cells (Marrone and Mason 2003).

Besides mutations in the *X*-linked *DKC1* gene, less severe forms of DC are associated with autosomal mutations in the *TERT* gene that encodes telomerase reverse transcriptase (Yamaguchi et al. 2005) or in the *TERC* gene that encodes the RNA component of telomerase (Vulliamy et al. 2001; Marrone et al. 2007). These mutations cause a haplo-insufficiency in functional telomerase leading to shortened telomeres. Using zebrafish, Pereboom et al. (2011) showed that loss of Nop10, one of the other three proteins within box H/ACA snoRNPs besides dyskerin (the other being Nhp2), caused a failure in 18S rRNA processing, loss of 40S ribosomal subunits, and a loss of hematopoietic stem cells. Similar to the loss of treacle in embryonic neural crest cells, these hematopoietic cells in zebrafish could survive if they carried a loss-of-function *p53* allele indicating a p53-dependent nucleolar stress. Interestingly,

however, telomere length in these cells was not restored, suggesting that nucleolar stress rather than shortened telomeres was the principal defect in the zebrafish model of DKC when nucleolar pseudouridylase activity is impaired.

Thumati et al. (2013) however, expressed TERT and TER in fibroblasts from *X*-linked DC patients to restore stable telomere maintenance but still in the presence of the mutant dyskerin protein. These cells continued to show slight but reproducible depletions of pseudouridine in the rRNA, but compared to wild type cells that also expressed exogenous TERT and TER, there were no detectable differences in protein synthesis, internal ribosome entry site translation initiation, in tolerances to ionizing radiation, or in endoplasmic reticulum stress in these modified DC cells. Thumati et al., (2013) proposed therefore, DC etiology is based primarily on the loss of telomere maintenance rather than on the loss of ribosome function.

1.6.3 Diamond-Blackfan anemia (DBA)

DBA in humans is a diverse collection of clinical disorders resulting from mutations consistently observed in genes encoding 40S subunit ribosomal proteins RpS7, RpS10, RpS17, RpS19, RpS24, or RpS26, or in genes encoding 60S subunit ribosomal proteins RpL5, RpL11, RpL26, or RpL35A (Ellis 2014; Gazda et al. 2012; Vlachos et al. 2013). Most are missense or nonsense mutations, but deletions have also been observed (Farrar et al. 2011; Landowski et al. 2013). All appear to be haplo-insufficiency-type mutations meaning that the wild type allele cannot provide sufficient product to prevent the disorder. DBA phenotypes vary depending on the particular mutation. While DBA patients could

display short stature, an increased risk of malignancies, craniofacial, thumb, urogenital, and heart defects (Narla and Ebert 2010; Ellis 2014), the principle defect is congenital bone marrow failure (erythroid precursor failure) leading to anemia, macrocytosis, and reticulocytopenia (Lipton and Ellis 2009). Loss of erythroid precursor cells occurs by apoptosis (Perdahl et al. 1994) due to p53 accumulation and activation (Dutt et al. 2011; Jaako et al. 2011). The zebra fish model for DBA similarly shows developmental defects and failures in erythropoiesis upon loss of RpL11 or RpS19 (Chakraborty et al. 2009; Danilova et al. 2010; Taylor et al. 2012). The developmental defects can be rescued by depleting p53, but the erythropoietic defects appear to be p53-independent (Torihara et al. 2011; Yadav et al. 2014). Interestingly, both the developmental defects and the erythroid defects in RpL35A-deficient zebra fish embryos could be improved by stimulating the mTOR pathway with either leucine or arginine treatments. This suggests that the efficiency in protein translation by a limited number of functional ribosomes may have been bolstered by the now hyper-activated mTOR pathway.

Related to these findings in zebrafish, Narla and Ebert (2010) suggested that loss of erythroid progenitors by apoptosis could occur by one of two mechanisms. In the first pathway, loss of the ribosomal proteins could induce nucleolar stress leading to p53-dependent apoptosis as described above. If this mechanism is correct, we have to assume that erythroid progenitors have a higher demand for functional ribosomes than most other stem/progenitor cells within the body. In the second pathway, insufficient ribosomes would cause an

under-production of hemoglobin in these erythroid progenitor cells, leading to an accumulation of excess heme that then induces oxidative stress leading to apoptosis and loss of the erythroid progenitors (Ellis 2014). This argues for both p53-dependent and independent nucleolar stress responses not only in the same organism, but perhaps within the same cell. We describe various other p53-independent nucleolar stress responses below.

1.6.4 5q- syndrome

The 5q- syndrome in humans is another disease associated with erythroid failure. A deletion on the long arm of human chromosome 5 eliminates several genes, but a systematic RNAi screen identified RpS14 as the critical gene associated with erythroid failure when haplo-insufficient (Ebert et al. 2008; Ebert 2009). The loss of RpS14 increases the 32S/18S processing ratio in cells derived from patients, and ectopic expression of RpS14 can rescue these cells. Cells expressing RpS14 shRNAs recapitulated the syndrome as these cells were deficient in 40S subunits (Ebert et al. 2008).

1.6.5 Schwachman-Diamond syndrome (SDS)

SDS is another failure in hematopoiesis, but it also presents exocrine pancreatic failures and increased risks to myelodysplasia and leukemia. The syndrome is associated with hypomorphic mutations in the *SBDS* (*Schwachman-Bodian-Diamond Syndrome)* gene (Boocock et al. 2003). The SBDS protein is well conserved from archaea to vertebrates, and is likely multi-functional (Johnson and Ellis 2011). SBDS co-enriches with the 60S subunit presumably in the cytoplasm; Finch et al. (2011) report that mouse SBDS acts in the cytoplasm

to release eIF6 from the large 60S subunit by stimulating the GTPase activity of elongation factor-like 1 (EFL1). Mechanistic similarities between SBDS and the bacterial ribosome recycling factor (RRF) support the role of SBDS in activating ribosomes for protein translation. Finch et al. (2011) used a liver-specific deletion of exon 2 in mouse SBDS, which uncoupled GTP hydrolysis by EFL1 from the release of eIF6. It is unknown if other SBDS mutations associated with SDS affect the same coupling mechanism (Johnson and Ellis 2011). SBDS also forms a protein complex with nucleophosmin presumably within nucleoli as determined by reciprocal co-immuno-precipitations (Ganapathi et al. 2007). While mutations in SBDS do not seem to affect nucleophosmin's abundance or nucleolar localization, interaction between SBDS and nucleophosmin suggests that SBDS could play a role in ribosome biosynthesis. Indeed, bone marrow cells from SDS patients showed dysregulation in genes involved with pre-rRNA transcription and processing, as well as dysregulation in many of the genes encoding ribosomal proteins (Rujkijyanont et al. 2009).

1.6.6 Ribosomopathies in non-mammalian metazoans

We already mentioned above several contributions from zebrafish to our understanding of ribosomopathies. The rDNA-deficient *0-nu* mutation in *Xenopus* was instrumental in defining the nucleolus as the site for ribosome biogenesis (Brown and Gurdon 1964). Tadpoles homozygous for the mutation fail to synthesize 18S and 28S rRNA; they have only maternal rRNA provided by the fertilized oocyte, but without the ability to synthesize new ribosomes, they die in the early swimming stages some three days post fertilization.

As we begin to transition toward p53-independent forms of nucleolar stress (see below), we briefly describe ribosomopathies in *C. elegans* and *Drosophila*, both of which have functional p53, but lack MDM2. Lee et al. (2014) recently showed that *dao-5* in *C. elegans* encodes a Nopp140 homologue. A null mutation in *dao-5* disrupts rRNA synthesis leading to delays in gonadogenesis and an increased incidence of apoptosis in the germ line. An intriguing study in *C. elegans* by Fuhrman et al. (2009) showed that mutation in the conserved nucleolar protein, NOL-6, actually enhanced resistance to bacterial infection (*e.g.* the mutation enhanced innate immunity) by activating p53/ CEP-1 and thus its target gene, *SYM-1*. This study linked the nucleolus and p53 to an ancient form of innate immunity, further establishing the nucleolus as a stress response organelle.

The list of ribosomopathies is far from complete if one considers the many *Drosophila* mutations known to disrupt ribosome biogenesis or function. Some of these mutations have been known for decades. For instance, deletions in rDNA transcription units referred to as *bobbed (bb)* mutations have been well studied since the discovery of bb^{1} by Calvin Bridges in 1915 (Morgan et al. 1925; Ritossa 1976). The vast majority of *Minute* genes encode ribosomal proteins; one gene encodes a translation initiation factor (Lambertsson 1998; Marygold et al. 2007). Mutations in these genes lead to haplo-insufficient phenotypes of delayed development, shortened and thin bristles, and reduced viability and fertility. Other *Drosophila* genes known to encode nucleolar processing/assembly factors have also been characterized in terms of their mutant phenotype; those that have been

better characterized include *minifly* (Giordano et al. 1999), *modulo* (Perrin et al. 1998; Perrin et al. 1999; Perrin et al. 2003), *viriato* (Marinho et al. 2011), *dribble* (Chan et al. 2001), *jumeaux* (Hofman et al. 2010), *pitchoune* (Zaffran et al. 1998), and *Nopp140* (Cui and DiMario 2007; James et al. 2013). The *minifly* gene (also called *Nop60B*) encodes a pseudouridylase homologous to human *DCK1*. Mutations in *minifly* not only inhibit pseudouridylation of rRNA, but also disrupt normal pre-rRNA cleavage patterns. This leads to reduced body size (thus the name) and to several other developmental abnormalities (Giordano et al. 1999; Kauffman et al. 2003; Tortoriello et al. 2010). Modulo is a multi-functional, nucleolin-like protein in *Drosophila* that locates to nucleoli, but also to non-nucleolar chromatin where it can affect (modulate) gene expression by position effect variegation. Interestingly, modulo locates to nucleoli when phosphorylated but to non-nucleolar chromatin when un-phosphorylated (Perrin et al. 1999). While its role in ribosome assembly remains unknown, nucleolar modulo also participates in centromere organization by interacting with the Chromosome Alignment 1 protein (CAL1), a centromere assembly factor required for the localization of the H3-variant, CENP-A (CID in *Drosophila*) (Chen et al. 2012). As in mammalian systems, nucleolar activity in *Drosophila* is regulated by Myc; Grewal et al. (2005) demonstrated the necessity of Myc in upregulating RNA Pol I transcription during *Drosophila* development. The *modulo*, *viriato*, *pitchoune*, and *Nopp140* genes are also known target genes for Myc in controlling proliferation and growth (Perrin et al. 2003; Marinho et al. 2011; Zaffran et al. 1998).

Clearly, many nucleolar processing/assembly factors are multi-functional. Comparative siRNA screens of 625 nucleolar proteins in HeLa cells identified 286 that are required for pre-rRNA processing. Of these, 27% have either distinct or additional functions in pre-rRNA processing as compared to their yeast orthologs (Tafforeau et al. 2013). Thorough understandings of intracellular and whole-organism phenotypes caused by null or partial-loss-of function mutations in genes encoding these factors are critical before devising strategies to induce nucleolar stress in potential cancer therapies (see below). Toward this end, Neumüller et al. (2013) performed comparative genome-wide loss-of-function analyses of genes necessary for the regulation of nucleolar size (Pol I–mediated transcription) in both yeast and *Drosophila*. Their comparative approach defined an evolutionarily conserved network of genes required for cell growth. This gene network may provide new insights in limiting tumor cell growth.

1.7 p53 Independent Nucleolar Stress in Metazoans

We begin this section by describing metazoan cell cycle arrest induced by nucleolar stress but in p53-independent manners. Key papers include Donati et al. (2011), Iadevaia et al. (2010), and Li et al. (2009). Each example includes some disruption in ribosome biogenesis leading to nucleolar stress, involving E2F-1 down-regulation or $p27^{Kip1}$ expression, all resulting in cell cycle arrest.

1.7.1 p53-independent cell cycle control.

POLR1A encodes the catalytic subunit of RNA Pol I (Grummt 2003). Expressing siRNA to deplete POLR1A function specifically and effectively reduces nucleolar rDNA transcription without disturbing ribosome components

made by Pol II and Pol III (Donati et al. 2011). Silencing *POLR1A* to inhibit rDNA transcription in U2OS osteosarcoma and HCT-116 colon cancer cells lines (both are $p53^{+/+}$) resulted in p53 stabilization, increased expression of the cell cycle inhibitor p21, and a decrease in phosphorylated retinoblastoma protein (pRb). As expected, these events led to an accumulation of cells in G1 phase and a significant reduction in S-phase cells as measured by BrdU incorporation (Donati et al. 2011). To investigate the link between p53 and pRb, both *POLR1A* and *TP53* were silenced in U2OS and HCT-116 cells by siRNA expression. Similar to the previous result in $p53^{+/+}$ cells, depletion of both p53 and POLR1A activity resulted in a significant reduction of cells in S phase. In a second experiment, a dominant negative inactive form of murine p53 (p53DD) was exogenously expressed in HCT-116 cells; POLR1A-silencing in these p53-deficient cells also caused a significant reduction in DNA synthesis (Donati et al. 2011). With these two results, we can conclude that cell cycle arrest after POLR1A-silencing can occur in a p53-independent manner.

To assess pRb's control of cell cycle progression in the absence of rRNA synthesis, Donati et al. (2011) measured expression of E2F-1, the transcription factor whose activity is negatively regulated by pRb. After 48 hours of *POLR1A* silencing, E2F-1 expression was reduced in both $p53^{+/+}$ (U2OS) and p53-mutant (HCT-116 p53DD) cells. Both cell types arrested in G1. Since E2F-1 is primarily expressed in S phase, cells expressing p53DD and siRNA to target *POLR1A* were also treated with siRNAs to silence *Retinoblastoma 1* (*RB1*). Silencing of *RB1* and *POLR1A* in these p53-mutant cells actually rescued the cell cycle arrest

(Donati et al. 2011). In other words, after *POLR1A*-silencing, sufficient E2F-1 was made available to activate genes necessary for entry and progression through S phase, but only in the absence of pRb. However, after silencing *RB1* and *POLR1A* in a p53DD mutant background, overall E2F-1 protein levels still declined. These results indicate that down-regulation of E2F-1 expression after *POLR1A* silencing is not just a consequence of changes in cell cycle progression and regulation by pRb and other E2F-1 regulators must be involved.

MDM2 is known to bind E2F-1 in human cancer cells (PC3 and DU145 prostate cancer cells) and to protect it from proteasome-dependent degradation by displacing SCF^{SKP2}, the E2F-1 E3 ligase, in a p53-, $p14^{Arf}$-, and pRb-independent manner (Zhang et al. 2005). Donati et al. (2011) focused on discerning the role of RpL11, because it is an important regulator of MDM2 (Zhang et al. 2004). Silencing of *RPL11* caused an increase in POLR1A expression, likely as a consequence of *Myc* activation (Donati et al. 2011; Dai et al. 2007). In p53-mutant (HCT-116 p53DD) cells treated with siRNAs to deplete both *RpL11* and *POLR1A* mRNA levels, E2F-1 protein levels did not change. These results contrast with those presented above; recall that in cells expressing RpL11, POLR1A depletion caused a significant decrease of E2F-1 protein levels. Therefore, availability of RpL11 is necessary for the down-regulation of E2F-1 (Donati et al. 2011). The model presented by Donati et al. (2011) suggests that ribosomal stress releases RpL11 that then binds to MDM2 (Figure 1.4, A). Without an association with MDM2, E2F-1 becomes unstable and is eventually degraded, resulting in cell cycle arrest at G1 (Donati et al. 2011; Zhang et al.

FIGURE 1.4. p53-Independent Responses to Nucleolar Stress. (A) Donati et al. (2011) expressed RNAi to silence *POLR1A*, a subunit of Pol I, in order to mimic nucleolar stress in p53-deficient HCT-110 human cancer cells. Donati et al. (2011) propose a model in which, during perturbations in ribosome biogenesis, modeled by silencing of POLR1A, RpL11 is released from ribosomes and subsequently associates with MDM2. The E2F-1-MDM2 interaction is severed, leading to proteasomal degradation of E2F-1 and cell cycle arrest. (B) In $p53^{-/-}$ erythroid cells, PIM1 kinase normally associates with RpS19. PIM1 kinase also phosphorylates the cell cycle inhibitor $p27^{Kip1}$ at Thr157, thus marking it for degradation, allowing normal cell cycle progression. Iadevaia et al. (2010) disrupted the RpS19/PIM1 kinase interaction, either by expressing RNAi against RpS19 or applying treatments known to induce nucleolar stress in human erythroleukemic TF-1 ($p53^{+/+}$) and K562 ($p53^{-/-}$) cell lines. PIM1 kinase, being unable to associate with the small subunit of the ribosome, is degraded, allowing $p27^{Kip1}$ stabilization, cell cycle arrest, and apoptosis, even in K562 ($p53^{-/-}$) cells (Iadevaia et al. 2010). (C) Russo et al. (2013) overexpressed RpL3 in order to mimic a disruption of ribosome biogenesis. Upon RpL3 overexpression, a multi-protein complex containing RpL3, Sp1, and NPM formed at the *p21* gene promoter, activating its expression, which resulted in cell cycle arrest or apoptosis. (D) Arf functions as a negative regulator of ribosome biogenesis. In $Arf^{+/+}$ murine embryonic fibroblasts (MEFs), Arf associates with DDX5, a DEAD-box RNA helicase, sequestering it in the nucleoplasm, allowing normal ribosome production. In $Arf^{-/-}$ MEFs, DDX5 localizes to the rDNA promoters in the nucleolus, resulting in increased ribosome production. In $p53^{-/-}$, $Mdm2^{-/-}$, $Arf^{-/-}$ MEFs, exogenous expression of HA-Arf resulted in reduced ribosome production once again (Saporita et al. 2011).

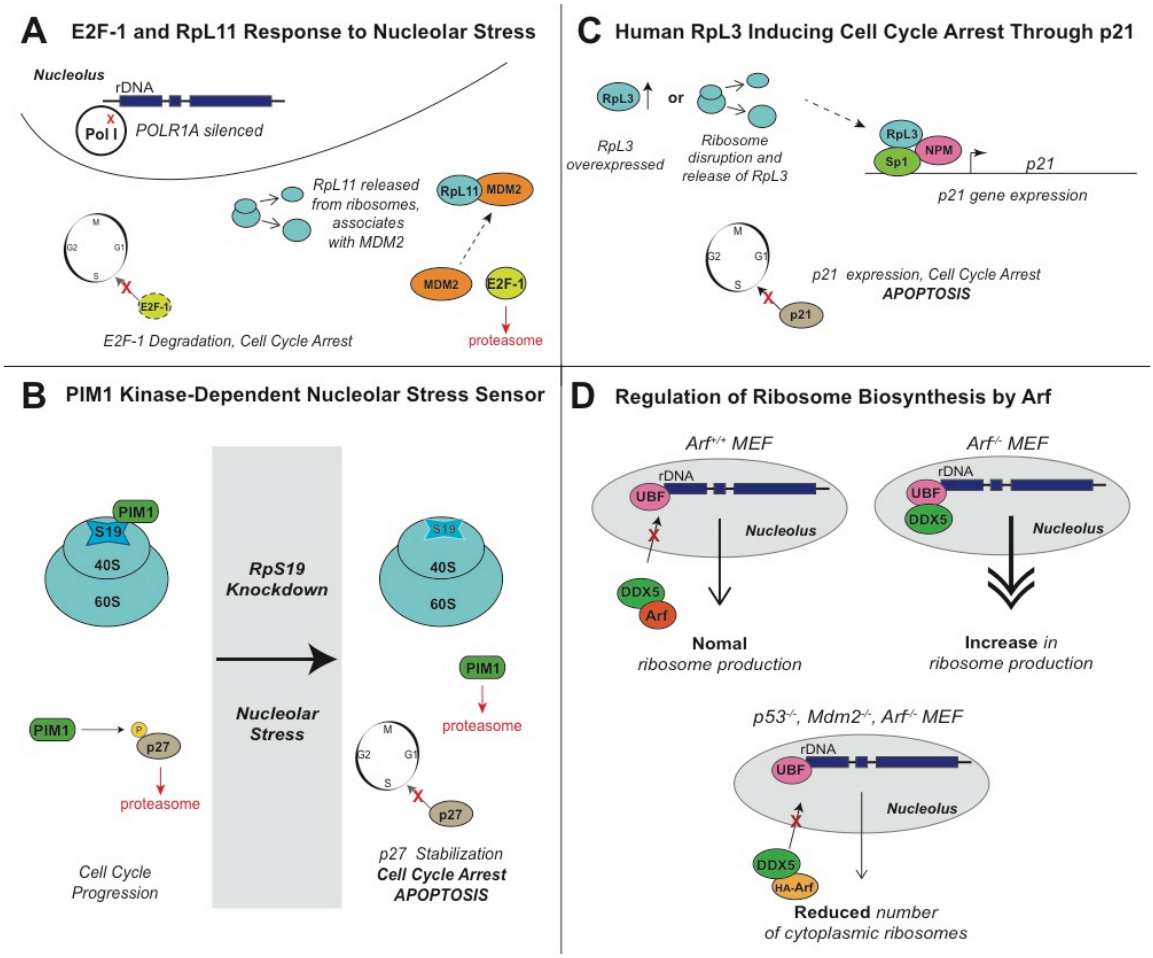
A E2F-1 and RpL11 Response to Nucleolar Stress
Nucleolus
rDNA
Pol I
POLR1A silenced
RpL11 released from ribosomes, associates with MDM2
RpL11
MDM2
MDM2
E2F-1
proteasome
E2F-1 Degradation, Cell Cycle Arrest
C Human RpL3 Inducing Cell Cycle Arrest Through p21
RpL3
or
RpL3 overexpressed
Ribosome disruption and release of RpL3
RpL3
NPM
Sp1
p21
p21 gene expression
p21
p21 expression, Cell Cycle Arrest
APOPTOSIS
B PIM1 Kinase-Dependent Nucleolar Stress Sensor
PIM1
S19
40S
60S
RpS19 Knockdown
Nucleolar Stress
PIM1
p27
proteasome
Cell Cycle Progression
S19
40S
60S
PIM1
proteasome
p27
p27 Stabilization
Cell Cycle Arrest
APOPTOSIS
D Regulation of Ribosome Biosynthesis by Arf
Arf+/+ MEF
rDNA
UBF
Nucleolus
DDX5
Arf
Nomal
ribosome production
Arf-/- MEF
rDNA
UBF
DDX5
Nucleolus
Increase in
ribosome production
p53-/-, Mdm2-/-, Arf-/- MEF
rDNA
UBF
Nucleolus
DDX5
HA-Arf
Reduced number
of cytoplasmic ribosomes

2005). In summary, Donati et al. (2011) demonstrated that the inhibition of rRNA synthesis down-regulates the expression of E2F-1, which in cells lacking p53, hinders cell cycle progression in a pRb-dependent manner. Degradation of E2F-1 results from its release from MDM2; instead, RpL11 binds MDM2 during the ribosomal stress response.

While considering the study by Donati et al. (2011), it is important to note that an inhibition in rRNA synthesis is not always associated with the down-regulation of E2F-1. Previous studies investigating the link between nucleolar stress and the cell cycle have found that treatment with certain DNA-damaging drugs (actinomycin D, cisplatin, or etoposide) causes an accumulation of E2F-1 (Lin et al. 2011; Stevens et al. 2003). However, in current efforts to develop anti-neoplastic drugs that target p53-deficient cancer cells, the ability to specifically target Pol I activity, reduce rRNA synthesis, and down-regulate E2F-1 to induce cell cycle arrest without genotoxic effects should prove most useful, in essence preventing new mutations that may give these cancer cells an ability to evade cell death (Donati et al. 2011).

Besides E2F-1 and Rb, other regulators affect p53-independent nucleolar stress. For example, PIM1 is a constitutively active serine/threonine kinase involved in cell cycle regulation and apoptosis (Wang et al. 2001; Bachmann and Moroy 2005). Yeast two-hybrid screens and co-immunoprecipitation experiments showed that PIM1 interacts with RpS19 and co-sediments with ribosomes in sucrose gradients (Chiocchetti et al. 2005). Iadevaia et al. (2010) examined the PIM1/ribosome interaction by expressing RNAi against RpS19 or by applying

treatments (such as actinomycin D, camtothecin, and cisplatin) to disrupt ribosome synthesis in human erythroleukemic TF-1 ($p53^{+/+}$) and K562 ($p53^{-/-}$) cell lines. They then measured the resulting expression of PIM1 (Figure 1.4, B), and showed that nucleolar stress caused a drop in PIM1 protein levels due to proteasomal degradation. With the loss of PIM1, levels of the cell cycle inhibitor $p27^{Kip1}$ increased with a corresponding block in cell division, even in $p53^{-/-}$ cells (K562 cells) (Iadevaia et al. 2010). PIM1 kinase phosphorylates Threonine-157 in $p27^{Kip1}$, marking the protein for degradation (Larrea et al. 2009). Indeed, lower levels of Thr157-phosphorylated $p27^{Kip1}$ were present after PIM1 destabilization in both $p53^{+/+}$ and $p53^{-/-}$ cells as measured by immunoblot. Therefore, a decrease of PIM1 activity leads to stabilization and accumulation of $p27^{Kip1}$ and consequently cell cycle arrest regardless of the p53 status of the cell. It is currently unclear if PIM1-dependent sensing of nucleolar stress acts independently or concurrently with known p53-dependent pathways (Iadevaia et al. 2010).

Another example involves PeBoW, the nucleolar complex in mammalian cells that plays an essential role in processing pre-rRNA during 60S ribosomal subunit assembly. The complex is comprised of pescadillo (Pes1), Bop1 (block of proliferation), and WDR12 (WD repeat) proteins (Lapik et al. 2004; Grimm et al. 2006). In a study linking the function of pescadillo to human breast cancer, Li et al. (2009) surveyed seven breast cancer cell lines, all of which demonstrated up-regulation of pescadillo at the mRNA and protein levels compared to normal breast epithelial tissue. Knockdown of pescadillo expression by RNAi in both

p53$^{-/-}$ (MDA-MB-435) and *p53*$^{+/+}$ (ZR-75-30) breast cancer cells led to an inhibition of cell division and to a decrease in the cells' colony forming ability on soft agar (Li et al. 2009). Pescadillo depletion also led to decreased expression of the cell cycle protein cyclin D1, up-regulation of the CDK inhibitor $p27^{Kip1}$, and consequent reduction of pRb phosphorylation, which led to cell cycle arrest in both *p53*$^{-/-}$ and *p53*$^{+/+}$ breast cancer cell lines (Li et al. 2009).

1.7.2 Drug induced nucleolar stress in the absence of p53

More than 50% of human cancers lack functional p53 (Soussi et al. 2000). For instance, deletion of *p53* has been reported in 10% of newly diagnosed multiple myeloma (MM) tumors; also, the occurrence of a *p53* deletion is much greater in advanced and extra-medullary tumors, which correlates with a poor prognosis (Avet-Loiseau et al. 2007; Jakubowiak et al. 2013). Therefore, drugs that trigger cell death in *p53*-null cells could have great potential in the treatment of many cancers. As cyclin dependent kinases (CDKs) represent a large family of proteins that regulate the cell cycle and transcription (Malumbres et al. 2009), small molecule multi-targeted CDK inhibitors (CDKIs) have shown anti-tumor activity regardless of the p53 status of the tumor cell. The compound RGB-286638, a new type of indenopryazole family of cyclin dependent kinase (CDK) inhibitors, is potent against transcriptional-type CDKs in both *p53*-wild type and *p53*-null MM cells (Cirstea et al. 2013).

To investigate the dose- and time-dependent effects of RGB-286638 treatment, Cirstea et al. (2013) used both *p53*-wild type (MM.1S, MM.1R, and H929) and *p53*-null MM cells (U266, OPM1, RPMI). Cell viability was measured

48 hours after a 50 nM RGB-286638 treatment; *p53*-wild type cells (MM1.S, which had p53 stabilization and activation) were slightly more sensitive to the treatment than *p53*-null cells. Apoptosis was induced in both *p53*-wild type and *p53*-null cells, as measured by cleavage of PARP and activation of caspases-8, -9, and -3 after a 4-hour treatment with RGB-286638. Expression of shRNA to knock down p53 function in MM.1S cells led to a partial rescue of apoptosis (14% of cells), suggesting that p53 does have some role in RGB-286638-induced cell death. RGB-286638 treatment (50 nM) of *p53*-mutant cells caused a reduction in total RNA synthesis after 2 hours and a larger, significant reduction after 24 hours as measured by [^{3}H]-uridine incorporation. Additionally, RGB-286638 treatment (50 nM) of *p53*-wild type cells for 3 hours triggered formation of numerous nuclear speckles as seen by immunofluorescence, which is indicative of nucleolar segregation. These results indicate that the CDK inhibitor, RGB-286638 can induce cell death in *p53*-wild type MM cells by activation of p53, as well as in *p53*-null MM cells through p53-independent mechanisms. Significant advances in targeting cancer cells that lack functional p53 requires a thorough understanding of predictably latent, more ancestral mechanisms that lead to cell cycle arrest or apoptosis in the absence of p53.

1.7.3 p53-independent autophagy

Autophagy is a pro-survival process that involves sequestration of cytoplasm into membrane bound vesicles that fuse with lysosomes resulting in the recycling of cellular components (Mizushima and Komatsu 2011). Boglev et al. (2013) reported a newly discovered link between nucleolar stress and the

induction of autophagy, which occurs in a p53-independent manner. Boglev et al. (2013) described the novel zebrafish mutant *titania* (*tti*^{s450}), a recessive lethal mutation located in *pwp2h,* the gene that encodes a subunit of the small ribosomal subunit processome. Pwp2h is especially necessary for 18S rRNA maturation during ribosome biogenesis. In yeast, Pwp2h was shown to be an essential scaffold component of the 90S pre-ribosomal processome, aiding in the interaction of proteins between the U3 snoRNP and the 5' end of pre-rRNA (Baserga 1997; Dosil and Bustelo 2004). *titania*^{s450} larvae exhibit defects in intestinal, liver, pancreas, and craniofacial development. Northern blots and polysome profiles using *titania*^{s450} larvae showed an accumulation of rRNA processing intermediates and a reduction of 40S subunits and 80S monosomes, respectively (Boglev et al. 2013). These results support previous findings that Pwp2h is necessary for proper maturation of the small ribosomal subunit. Transmission electron microscopic comparisons of intestinal epithelial tissues between *titania*^{s450} and wild type larvae indicated the presence of autophagosome- and autolysosome-like structures present in *titania*^{s450} larvae. Immunohistochemical studies were also conducted using mCherry-LC3III, the membrane-bound mammalian orthologue of Atg8a and a robust marker for autophagosome formation (Boglev et al. 2013). The results of this experiment confirmed the TEM results, showing intestinal epithelial cells that had lost Pwp2h function experienced significantly more autophagy compared to similar wild type tissues. Autophagy induction in *titania*^{s450} larvae extends their lifespan and prolongs the survival of the intestinal cells (Boglev et al. 2013). Expression of a

p53 mutant, which is unable to bind DNA, failed to rescue the autophagy phenotype in *titania*^{s450} larvae. Autophagy induction in *titania*^{s450} larvae is also independent of the level of activation of the Tor pathway and the levels of RpS6, a downstream target of Tor activity (Boglev et al. 2013). From this study, we can conclude that autophagy is a survival mechanism that can be induced by ribosomal stress, even in p53- and Tor- independent manners. In the context of cancer research, it is important to consider that certain therapeutic agents may promote autophagy, contributing to cancer cells' evasion of cell death (Boglev et al. 2013).

1.7.4 Role of ribosomal proteins in p53-independent nucleolar stress

c-Myc is a master regulator of cell division, as it controls the transcription of all three RNA polymerases and therefore affects all steps in ribosome biogenesis. c-Myc facilitates the recruitment of SL1 to Pol I promoters and controls expression of UBF, which is essential for Pol I transcription (Poortinga et al. 2004). c-Myc also facilitates expression of ribosomal proteins by increasing Pol II transcription and enhances Pol III activity by interacting with TFIIIB (van Riggelel et al. 2010). When over-expressed, RpL11 binds both c-Myc and its mRNA, which promotes degradation of this mRNA, thus revealing an elegant auto-regulatory feedback mechanism as c-Myc also activates expression of RpL11 (Dai et al. 2007). Over-expression of RpL11 was used to mimic what can occur in cells during ribosomal stress; specifically, excess RpL11 is available to bind proteins involved in the stress response (Bursać et al. 2012). RpL11 and c-Myc were expressed from a recombinant adenovirus, and BrdU incorporation

was used to monitor cell cycle progression (Dai et al. 2007). While over-expression of c-Myc alone significantly increased the number of U2OS cells undergoing DNA synthesis as expected, co-expression of RpL11 and c-Myc reduced the number of cells in S phase, suggesting that excess RpL11 hindered c-Myc function. The same experiment using *p53*-null MEF cells also generated RpL11-dependent cell cycle arrest. Immuno-precipitation analysis revealed that c-Myc and RpL11 interact in both *Arf*-null U2OS cells and in *p53*$^{-/-}$*mdm2*$^{-/-}$ MEF cells. On the other hand, transient RNAi depletion of RpL11 led to an increase in c-Myc protein levels (Dai et al. 2007). RpL11 may also inhibit c-Myc activity by preventing the recruitment of its co-activator, TRRAP, to c-Myc target genes transcribed by Pol I and Pol II (Dai et al. 2007). These findings suggest an expanded role of RpL11, beyond its well-studied interaction with MDM2 during ribosomal stress leading to p53 activation and apoptosis (described above).

RpL11 is not the only ribosomal protein reported to have extra-ribosomal function during p53-independent nucleolar stress. Russo et al. (2013) described a new p53-independent role for RpL3 in modulating cell cycle progression through its positive regulation of p21 expression (Figure 1.4, C). p21 is a main inhibitor of cyclin dependent kinases and its p53-dependent expression results in cell cycle arrest at the G1/S phase transition. Russo et al. (2013) over-expressed RpL3 in an attempt to mimic situations of altered ribosome biogenesis. As mentioned before, during nucleolar stress, certain ribosomal proteins can accumulate either by *de-novo* synthesis or by protection from degradation when ribosomes disassemble (Bursać et al. 2012; Fumagalli et al. 2009; Sun et al.

2008). In human Calu-6 cells, which lack a functional p53, over-expression of RpL3 led to a corresponding dose-dependent increase in *p21* expression as measured by RT-PCR (Russo et al. 2013). ChIP assays suggested that RpL3 interacts with the promoter of p21, but mobility shift assays (EMSA) revealed that RpL3 does not bind to the promoter directly, so other factors must be involved (Russo et al. 2013). ChIP assays identified nucleophosmin (NPM), a regulator of RpL3 alternative splicing, and Sp1, a known regulator of *p21* expression, present at the *p21* gene promoter with RpL3 (Figure 1.4, C) (Russo et al. 2013; Russo et al. 2011; Kutsodontis et al. 2002). In addition, luciferase expression assays engineered with the Sp1 promoter showed that RpL3 and Sp1 expression had a greater positive effect on *p21* expression than did expression of either RpL3 or Sp1 alone (Russo et al. 2013). These data suggest a model in which over-expression of RpL3 causes the formation of a multi-protein complex containing at minimum RpL3, NPM, and Sp1; this complex binds to the *p21* promoter, causing an up-regulation of *p21* expression thus leading to either cell cycle arrest or mitochondrial-dependent apoptosis (Figure 1.4, C) (Russo et al. 2013).

1.7.5 p53-independent functions of Arf

$p19^{Arf}$ (Arf) functions as a tumor-suppressor in mammals, but it also functions in the regulation of ribosome biogenesis; specifically, Arf regulates nucleolar export of nucleophosmin (NPM1) as well as MDM2, suggesting that it plays a role as a nucleolar stress sensor or monitor of nucleolar function (Brady et al. 2004). Sugimoto et al. (2003) demonstrated that nucleolar Arf inhibits pre-rRNA processing, retarding the processing of 47/45S and 32S precursors. This

experiment was conducted using NIH-3T3 cells, which lack endogenous *Ink4a-Arf* alleles, so exogenous Arf was expressed using a zinc-inducible metallothionin promoter. Arf's interference with pre-rRNA processing and its interaction with the 5.8S rRNA require the N-terminus of Arf, but neither MDM2 nor p53 (Sugimoto et al. 2003). However, this finding did not quite elucidate the mechanism by which Arf regulates rRNA processing.

To approach this mechanism, Saporita et al. (2011) performed a proteomics screen using wild type and *Arf*$^{-/-}$ mouse embryonic fibroblasts (MEFs) to determine how levels of Arf might affect nucleolar composition and function. DDX5, a DEAD-box RNA helicase (also known as p68), was among the proteins enriched in the nucleolus upon Arf depletion. There, it associates with UBF at rDNA promoter sites (O'Sullivan et al., 2002). Arf prevents DDX5 from localizing to nucleoli in a p53-independent fashion (Figure 1.4, D) (Saporita et al. 2011). In the *Arf*$^{-/-}$ MEFs, DDX5 occupancy at rDNA promoters was 2-fold greater than that in wild type cells. DDX5 localization at rDNA promoters resulted in an increase in rRNA synthesis and processing. Increased production of 47S rRNA transcripts still occurred upon expression of an ATP-binding mutant of DDX5, therefore the helicase activity of DDX5 is not necessary for enhanced Pol I transcription. Conversely, knockdown of DDX5 by shRNA reduced cell division of *Arf*$^{-/-}$ and *p53*$^{-/-}$ MEFs. To further investigate p53-independent functions of Arf, the authors used a triple knockout MEF line (*p53*$^{-/-}$, *Mdm2*$^{-/-}$, *Arf*$^{-/-}$), thus eliminating the entire Arf-MDM2-p53 cascade. Expression of HA-tagged Arf in these cells resulted in a reduced number of cytoplasmic ribosomes in the polysome fraction of sucrose

gradients (Figure 1.4, D). These results are consistent with earlier observations indicating Arf actually inhibits ribosome biogenesis in a p53-independent manner. Saporita et al. (2011) concluded that Arf acts to protect against non-oncogene driven ribosome biogenesis in order to prevent cell transformation.

1.7.6 p53-independent nucleolar stress in *Drosophila melanogaster*

To this point, our discussion has described p53-independent nucleolar (ribosomal) stress in vertebrate (mammalian) cells where the p53-independent pathways remain minor compared to the preferred MDM2- and p53-dependent pathways. *C. elegans* and *Drosophila* express p53, but they lack MDM2 and Arf, so nucleolar stress in these organisms is necessarily quite different than in mammalian cells. Is p53 required for nucleolar stress in *Drosophila*? If p53 is not required for nucleolar stress in *Drosophila*, what forms of nucleolar stress occur in *Drosophila*, and how are they activated? If similar mechanisms still exist in mammalian cells but remain latently silent, can oncologists one day induce these pathways as therapies to target cancer cells that lack p53?

1.7.7 Functions of p53 in *Drosophila melanogaster*

In vertebrates, the p53 paralogs p63 and p73 present a challenge in studying p53 function (Stiewe 2007). *D. melanogaster*, however, contains one *p53* gene (*Dp53*) within the haploid genome, and it is highly conserved in gene structure compared to mammalian p53. The single *Dp53* gene, however, contains two alternative promoters that can give rise to three possible protein isoforms: Dp53, DΔNp53 (discovered first), and Dp53ΔC (the third of which has not been experimentally confirmed) (Marcel et al. 2011). *Dp53*-null flies are

viable and fertile. Apart from a defect in primordial germ cells, no developmental defects are observed in these *Dp53*-null flies (Brodsky et al. 2004; Yamada et al. 2008). While conserved in sequence, the activation of Dp53 in flies is quite different than activation of p53 in mammalian cells. There are no obvious MDM2 homologues in *D. melanogaster*, suggesting that either Dp53 is not regulated by protein turnover, or the sequence of the fly homolog of MDM2 is too dissimilar from its mammalian counterpart to have been identified already by sequence searches (Brodsky et al. 2004). Additionally, Dp53 does not contain a conserved MDM2 binding domain like mammalian p53, supporting the fact that Dp53 is not regulated by MDM2 association and protein degradation as it is in mammals (Sekelsky et al. 2000).

The consequence of activating Dp53 in *D. melanogaster* is also quite different than activating p53 in mammals; Dp53 is unable to induce cell cycle arrest upon radiation treatment nor is it able to activate *decapo*, the gene encoding the p21 homolog (Brodsky et al. 2004; Ollmann et al. 2000; Akdemir et al. 2007; Brodsky et al. 2000). While cell cycle control may not respond to Dp53, the pro-apoptotic function of Dp53 seems to be conserved, as both Dp53 and DΔNp53 are capable of activating apoptosis, but through distinct mechanisms involving different pro-apoptotic regulators, reaper, hid and grim, that are often referred to the RHG proteins. The RHG proteins are pro-apoptotic, because they inhibit *Drosophila* Inhibitor of Apoptosis (DIAP). Over-expression of Dp53 selectively induced robust expression of *reaper* while expression of DΔNp53 preferentially induced *hid* expression (Dichtel-Danjoy et al. 2013).

1.7.8 p53-independent nucleolar stress in *D. melanogaster*.

As described above, TIF-IA is a critical transcription initiation factor for RNA Pol I, and as in mammals it is required for ribosome biogenesis in *Drosophila* (Grewal et al. 2007). In flies, loss of TIF-IA induces p53-independent phenotypes; *tifia*$^{-/-}$ *p53*$^{-/-}$ had the same growth arrest as *tifia*$^{-/-}$ larvae. This finding contrasts with studies using mammalian cells, where cell cycle arrest and apoptosis caused by the loss of TIF-IA could be rescued upon genetic loss of p53 (Yuan et al. 2005).

Brodsky et al. (2004) described a DNA damage-induced pathway that arrests the cell cycle and initiates apoptosis in *Drosophila*. After treating larval imaginal eye and wing discs with ionizing radiation (IR), Dp53 protein levels did not change, but its phosphorylation pattern changed; this phosphorylation is sufficient for its activation (Brodsky et al. 2004). MNK (Chk2 in *Drosophila*) is required for IR-induced phosphorylation/activation of Dp53, and MNK along with Dp53 are required for IR-induced gene expression in *Drosophila* (Brodsky et al. 2004). Microarray and qPCR methods identified several genes activated by IR treatment. Reaper, Sickle, and Hid (the RHG proteins) were up regulated within 30 minutes of IR treatment. Mutant *Dp53*$^{-/-}$*, MNK*$^{-/-}$ cells failed to activate apoptosis and gene expression upon IR treatment, suggesting that MNK is required for phosphorylation of p53 following IR-induced damage. As visualized by an antibody specific for mitotic cells (anti-histone H3), IR-induced cell cycle arrest at G2 still occurred in Dp53-deficient cells (Brodsky et al. 2004). Also, *decapo* (p21 homolog) was repressed following IR treatment of Dp53-deficient

cells, adding evidence to previous reports that Dp53 is not necessary for cell cycle arrest at G2 (Brodsky et al. 2004). On the other hand, ATR and GPRS (Chk1 in *Drosophila*) were necessary for G2 cell cycle arrest upon IR treatment (Brodsky et al. 2004).

Brodsky et al. (2004) also observed that IR induced a p53-independent decrease in the mRNA levels of at least 17 genes, many of which were developmental regulators. The authors favor a model that includes MNK (Chk2)-dependent cell cycle delay upon IR treatment with developmental gene induction as a secondary effect (Brodsky et al. 2004). They conclude that MNK activates diverse pathways including Dp53-dependent gene expression. The phosphorylation of p53 by MNK (Chk2) is conserved among metazoans. MNK, however, has Dp53-independent roles as well. For meiotic checkpoint regulation, MNK activation requires MEI-41 (ATR) (Brodsky et al. 2004). MNK, but not p53, is also necessary for damage-induced inactivation of centrosomes (Takada et al. 2003). The presence of MDM2 in mammals likely adds an evolutionarily advanced layer of control over p53 timing and function (Brodsky et al. 2004).

McNamee and Brodsky (2009) also described a Dp53-independent, but JNK- and HID-dependent apoptotic pathway that was activated after ionizing radiation (IR) treatment, which likely caused a haplo-insufficiency of ribosomal proteins. In flies, ribosomal protein genes are spread throughout the genome (Perrin et al. 1998), therefore chromosomal breaks prior to mitosis often cause segmental aneuploidy of the ribosomal protein genes resulting in a *Minute* phenotype in the daughter cells. McNamee and Brodsky (2009) treated larval

wing discs with ionizing radiation (IR), and then counted the number of shorter, thinner *Minute* bristles after the adult flies eclosed. There was no difference in the number of defective (*Minute*) bristles after IR treatment and in several lines that either harbored $Dp53^{-/-}$ or $Dp53^{+/+}$ genotypes. Thus, Dp53 function was not necessary for the elimination of cells that were haplo-insufficient for ribosomal protein genes (the *Minute* phenotype).

Phenotypes normally associated with the *Minute* phenotype involve increased activity of c-Jun N-terminal kinase (JNK) and Brinker (brk, the upstream kinase and activator of JNK), and reduced expression of the survival factor *decapentaplegic* (*dpp*) (Moreno et al. 2002; Tyler et al. 2007). Indeed, *brk* expression was observed in wild type cells 4 hours after IR treatment, which was sufficient to activate JNK-dependent apoptosis (McNamee and Brodsky 2009; Martin et al. 2004).

McNamee and Brodsky (2009) also monitored the activity of JNK after IR treatment of imaginal disc cells. An important downstream target of JNK signaling is *puckered* (*puc*), which encodes the JNK phosphatase that acts as a repressor of JNK function, forming a negative regulatory loop. Recall, IR-treated cells likely have mutations in genes encoding ribosomal proteins, which, as described earlier, would be considered *Minute* mutations. JNK activity in these cells can be modulated by way of changing *puc* expression. There was a 3- to 4-fold increase in apoptosis in $puc^{-/+}$, $p53^{-/-}$ mutant wing discs compared to $puc^{+/+}$, $p53^{-/-}$ cells at 16 to 24 hours following IR treatment as visualized by anti-cleaved caspase staining. So, with only one functional copy of *puc* present, JNK activity was

increased in *p53*$^{-/-}$ cells, and apoptosis was able to proceed more efficiently. Conversely, over-expression of *puc* led to greater negative regulation on JNK activity, reduced *hid* expression, and apoptosis. These results indicate that the JNK pathway plays an important role in the elimination of *Minute* wing disc cells upon IR treatment. JNK activates the transcription of *hid* (which then leads to activation of the caspase pathway, including caspase-3). Therefore p53-independent apoptosis utilizes the same core apoptotic machinery that is activated in most *Drosophila* cell stress and developmental signals (McNamee and Brodsky 2009).

McNamee and Brodsky (2009) further investigated cell cycle regulation along with reducing the level of negative feedback signaling after IR treatment of wing discs. *Drosophila grp* is the *Chk1* kinase homolog (Fogarty et al. 1997). Triple mutant wing discs (*grp*$^{-/-}$*, puc*$^{-/+}$*, Dp53*$^{-/-}$*)* displayed higher levels of apoptosis, as visualized by anti-caspase 3 staining, compared to either *grp*$^{-/-}$*, Dp53*$^{-/-}$ or *puc*$^{-/+}$*, Dp53*$^{-/-}$ double mutant wing discs (Takada et al. 2003). Therefore, decreasing the negative feedback signal from puc to JNK further increased the number of cells that underwent p53-independent apoptosis following IR (McNamee and Brodsky 2009). In *Dp53*$^{-/-}$ and *mnk*$^{-/-}$ mutant discs, IR-induced apoptosis was seen only after cells recovered from DNA-damage induced cell cycle delay (McNamee and Brodsky 2009). The apoptotic response was accelerated in these double mutant discs that failed to arrest at G2/M due to mutations in *grp (Chk1)*. Overall, these results suggest that cell cycle arrest helps

delay p53-independent activation of JNK signaling and apoptosis following IR (McNamee and Brodsky 2009).

McNamee and Brodsky (2009) concluded that this p53-independent pathway acts in parallel with the canonical DNA damage response pathway to eliminate cells with altered genomes following IR. Also, JNK activation acts as compensation upon loss of p53 to preserve genome integrity, and that JNK may be activated upon loss of certain genes, such as the ribosomal genes in aneuploid cells. In support of these conclusions, Titen and Golic (2008) reported that p53-independent apoptosis is activated upon telomere loss only if the resultant chromosome leads to aneuploidy.

1.7.9 Direct nucleolar stress responses induced in *Drosophila*

As described above, Nopp140 is an assembly nucleolar factor or chaperone for Box C/D and Box H/ACA snoRNP complexes that modify pre-rRNA during ribosome biogenesis. Loss of Nopp140 function upon expression of shRNA leads to several phenotypes in *D. melanogaster.* These include apoptosis within larval imaginal wing disc cells, autophagy of larval polyploid gut cells, an increase in activated phospho-JNK levels, a reduction of RpL23a and RpL34 protein levels as visualized by immuno-blot, reduction of cytoplasmic ribosomes as seen by TEM, and a reduction of protein synthesis as measured by metabolic labeling assays (Chapter 2, James et al. 2013). Apoptosis occurred after expressing *Nopp140-RNAi* within the larval wing discs as observed by immunofluorescence with an anti-cleaved caspase-3 antibody. The UAS-Gal4 system used to express Nopp140-RNAi in wing discs only is diagrammed in

Figure 1.5. When these larvae eclosed as flies, their wings showed a vestigial-like phenotype in which they were shriveled and blistered. Following the murine Treacher Collins study by Jones et al. (2008) in which nucleolar stress was rescued by the depletion of p53 (described above), we reasoned that blocking Dp53 function would rescue this wing phenotype.

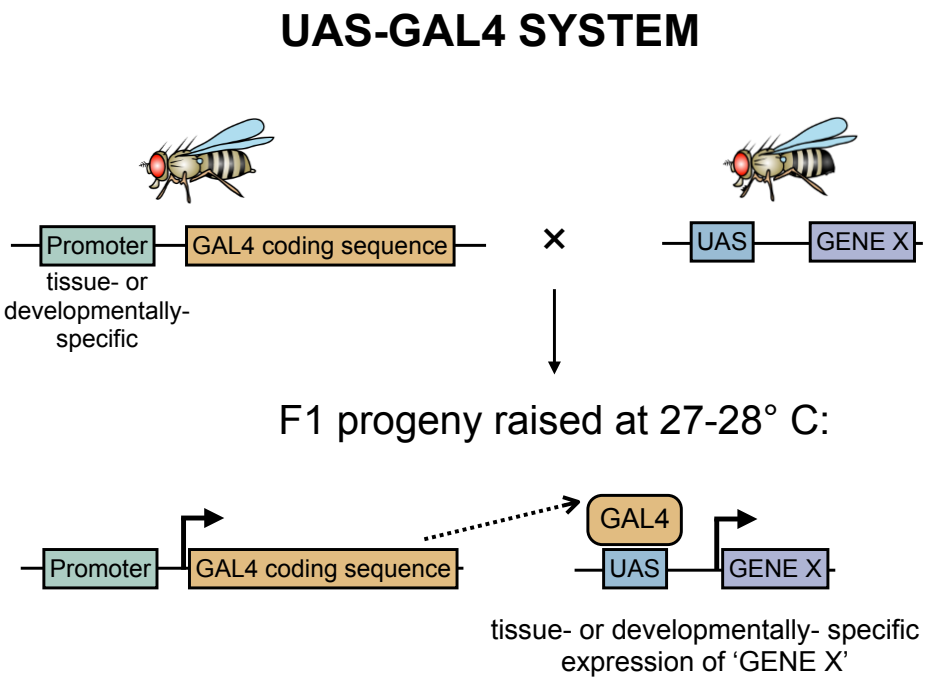

FIGURE 1.5. The UAS-GAL4 System in *D. melanogaster*: developed for temporal and spatial regulation of ectopically-expressed genes. Parent lines, one containing the GAL4 coding sequence under the regulation of a promoter sequence that is tissue- or developmental stage- specifically regulated and the other contains a "GENE X" sequence downstream of five upstream activating sequence (UAS) sites. In F1 progeny, both the *Promoter-GAL4* and *UAS-GENE X* constructs are present. UAS sites specifically allow GAL4 binding; GAL4 is a yeast transcription factor that when bound to the UAS sequence as a tetramer, activates the expression of "GENE X" only at temperatures near 27-28 °C. "GENE X" may be cDNA for the expression of a protein or encoding shRNA to knockdown the expression of a gene through RNAi. This system allows the expression of GENE X to occur either in certain tissues or at certain developmental stages, depending on the promoter used and the temperature at which the flies are kept. This system was developed by Brand and Perrimon (1993).

However, expressing *Nopp140-RNAi* in the *Dp53*$^{-/-}$ background failed to rescue the apoptosis in wing disc cells and the resulting shriveled (vestigial) wing phenotype. Thus, a Dp53-independent pathway involving JNK must activate apoptosis upon depletion of Nopp140. Our findings supported the observations of McNamee and Brodsky (2009).

1.8 Prospects and Conclusion

We have seen how ribosomal proteins in mammalian cells, released under nucleolar stress conditions, bind and suppress MDM2 leading to p53 stabilization and/or activation that then induces cell cycle arrest or apoptosis. Discovery of this phenomenon has rekindled our attempts at selectively inducing nucleolar stress in highly metabolic cancer cells, hopefully forcing these cells into cycle arrest or apoptosis while normal cells with reduced requirements for ribosome synthesis remain relatively unscathed. These are exciting times for nucleolar biologists as they work with structural biochemists and organic chemists to devise new drugs that specifically block ribosome biogenesis at the level of Pol I transcription or pre-rRNA processing in the hopes of inducing nucleolar stress as an effective cancer treatment. Many types of cancer cells, however, lack functional p53, and the question remains: can oncologists still use nucleolar stress as an effective strategy in treating these p53-minus cancers? We cited several examples of mammalian cells undergoing p53-independent cycle arrest upon nucleolar stress, but the detailed mechanisms of how this comes about remain sketchy. Future studies will likely reveal the details of p53-independent nucleolar stress mechanisms that either remain generally silent in mammalian

cells due to evolutionary emergence of the predominant MDM2-p53 pathway, or are active in mammalian cells but have simply gone unrecognized. A careful examination of nucleolar stress in non-mammalian systems such as yeast that lacks p53 or *C. elegans* and *Drosophila* that express p53 but lack MDM2, may reveal conserved aspects of p53-independent nucleolar stress pathways throughout the eukaryotes. Our full understanding of these p53-independent pathways may likewise reveal targets for effective cancer treatments.

1.9 Scope and Aims of Thesis

The purpose of this thesis is to present newly ascribed functions of Nopp140, a nucleolar and Cajal Body protein in *D. melanogaster,* and the cellular response induced by nucleolar stress. As previously mentioned in this chapter, nucleolar stress is defined as any disturbance in the ribosome biogenesis pathway, which originates in the nucleolus. Basic research geared toward understanding the most fundamental cellular processes such as ribosome biogenesis is critical; still, we do not understand all the details of this intricate, yet necessary process. Every cell, especially those undergoing rapid cell cycle progression, has a huge demand for protein synthesis, and thus a functional ribosome biogenesis pathway. Utilizing *D. melanogaster* as a model organism, we are able to study the ribosome biogenesis pathway, which is common to metazoans.

Nopp140 is a proposed ribosome assembly factor, specifically participating in the shuttling of small nucleolar ribonucleoprotein (snoRNP) complexes from the Cajal body in the nucleoplasm to the nucleolus. Once in the

nucleolus, these snoRNPs where they modify certain nucleotides of pre-rRNA before their assembly with ribosomal proteins into the small and large ribosomal subunits. If Nopp140 function is lost, we hypothesized that the cell would not be able to make functional ribosomes, thus inducing nucleolar stress. We have mainly utilized loss-of-function techniques, including RNAi expression (Chapters 2 and 4) and gene knockout (Chapters 3 and 4), to assay the consequence of Nopp140 loss. The goal of this thesis is to describe phenotypes attributed to the loss of Nopp140 (induced nucleolar stress). Some phenotypes observed upon loss of Nopp140 (and described in Chapters 2 and 3 of this thesis) include a loss of 2'-*O*-methylation of certain rRNA nucleotides, a reduction of cytoplasmic ribosomes as observed by TEM and an organism-wide reduction in protein synthesis, cell stress responses including autophagy in polyploid gut cells and apoptosis in diploid imaginal discs, and lethality in the 2nd or 3rd larval instar stages. Chapter 4 describes more recent efforts that involve knock-down of Nopp140 function in the eye discs and resultant development of the adult eye, gene knockout organism-wide to assay the expression of stress related genes (apoptosis and autophagy related), and over-expression of Nopp140 in the larval wing discs and the consequence of this on adult wing development. By studying phenotypes induced by loss- and gain-of-Nopp140 function, we can better understand the role Nopp140 has in ribosome biogenesis in *D. melanogaster*.

Expanding the scope of this work, our results can be applied to studies in human health. Human diseases attributed to perturbations in ribosome biogenesis are collectively referred to as Ribosomopathies (see section 1.6 of

this chapter). Recently, studies aimed at finding new cancer treatments have focused on inducing nucleolar stress, since cancer cells have such a high threshold for ribosomes (see section 1.5 of this chapter). Interestingly, our studies have revealed that certain diploid cell populations undergo p53-independent apoptosis upon loss of Nopp140 (induced nucleolar stress) (Chapter 2). This finding is significant, as up to 50% of human cancer cell types do not have a functional p53. However, many cancer drugs utilize the p53 pathway to induce cell death, so these drugs would not be effective in p53-null or p53-inactivated cancer cells. Perhaps our result has alluded to a latent p53-independent cell death program that involves the stress kinase JNK in human cells.

Chapter 5 summarizes the results of this thesis and describes future work aimed at identifying upstream activators of JNK during nucleolar stress.

1.10 References

Akdemir F, Christich A, Sogame N, Chapo J, Abrams JM (2007) p53 directs focused genomic responses in *Drosophila*. Oncogene 26:5184–5193. http://dx.doi.org/10.1038/sj.onc.1210328.

Andersen JS, Lam YW, Leung AKL, Ong A-E, Lyon CE, Lamond AI, Mann M (2005) Nucleolar proteome dynamics. Nature 433:77-83. http://dx.doi.org/10.1038/nature03207.

Andrews WJ, Panova T, Normand C, Gadal O, Tikhonova IG, Panov KI (2013) Old drug, new target: Ellipticines selectively inhibit RNA polymerase I transcription. J Biol Chem 288:4567-4582. http://dx.doi.org/10.1074/jbc.M112.411611.

Argentini M, Barboule N, Wasylyk B (2001) The contribution of the acidic domain of MDM2 to p53 and MDM2 stability. Oncogene 20:1267-1275. http://dx.doi.org/10.1038/sj.onc.1204241.

Armache JP, Jarasch A, Anger AM, Villa E, Becker T, Bhushan S, et al. (2010a) Cryo-EM structure and rRNA model of a translating eukaryotic 80S ribosome at 5.5-Å resolution. Proc Natl Acad Sci 107:19748-19753. http://dx.doi.org/10.1073/pnas.1009999107.

Armache JP, Jarasch A, Anger AM, Villa E, Becker T, Bhushan S, et al. (2010b) Localization of eukaryotic-specific ribosomal proteins in a 5.5- Å cryo-EM map of the 80S eukaryotic ribosome. Proc Natl Acad Sci 107:19754-19759. http://dx.doi.org/10.1073/pnas.1010005107.

Armistead J, Triggs-Raine, B (2014) Diverse diseases from a ubiquitous process: The ribosomopathy paradox. FEBS Lett. http://dx.doi.org/10.1016/j.febslet.2014.03.024.

Avet-Loiseau H, Attal M, Moreau P, Charbonnel C, Garban F, Hulin C, et al. (2007) Genetic abnormalities and survival in multiple myeloma: the experience of the Intergroupe Francophone du Myelome. Blood 109:3489–3495. http://dx.doi.org/10.1182/blood-2006-08-040410.

Avitabile D, Bailey B, Cottage CT, Sundararaman B, Joyo A, McGregor M, et al. (2011) Nucleolar stress is an early response to myocardial damage involving nucleolar proteins nucleostemin and nucleophosmin. Proc Natl Acad Sci 108:6145-6150. http://dx.doi.org/10.1073/pnas.1017935108.

Bachmann M, Moroy T (2005) The serine/threonine kinase Pim-1. Int J Biochem Cell Biol 37:726-730. http://dx.doi.org/10.1016/j.biocel.2004.11.005.

Bai B, Moore HM, Laiho M (2013) CRM1 and its ribosome export adaptor NMD3 localize to the nucleolus and affect rRNA synthesis. Nucleus 4:315-325. http://dx.doi.org/10.4161/nucl.25342.

Baserga R (1997) The path less traveled by. Endocrinology 138:2217-8. http://dx.doi.org/10.1210/en.138.6.2217.

Ben-Shem A, Garreau de Loubresse N, Melnikov S, Jenner L, Yusupova G, Yusopova M (2011) The structure of the eukaryotic ribosome at 3.0 Å resolution. Science 334(6062):1524-1529. http://dx.doi.org/10.1126/science.1212642.

Bhat KP, Itahana K, Jin, A, Zhang Y (2004) Essential role of ribosomal protein L11 in mediating growth inhibition-induced p53 activation. EMBO J 23:2402-2412. http://dx.doi.org/10.1038/sj.emboj.7600247.

Birnstiel ML, Wallace H, Sirlin JL, Fischberg M (1966) Localization of the ribosomal DNA complements in the nucleolar organizer region of *Xenopus laevis*. National Cancer Institute monograph 23:431-47.

Bleichert F, Baserga SJ (2007) The long unwinding road of RNA helicases. Mol Cell 27:339-52. http://dx.doi.org/10.1016/j.molcel.2007.07.014.

Boglev Y, Badrock AP, Trotter AJ, Du Q, Richardson EJ, Parslow AC, Markmiller SJ, Hall NE, de Jong-Curtain TA, Ng AY, et al. (2013) Autophagy induction is a Tor- and Tp53-independent cell survival response in a zebrafish model of disrupted ribosome biogenesis. PLoS Genetics 9:e1003279. http://dx.doi.org/10.1371/journal.pgen.1003279.

Boisvert F-M, van Koningsbruggen S, Navascués J, Lamond AI (2007) The multifunctional nucleolus. Nat Rev Mol Cell Bio 8:574-585. http://dx.doi.org/10.1038/nrm2184.

Boocock GRB, Morrison JA, Popovic M, Richards N, Ellis L, Durie PR, Rommens JM (2003) Mutations in SBDS are associated with Schwachman-Diamond syndrome. Nat Genet 33:97-101. http://dx.doi.org/10.1038/ng1062.

Boulon S, Westman BJ, Hutten S, Boisvert F-M, Lamond AI (2010) The nucleolus under stress. Mol Cell 40:216-227. http://dx.doi.org/10.1016/j.molcel.2010.09.024.

Brady, SN, Yu Y, Maggi LB, Weber JD (2004) ARF impedes NPM/B23 shuttling in an Mdm2-sensitive tumor suppressor pathway. Mol Cell Biol 24:9327-9338. http://dx.doi.org/10.1128/MCB.24.21.9327-9338.2004.

Brand A, Perrimon N (1993) Targeted gene expression as a means of altering cell fates and generating dominant phenotypes. Development 118:401-415.

Brodsky MH, Nordstrom W, Tsang G, Kwan E, Rubin GM, Abrams JM (2000) *Drosophila* p53 binds a damage response element at the *reaper* locus. Cell 101:103-113. http://dx.doi.org/10.1016/S0092-8674(00)80627-3.

Brodsky MH, Weinert BT, Tsang G, Rong YS, McGinnis NM, Golic KG et al. (2004) *Drosophila melanogaster* MNK/Chk2 and p53 regulate multiple DNA repair and apoptotic pathways following DNA damage. Mol Cell Biol 24:1219-1231. http://dx.doi.org/10.1128/MCB.24.3.1219-1231.2004.

Brooks CL, Gu W (2006) p53 ubiquitination: Mdm2 and beyond. Mol Cell 21:307–315. http://dx.doi.org/10.1016/j.molcel.2006.01.020.

Brown DD, Gurdon JB (1964) Absence of ribosomal RNA synthesis in the anucleate mutant of *Xenopus laevis*. Proc Nat Acad Sci USA 51:139-146.

Burger K, Mühl B, Harasim T, Rohrmoser M, Malamoussi, A, Orban M, Kellener M, Gruber-Eber A, Kremmer E, Hölzel M, Eick D (2010) Chemotherapeutic

drugs inhibit ribosome biogenesis at various levels. J Biol Chem 285:12416-12425. http://dx.doi.org/10.1074/jbc.M109.074211.

Bursać S, Brdovčak MC, Pfannkuchen M, Orsolić I, Golomb L, Zhu Y, Katz C, Daftuar L, Grabušić K, Vukalić I, Filić V, Oren M, Prives C, Volarević S (2012) Mutual protection of ribosomal proteins L5 and L11 from degradation is essential for p53 activation upon ribosomal biogenesis stress. Proc Natl Acad Sci 109:20467-20472. http://dx.doi.org/10.1073/pnas.1218535109.

Busch H, Smetana K (1970) The Nucleolus. Academic Press, New York.

Chakraborty A, Uechi T, Higa S, Torihara H, Kenmochi N (2009) Loss of ribosomal protein L11 affects zebrafish embryonic development through a p53-dependent apoptotic response. PLoS ONE 4:e4152. http://dx.doi.org/10.1371/journal.pone.0004152.

Chan HYE, Brogna S, O'Kane CJ (2001) Dribble, the *Drosophila* KRR1p homologue, is involved in rRNA processing. Mol Biol Cell 12:1409-1419. http://dx.doi.org/10.1091/mbc.12.5.1409.

Chen C-C, Greene E, Bowers SR, Mellone BG (2012) A role for the CAL1-partner modulo in centromere integrity and accurate chromosome segregation in *Drosophila*. PLoS One 7:e45094. http://dx.doi.org/10.1371/journal.pone.0045094.

Chen D, Zhang Z, Li M, Wang W, Li Y, Rayburn ER, Hill DL, Wang H, Zhang R (2007) Ribosomal protein S7 as novel modulator of p53-MDM2 interaction: binding to MDM2, stabilization of p53 protein, and activation of p53 function. Oncogene 26:5029-5037. http://dx.doi.org/10.1038/sj.onc.1210327.

Chen S, Seiler, J, Santiago-Reichelt M, Felbel K, Grummt I, Voit R (2013) Repression of RNA polymerase I upon stress is caused by inhibition of RNA-dependent deacetylation of PAF53 and SIRT7. Mol Cell 52:303-313. http://dx.doi.org/10.1016%2Fj.molcel.2013.10.010.

Chiocchetti A, Gibello L, Carando A, Aspesi A, Secco P, Garelli E et al. (2005) Interactions between RPS19, mutated in Diamond–Blackfan anemia, and the PIM-1 oncoprotein. Haematologica 90:1453-1462.

Cioce M, Boulon S, Matera AG, Lamond AI (2006) UV-induced fragmentation of Cajal bodies. The Journal of Cell Biology 175:401-13.

Cirstea IC, Gremer L, Dvorsky R, Zhang SC, Piekorz RP, Zenker M, Ahmadian MR (2013) Diverging gain-of-function mechanisms of two novel KRAS mutations associated with Noonan and cardio-facio-cutaneous syndromes. Human Molecular Genetics 22:262-70. http://dx.doi.org/10.1093/hmg/dds426.

Colombo E, Alcalay M, Pelicci PG (2011) Nucleophosmin and its complex network: a possible therapeutic target in hematological diseases. Oncogene 30:2595-2609. http://dx.doi.org/10.1038/onc.2010.646.

Colombo E, Bonetti P, Denchi EL, Martinelli P, Zamponi R, Marine J-C, Helin K, Falini B, Pelicci PG (2005) Nucleophosmin is required for DNA integrity and $p19^{Arf}$ protein stability. Mol Cell Biol 25:8874-8886. http://dx.doi.org/10.1128/MCB.25.20.8874-8886.2005.

Cong R, Das S, Bouvet P (2011) The multiple properties and functions of nucleolin. In: Olson MOJ (ed) The Nucleolus, Protein Reviews. Springer, New York, NY, pp 185-212. http://dx.doi.org/10.1007/978-1-4614-0514-6_9.

Cui Z, DiMario PJ (2007) RNAi knockdown of Nopp140 induces *Minute*-like phenotypes in *Drosophila.* Mol Biol Cell 18:2179-91. http://dx.doi.org/10.1091/mbc.E07-01-0074.

Dai M-S, Arnold H, Sun X-X, Sears R, Lu H (2007) Inhibition of c-Myc activity by ribosomal protein L11. EMBO J 26:3332-3345. http://dx.doi.org/10.1038/sj.emboj.7601776.

Dai M-S, Lu H (2004) Inhibition of MDM2 mediated p53 ubiquitination and degradation by ribosomal protein L5. J Biol Chem 279:44475-44482. http://dx.doi.org/10.1074/jbc.M403722200.

Dai M-S, Sun X-X, Lu H (2008) Aberrant expression of nucleostemin activates p53 and induces cell cycle arrest via inhibition of MDM2. Mol Cell Biol 28:4365-4376. http://dx.doi.org/10.1128/MCB.01662-07.

Dai M-S, Zeng SX, Jin Y, Sun X-X, David L, Lu H (2004) Ribosomal protein L23 activates p53 by inhibiting MDM2 function in response to ribosomal perturbation but not to translation inhibition. Mol Cell Biol 24:7654-7668. http://dx.doi.org/10.1128/MCB.24.17.7654-7668.2004.

Daniely Y, Dimitrova DD, Borowiec JA (2002) Stress-dependent nucleolin mobilization mediated by p53-nucleolin complex formation. Mol Cell Biol 22:6014-6022. http://dx.doi.org/10.1128/MCB.22.16.6014-6022.2002.

Danilova N, Sakamoto KM, Lin S (2010) Ribosomal protein L11 mutation in zebrafish leads to haematopoietic and metabolic defects. Br J Haematol 152:217-228. http://dx.doi.org/10.1111/j.1365-2141.2010.08396.x.

Dauwerse JG, Dixon J, Seland S, Ruivenkamp CAL, van Haeringen A, Hoefsloot LH, et al. (2011) Nat Genet 43:20-22. http://dx.doi.org/10.1038/ng.724.

Dichtel-Danjoy ML, Ma D, Dourlen P, Chatelain G, Napoletano F, Robin M, Corbet M, Levet C, Hafsi H, Hainaut P, et al. (2013) *Drosophila* p53 isoforms differentially regulate apoptosis and apoptosis-induced proliferation. Cell Death and Differentiation 20:108-16. http://dx.doi.org/10.1038/cdd.2012.100.

Dixon J, Edwards SJ, Anderson I, Brass A, Scambler PJ, Dixon MJ (1997) Identification of the complete coding sequence and genomic organization of the Treacher Collins syndrome gene. Genome Research 7:223-34.

Dixon J, Jones NC, Sandell LL, Jayasinghe SM, Crane J, Rey J-P, Dixon M, Trainor PA (2006) *Tcof1*/Treacle is required for neural crest cell formation and proliferation deficiencies that cause craniofacial abnormalities. Proc Nat Acad Sci USA 103:13403-13408. http://dx.doi.org/10.1073/pnas.0603730103.

Donati G, Brighenti E, Vici M, Mazzini G, Trere D, Montanaro L, et al. (2011) Selective inhibition of rRNA transcription down regulates E2F-1: a new p53-independent mechanism linking cell growth to cell proliferation. J Cell Sci 124:3017-28. http://dx.doi.org/10.1242/jcs.086074.

Donati G, Peddigari S, Mercer CA, Thomas G (2013) 5S ribosomal RNA is an essential component of a nascent ribosomal precursor complex that regulates the Hdm2-p53 checkpoint. Cell Rep 4:87-98. http://dx.doi.org/10.1016/j.celrep.2013.05.045.

Dosil M, Bustelo XR (2004) Functional characterization of Pwp2, a WD family protein essential for the assembly of the 90S pre-ribosomal particle. J Biol Chem 279:37385–37397. http://dx.doi.org/10.1074/jbc.M404909200.

Drygin D, Lin A, Bliesath J, Ho CB, O'Brien SE, Proffitt C, et al. (2011) Targeting RNA polymerase I with an oral small molecule CX-5461 inhibits ribosomal RNA synthesis and solid tumor growth. Cancer Res 71:1418-1430. http://dx.doi.org/10.1158/0008-5472.CAN-10-1728.

Drygin D, O'Brien SE, Hannan RD, McArthur GA, Von Hoff DD (2013) Targeting the nucleolus for cancer-specific activation of p53. Drug Discov Today. http://dx.doi.org/10.1016/j.drudis.2013.08.012.

Drygin D, Siddiqui-Jain A, O'Brien S, Schwaebe M, Lin A, Bliesath J, et al. (2009) Anticancer activity of CX-3543: a direct inhibitor of rRNA biogenesis. Cancer Res 69:7653-7661. http://dx.doi.org/10.1158/0008-5472.CAN-09-1304.

Du X, Rao MR, Chen XQ, Wu W, Mahalingam S, and Balasundaram D (2006) The homologous putative GTPase Grn1p from fission yeast and the human GNL3L are required for growth and play a role in processing of nucleolar pre-rRNA. Mol Biol Cell 17:460-474. http://dx.doi.org/10.1091/mbc.E05-09-0848.

Dutt S, Narla A, Lin K, Mullally A, Abayasekara N, Megerdichian C, et al. (2011) Haploinsufficiency for ribosomal protein genes causes selective activation of p53 in human erythroid progenitor cells. Blood 117: 2567-2576. http://dx.doi.org/10.1182/blood-2010-07-295238.

Ebert BL, Pretz J, Bosco J, Chang CY, Tamayo P, Galili N, Raza A, Root DE, Attar E, Ellis SR Golub TR (2008) Identification of RPS14 as a 5q- syndrome gene by RNA interference screen. Nature 451:335-339. http://dx.doi.org/10.1038/nature06494.

Ebert BL (2009) Deletion 5q in myelodysplastic syndrome: a paradigm for the study of hemizygous deletions in cancer. Leukemia 23:1252-1256. http://dx.doi.org/10.1038/leu.2009.53.

Edström JE, Grampand N, Schor N (1961) The intracellular distribution and heterogeneity of ribonucleic acid in starfish oocytes. J Biophys Biochem Cytol 11:549-557. http://dx.doi.org/10.1083/jcb.11.3.549.

Ellis SR (2014) Nucleolar stress in Diamond Blackfan anemia pathophysiology. Biochim Biophys Acta 1842:765-768. http://dx.doi.org/10.1016/j.bbadis.2013.12.013.

Farrar JE, Vlachos A, Atsidaftos E, Carlson-Donohoe H, Markello TC, Arceci RJ, Ellis SR, Lipton JM, Bodine DM (2011). Ribosomal protein gene deletions in Diamond-Blackfan anemia. Blood 118:6943-6951. http://dx.doi.org/10.1182/blood-2011-08-375170.

Finch AJ, Hilcenko C, Basse N, Drynan LF, Goyenechea B, Menne TF, Gonzalez Fernandez A, Simpson P, D'Santos CS, Arends MJ, et al. (2011) Uncoupling of GTP hydrolysis from eIF6 release on the ribosome causes Shwachman-Diamond syndrome. Genes and Development 25:917-29. http://dx.doi.org/10.1016/s0145-2126(11)70040-6.

Fogarty P, Campbell SD, Abu-Shumays R, de Saint Phalle B, Yu KR, Uy GL, et al. (1997) The *Drosophila grapes* gene is related to checkpoint gene *chk1*/*rad27* and is required for late syncytial division fidelity. Curr Biol 7:418-426. http://dx.doi.org/10.1016/S0960-9822(06)00189-8.

French SL, Osheim YN, Schneider DA, Sikes ML, Fernandez CF, Copela LA, Misra VA, Nomura M, Wolin SL, and Beyer AL (2008) Visual analysis of the yeast 5S rRNA gene transcriptome: regulation and role of La protein. Mol Cell Biol 28:4576-4587. http://dx.doi.org/10.1128/MCB.00127-08.

Fuhrman LE, Goel AK, Smith J, Shianna KV, Aballay A (2009) Nucleolar proteins suppress *Caenorhabditis elegans* innate immunity by inhibiting p53/CEP-1. PLoS Genetics 5:e1000657. http://dx.doi.org/10.1371/journal.pgen.1000657.

Fumagalli S, Di Cara A, Neb-Gulati A, Natt F, Schwemberger S, Hall J, Babcock GF, Bernardi R, Pandolfi PP, Thomas G (2009) Absence of nucleolar disruption after impairment of 40S ribosome biogenesis reveals an RpL11-translation-dependent mechanism of p53 induction. Nat Cell Biol 11:501-508. http://dx.doi.org/10.1038/ncb1858.

Ganapathi KA, Austin KM, Lee C-S, Dias A, Malsch MM, Reed R, Shimamura A (2007) The human Shwachman-Diamond syndrome protein, SBDS, associates with ribosomal RNA. Blood 110:1458-1465. http://dx.doi.org/10.1182/blood-2007-02-075184.

Gazda HT, Preti M, Sheen MR, O'Donohue MF, Vlachos A, Davies SM, et al. (2012) Frameshift mutation in p53 regulator RPL26 is associated with multiple physical abnormalities and a specific pre-ribosomal RNA processing defect in Diamond-Blackfan anemia. Hum Mutat 33:1037-1044. http://dx.doi.org/10.1002/humu.22081.

Ginisty H, Sicard H, Roger B, Bouvet P (1999) Structure and functions of nucleolin. J Cell Sci 112:761-772.

Giordano E, Peluso I, Senger S, Furia M (1999) *minifly*, a *Drosophila* gene required for ribosome biogenesis. J Cell Biol 144:1123-1133. http://dx.doi.org/10.1083/jcb.144.6.1123.

Golomb L, Volarevic S, Oren M (2014) p53 and ribosome biogenesis stress: The essentials. FEBS Lett. http://dx.doi.org/10.1016/j.febslet.2014.04.014.

Gonzales B, Henning D, So RB, Dixon J, Dixon MJ, Valdez BC (2005) The Treacher Collins syndrome (*TCOF1*) gene product is involved in pre-rRNA methylation. Hum Mol Genet 14:2035-2043. http://dx.doi.org/10.1093/hmg/ddi208.

Goodfellow SJ, Zomerdijk JCBM (2012) Basic mechanisms in RNA polymerase I transcription of the ribosomal RNA genes. Subcell Biochem 61: 211-236. http://dx.doi.org/10.1007/978-94-007-4525-4_10.

Grewal SS, Evans JR, Edgar BA (2007) *Drosophila* TIF-IA is required for ribosome synthesis and cell growth and is regulated by the TOR pathway. J Cell Biol 179:1105-13. http://dx.doi.org/10.1083/jcb.200709044.

Grewal SS, Li L, Orian A, Eisenman RN, Edgar BA (2005) Myc-dependent regulation of ribosomal RNA synthesis during *Drosophila* development. Nat Cell Biol 7:295-302. http://dx.doi.org/10.1038/ncb1223.

Grimm T, Hölzel M, Rohrmoser M, Harasim T, Malamoussi A, Gruber-Eber A, et al. (2006) Dominant-negative Pes1 mutants inhibit ribosomal RNA processing

and cell proliferation via incorporation into the PeBoW complex. Nucleic Acids Res 34:3030-43. http://dx.doi.org/10.1093/nar/gkl378.

Grob A, Colleran C, McStay B (2011) UBF an essential player in maintenance of active NORs and nucleolar formation. In: Olson MOJ (ed) The Nucleolus, Protein Reviews. Springer, New York, NY, pp 83-103 http://dx.doi.org/10.1007/978-1-4614-0514-6_5.

Grummt I (2003) Life on a planet of its own: regulation of RNA polymerase I transcription in the nucleolus. Genes Dev 17:1691-1702. http://dx.doi.org/10.1101/gad.1098503R.

Grummt I (2013) The nucleolus-guardian of cellular homeostasis and genome integrity. Chromosoma 122:487-497. http://dx.doi.org/10.1007/s00412-013-0430-0.

Hadjiolov AA (1985) The nucleolus and ribosome biogenesis. Springer-Verlag.

Hariharan N, Sussman MA (2014) Stressing on the nucleolus in cardiovascular disease. Biochem Biophys Acta 1842:798-801. http://dx.doi.org/10.1016/j.bbadis.2013.09.016.

He F, DiMario P (2011) Structure and function of Nopp140 and Treacle. In: Olson MJ (ed) The Nucleolus. Springer, New York, pp 253-278.

Hein N, Hannan KM, George AJ, Sanij E, Hannan RD (2013) The nucleolus: an emerging target for cancer therapy. Trends Mol Med 19:643-654. http://dx.doi.org/10.1016/j.molmed.2013.07.005.

Heitz E (1933) Über totale und partielle somatische heterpyknose, sowie strukturelle geschlectschromosemen bie *Drosophila funebris*. Z Zellforsch Mikroskop Anat 19:720-742. http://dx.doi.org/10.1007/BF02450275.

Hernandez-Verdun D (2011) Assembly and disassembly of the nucleolus during the cell cycle. Nucleus 2:189-194. http://dx.doi.org/10.4161/nucl.2.3.16246.

Hofmann A, Brünner M, Schwenemann A, Strödicke M, Karberg S, Klebes A, et al. (2010) The winged-helix transcription factor JUMU regulates development, nucleolus morphology and function, and chromatin organization of *Drosophila melanogaster*. Chromosome Res 18:307-324. http://dx.doi.org/10.1007/s10577-010-9118-y.

Hsu JK, Lin T, Tsai RYL (2012) Nucleostemin prevents telomere damage by promoting PML-IV recruitment to SUMOylated TRF1. J Cell Biol 197:613-624. http://dx.doi.org/10.1083/jcb.201109038.

Iadevaia V, Caldarola S, Biondini L, Gismondi A, Karlsson S, Dianzani I, et al. (2010) PIM1 kinase is destabilized by ribosomal stress causing inhibition of cell cycle progression. Oncogene 29:5490-9. http://dx.doi.org/10.1038/onc.2010.279.

Itahana K, Bhat KP, Jin A, Itahana Y, Hawke D, Kobayashi R, Zhang Y (2003) Tumor suppressor ARF degrades B23, a nucleolar protein involved in ribosome biogenesis and cell proliferation. Mol Cell 12:1151-1164. http://dx.doi.org/10.1016/S1097-2765(03)00431-3.

Jaako P, Flygare J, Olsson K, Quere R, Ehinger M, Henson A, et al. (2011) Mice with ribosomal protein S19 deficiency develop bone marrow failure and symptoms like patients with Diamond-Blackfan anemia. Blood 118:6087-6096. http://dx.doi.org/10.1182/blood-2011-08-371963.

Jakubowiak AJ, Siegel DS, Martin T, Wang M, Vij R, Lonial S et al. (2013) Treatment outcomes in patients with relapsed and refractory multiple myeloma and high-risk cytogenetics receiving single-agent carfilzomib in the PX-171-003-A1 study. Leukemia 27:2351-2357. http://dx.doi.org/10.1038/leu.2013.152.

James A, Cindass R Jr, Mayer D, Terhoeve, S, Mumphrey C, DiMario, P (2013) Nucleolar stress in *Drosophila melanogaster*. Nucleus 4:123-133. http://dx.doi.org/10.4161/nucl.23944.

Johnson AW, Ellis SR (2011) Of blood, bones, and ribosomes: is Swachman-Diamond syndrome a ribosomopathy? Genes and Development 25:898-900. http://dx.doi.org/10.1101/gad.2053011.

Jones NC, Lynn ML, Gaudenz K, Sakai D, Aoto K, Rey J-P, Glynn EF, Ellington L, Du C, Dixon J, Dixon MJ, Trainor PA (2008) Prevention of the neurocristopathy Treacher Collins syndrome through inhibition of p53 function. Nat Med 14:125-133. http://dx.doi.org/10.1038/nm1725.

Jordan, E G, and Cullis, C A (1982) The Nucleolus. Univeristy Press, Cambridge.

Kauffman T, Tran J, Dinardo S (2003) Mutations in *Nop60B*, the *Drosophila* homolog of human Dyskeratosis congenita 1, affect the maintenance of the germ-line stem cell lineage during spermatogenesis. Dev Biol 253:189-199. http://dx.doi.org/10.1016/S0012-1606(02)00013-1.

Kawai H, Wiederschain D, Yuan ZM (2003) Critical contribution of the MDM2 acidic domain to p53 ubiquitination. Mol Cell Biol 23:4939-4947. http://dx.doi.org/10.1128/MCB.23.14.4939-4947.2003.

Klinge S, Voigts-Hoffmann F, Leibundgut M, Arpagus S, Ban N (2011) Crystal structure of the eukaryotic 60S ribosomal subunit in complex with initiation factor 6. Science 334:941-948. http://dx.doi.org/10.1126/science.1211204.

Klinge S, Voigts-Hoffmann F, Leibundgut M, Ban N (2012) Atomic structures of the eukaryotic ribosome. Trends Biochem Sci 37:189-198. http://dx.doi.org/10.1016/j.tibs.2012.02.007.

Korgaonkar C, Hagen J, Tomkins V, Frazier AA, Allamargot C, Quelle FW, Quelle DE (2005) Nucleophosmin (B23) targets ARF to nucleoli and inhibits its function. Mol Cell Biol 25:1258–1271. http://dx.doi.org/10.1128/MCB.25.4.1258-1271.2005.

Koutsodontis G, Moustakas A, Kardassis D (2002) The role of Sp1 family members, the proximal GC-rich motifs, and the upstream enhancer region in the regulation of the human cell cycle inhibitor p21WAF-1/Cip1 gene promoter. Biochemistry 41:12771-12784. http://dx.doi.org/10.1021/bi026141q.

Kruhlak M, Crouch EE, Orlov M, Montano C, Gorski SA, Nussenzweig A, Misteli T, Phair RD, Casellas R (2007) The ATM repair pathway inhibits RNA polymerase I transcription in response to chromosome breaks. Nature 447:730–734. http://dx.doi.org/10.1038/nature05842 and http://dx.doi.org/10.1038/nature08110.

Kudron MM, Reinke V (2008) *C. elegans* nucleostemin is required for larval growth and germline stem cell division. PLoS Genet e1000181. http://dx.doi.org/10.1371/journal.pgen.1000181.

Lam YW, Lamond AI, Mann M, Andersen JS (2007) Analysis of nucleolar protein dynamics reveals the nuclear degradation of ribosomal proteins. Curr Biol 17:749-760. http://dx.doi.org/10.1016/j.cub.2007.03.064.

Lambertsson A (1998) The *minute* genes in *Drosophila* and their molecular functions. Advances in Genetics 38:69-134.

Landowski M, O'Donohue MF, Buros C, Ghazvinian R, Montel-Lehry N, Vlachos A, et al. (2013) Novel deletion of RPL15 identified by array-comparative genomic hybridization in Diamond-Blackfan anemia. Hum Genet 132:1265-1274. http://dx.doi.org/10.1007/s00439-013-1326-z.

Lapik YR, Fernandes CJ, Lau LF, Pestov DG (2004) Physical and functional interaction between Pes1 and Bop1 in mammalian ribosome biogenesis. Mol Cell 15:17-29. http://dx.doi.org/10.1016/j.molcel.2004.05.020.

Larrea MD, Wander SA, Slingerland JM (2009) p27 as Jekyll and Hyde: regulation of cell cycle and cell motility. Cell Cycle 8:3455-3461. http://dx.doi.org/10.4161/cc.8.21.9789.

Lee C-C, Tsai Y-T, Kao C-W, Lee L-W, Lai H-J, Ma T-H, et al. (2014) Mutation of a Nopp140 gene *dao-5* alters rDNA transcription and increases germ line apoptosis in *C. elegans*. Cell Death Disease 5:e1158. http://dx.doi.org/10.1038/cddis.2014.114.

Li J, Yu L, Zhang H, Wu J, Yuan J, Li X, et al. (2009) Down-regulation of pescadillo inhibits proliferation and tumorigenicity of breast cancer cells. Cancer Sci 100:2255-2260. http://dx.doi.org/10.1111/j.1349-7006.2009.01325.x.

Lin C-I, Yeh N-H (2009) Treacle recruits RNA polymerase I complex to the nucleolus that is independent of UBF. Biochem Biophys Res Commun 386:396-401. http://dx.doi.org/10.1016/j.bbrc.2009.06.050.

Lin T, Meng L, Lin T-C, Wu LJ, Pederson T, Tsai RYL (2014) Nucleostemin and GNL3L exercise distinct functions in genome protection and ribosome synthesis, respectively. J Cell Sci 127:2302-2312. http://dx.doi.org/10.1242/jcs.143842.

Lin WC, Lin FT, Nevins JR (2001) Selective induction of E2F1 in response to DNA damage, mediated by ATM dependent phosphorylation. Genes Dev 15:1833-1844.

Lipton JM, Ellis SR (2009) Diamond-Blackfan anemia: diagnosis, treatment, and molecular pathogenesis. Hematology/oncology clinics of North America 23:261-82. http://dx.doi.org/10.1016/j.hoc.2009.01.004.

Liu Y, Liang S, Tartakoff AM (1996) Heat shock disassembles the nucleolus and inhibits nuclear protein import and poly(A)$^+$ RNA export. EMBO J 15:6750-6757.

Llanos S, Clark PA, Rowe J, Peters G (2001) Stabilization of p53 by p14^{ARF} without relocation of MDM2 to the nucleolus. Nat Cell Biol 3:445-452. http://dx.doi.org/10.1038/35074506.

Lo D, Dai M, Sun X, Zeng SX, Lu H (2012) Ubiquitin- and MDM2 E3 ligase-independent proteasomal turnover of nucleostemin in response to GTP depletion. J. Biol Chem 287(13):10013-10020. http://dx.doi.org/10.1074/jbc.M111.335141.

Lo D, Lu H (2010) Nucleostemin, another nucleolar “twister” of the p53-MDM2 loop. Cell Cycle 9(16):3227-3232. http://dx.doi.org/10.4161/cc.9.16.12605.

Lohrum, MAE, Ludwig RL, Kubbutat MHG, Hanlon M, Vousden KH (2003) Regulation of HDM2 activity by the ribosomal protein L11. Cancer Cell 3:577-587. http://dx.doi.org/10.1016/S1535-6108(03)00134-X.

Ma H, Pederson T (2007) Depletion of the nucleolar protein nucleostemin causes G1 cell cycle arrest via the p53 pathway. Mol Biol Cell 18(7):2630-2635. http://dx.doi.org/10.1091/mbc.E07-03-0244.

Ma H, Pederson T (2008) Nucleostemin: a multiplex regulator of cell-cycle progression. Trends Cell Biol 18(12):575-579. http://dx.doi.org/10.1016/j.tcb.2008.09.003.

Malumbres M, Harlow E, Hunt T, Hunter T, Lahti JM, Manning G et al. (2009) Cyclin-dependent kinases: a family portrait. Nat Cell Biol 11: 1275–1276. http://dx.doi.org/10.1038/ncb1109-1275.

Marcel V, Dichtel-Danjoy M-L, Sagne C, Hafsi H, Ma D, Ortiz-Cuaran S, et al. (2011) Biological functions of p53 isoforms through evolution: lessons from animal and cellular models. Cell Death Differ 18:1815–1824. http://dx.doi.org/10.1038/cdd.2011.120.

Marechal V, Elenbaas B, Piette J, Nicolas J-C, Levine AJ (1994) The ribosomal L5 protein is associated with Mdm2 and Mdm2-p53 complexes. Mol Cell Biol 14:7414-7420.

Marinho J, Casares F, Pereira PS (2011) The *Drosophila Nol12* homologue *viriato* is a dMyc target that regulates nucleolar architecture and is required for dMyc-stimulated cell growth. Development 138:349-357. http://dx.doi.org/10.1242/dev.054411.

Marrone A, Mason PJ (2003) Dyskeratosis congenita. Cellular and molecular life sciences. CMLS 60:507-17.

Marrone A, Walne A, Tamary H, Masunari Y, Kirwan M, Beswick R, Vulliamy T, Dokal I (2007) Telomerase reverse-transcriptase homozygous mutations in autosomal recessive dyskeratosis congenital and Hoyeraal-Hreidarsson syndrome. Blood 110:4198-4205. http://dx.doi.org/10.1182/blood-2006-12-062851.

Martin FA, Pérez-Garijo A, Moreno E, Morata G (2004) The *brinker* gradient controls wing growth in *Drosophila*. Development 131:4921-4930. http://dx.doi.org/10.1242/dev.01385.

Marygold SJ, Roote J, Reuter G, Lambertsson A, Ashburner M, Millburn GH, Harrison PM, Yu Z, Kenmochi N, Kaufamn TC, Leevers SJ, and Cook KR (2007) The ribosomal protein genes and *Minute* loci of *Drosophila*

melanogaster. Genome Biol 8:R216.1-26. http://dx.doi.org/10.1186/gb-2007-8-10-r216.

Mayer C, Bierhoff H, Grummt I (2005) The nucleolus as a stress sensor: JNK2 inactivates the transcription factor TIF-IA and down-regulates rRNA synthesis. Gene Dev 19:933-941. http://dx.doi.org/10.1101/gad.333205.

Mayer C, Grummt I (2005) Cellular stress and nucleolar function. Cell Cycle 4:1036-1038. http://dx.doi.org/10.4161/cc.4.8.1925.

Mayer C, Zhao J, Yuan, X, Grummt I (2004) mTOR-dependent activation of the transcription factor TIF-IA links rRNA synthesis to nutrient availability. Gene Dev 18:423-434. http://dx.doi.org/10.1101/gad.285504.

McClintock B (1934) The relation of a particular chromosomal element to the development of the nucleoli in *Zea mays*. Z Zellforsch Mikroskop Anat 21:294-328. http://dx.doi.org/10.1007/BF00374060.

McNamee LM, Brodsky MH (2009) p53-independent apoptosis limits DNA damage-induced aneuploidy. Genetics 182:423-35. http://dx.doi.org/10.1534/genetics.109.102327.

Mekhail K, Rivero-Lopez L, Khacho M, Lee S (2006) Restriction of rRNA synthesis by VHL maintains energy equilibrium under hypoxia. Cell Cycle 5:2401-2413. http://dx.doi.org/10.4161/cc.5.20.3387.

Meng L, Lin T, Peng G, Hsu JK, Lee S, Lin A-Y, Tsai RYL (2013) Nucleostemin deletion reveals an essential mechanism that maintains the genomic stability of stem and progenitor cells. Proc Natl Acad Sci 110:11415-11420. http://dx.doi.org/10.1073/pnas.1301672110.

Meng L, Yasumoto H, Tsai RYL (2006) Multiple controls regulate nucleostemin partitioning between nucleolus and nucleoplasm. J Cell Sci 119:5124-5136. http://dx.doi.org/10.1242/jcs.03292.

Meulmeester E, Frenk R, Stad R, de Graaf P, Marine J-C, Vousden KH, et al. (2003) Critical role for a central part of Mdm2 in the ubiquitylation of p53. Mol Cell Biol 23:4929-4938. http://dx.doi.org/10.1128/MCB.23.14.4929-4938.2003.

Miller OL Jr, Beatty BR (1969) Visualization of nucleolar genes. Science 164:955-957. http://dx.doi.org/10.1126/science.164.3882.955.

Misteli T (2005) Going in GTP circles in the nucleolus. J Cell Biol 168:177-178. http://dx.doi.org/10.1083/jcb.200412038.

Mitchell JR, Wood E, Collins K (1999) A telomerase component is defective in the human disease dyskeratosis congenita. Nature 402:551-555. http://dx.doi.org/10.1038/990141.

Mizushima N, Komatsu M (2011) Autophagy: renovation of cells and tissues. Cell 147:728-741. http://dx.doi.org/10.1016/j.cell.2011.10.026.

Mochizuki T, Miyazaki H, Hara T, Furuya T, Imamura T, Watabe T, Miyazono K (2004) Roles for the MH2 domain of Smad7 in the specific inhibition of transforming growth factor-beta superfamily signaling. The Journal of biological chemistry 279:31568-74.

Montanaro L, Treré D, Derenzini M (2013) The emerging role of RNA polymerase I transcription machinery in human malignancy: a clinical perspective. Onco Targets Ther 6:909-916. http://dx.doi.org/10.2147/ott.s36627.

Moreno E, Basler K, Morata G (2002) Cells compete for decapentaplegic survival factor to prevent apoptosis in *Drosophila* wing development. Nature 416:755–759. http://dx.doi.org/10.1038/416755a.

Morgan TH, Bridges CB, Sturtevant AH (1925) The genetics of *Drosophila*. *Bibliographica Genetica* 2:1-262.

Moss T, Stefanovsky VY (2002) At the center of eukaryotic life. Cell 109:545–548. http://dx.doi.org/10.1016/S0092-8674(02)00761-4.

Narla A, Ebert BL (2010) Ribosomopathies: human disorders of ribosome dysfunction. Blood 115:3196-3205. http://dx.doi.org/10.1182/blood-2009-10-178129.

Názer E, Verdún RE, Sánchez DO (2012) Severe heat shock induces nucleolar accumulation of mRNAs in *Trypanosoma cruzi*. PLoS ONE 7:e43175. http://dx.doi.org/10.1371/journal.pone.0043715.

Neumüller RA, Gross T, Samsonova AA, Vinayagam A, Buckner M, Founk K, Hu Y, Sharifpoor S, Rosebrock AP, Andrews B, Winston F, Perrimon N (2013) Conserved regulators of nucleolar size revealed by global phenotypic analyses. Sci Signal 6:ra70. http://dx.doi.org/10.1126/scisignal.2004145.

O'Sullivan AC, Sullivan GJ, McStay B (2002) UBF binding in vivo is not restricted to regulatory sequences within the vertebrate ribosomal DNA repeat. Mol Cell Biol 22:657-668. http://dx.doi.org/10.1128%2FMCB.22.2.657-668.2002.

Ollmann M, Young LM, Di Como CJ, Karim F, Belvin M, Robertson S, et al. (2000) *Drosophila* p53 is a structural and functional homolog of the tumor

suppressor p53. Cell 101:91–101. http://dx.doi.org/10.1016/S0092-8674(00)80626-1.

Olson MOJ (2011) The Nucleolus. Springer, New York.

Olson, MOJ (2004) Sensing cellular stress: another new function for the nucleolus? Sci STKE pe10. http://dx.doi.org/10.1126/stke.2242004pe10.

Panse VG, Johnson AW (2010) Maturation of eukaryotic ribosomes: acquisition of functionality. Trends Biochem Sci 35:260-266. http://dx.doi.org/10.1016/j.tibs.2010.01.001.

Parlato R, Kreiner G (2013) Nucleolar activity in neurodegenerative diseases: a missing piece of the puzzle? J Mol Med 91:541-547. http://dx.doi.org/10.1007/s00109-012-0981-1.

Pederson T (1998) The plurifunctional nucleolus. Nucleic Acids Res 26:3871-3876. http://dx.doi.org/10.1093/nar/26.17.3871.

Perdahl EB, Naprstek BL, Wallace WC, Lipton JM (1994) Erythroid failure in Diamond-Blackfan anemia is characterized by apoptosis. Blood 83:645-50.

Pereboom TC, van Weele LJ, Bondt A, MacInnes AW (2011) A zebrafish model of dyskeratosis congenital reveals hematopoietic stem cell formation failure resulting from ribosomal protein-mediated p53 stabilization. Blood 118:5458-5465. http://dx.doi.org/10.1182/blood-2011-04-351460.

Perrin L, Banassayag C, Morello D, Pradel, J, Montagne J (2003) Modulo is a target of Myc selectively required for growth of proliferative cells in *Drosophila*. Mech Dev 120:645-655. http://dx.doi.org/10.1016/S0925-4773(03)00049-2.

Perrin L, Demakova O, Fanti L, Kallenbach S, Saingery S, Mal'ceva NI, Pimpinelli S, Zhimulev I, Pradel J (1998) Dynamics of the sub-nuclear distribution of Modulo and the regulation of position-effect variegation by nucleolus in *Drosophila*. J Cell Sci 111:2753-2761.

Perrin L, Romby P, Laurenti P, Berenger H, Kallenbach S, Bourbon, H-M, Pradel J (1999) The *Drosophila* modifier of variegation *modulo* gene product binds specific RNA sequences at the nucleolus and interacts with DNA and chromatin in a phosphorylation-dependent manner. J Biol Chem 274:6315-6323. http://dx.doi.org/10.1074/jbc.274.10.6315.

Perry RP, Hell A, Errera M (1961) The role of the nucleolus in ribonucleic acid and protein synthesis. I: Incorporation of cytidine into normal and nucleolar

inactivated HeLa cells. Biochim Biophys Acta 49:47-57. http://dx.doi.org/10.1016/0006-3002(61)90868-X.

Perry RP (1962) The cellular sites of synthesis of ribosomal and 4S RNA. Proc Nat Acad Sci USA 48:2179-2186.

Politz JC, Polena I, Trask I, Bazett-Jones DP, and Pederson T (2005) A nonribosomal landscape in the nucleolus revealed by the stem cell protein nucleostemin. Mol Biol Cell 16:3401-3410. http://dx.doi.org/10.1091/mbc.E05-02-0106.

Poortinga G, Hannan KM, Snelling H, Walkley CR, Jenkins A, Sharkey K, et al. (2004) MAD1 and c-MYC regulate UBF and rDNA transcription during granulocyte differentiation. EMBO J. 23:3325–3335. http://dx.doi.org/10.1038/sj.emboj.7600335.

Quelle DE, Zindy F, Ashmun RA, Sherr CJ (1995) Alternative reading frames of the INK4a tumor suppressor gene encode two unrelated proteins capable of inducing cell cycle arrest. Cell 83:993-1000.

Quin JE, Devlin JR, Cameron D, Hannan KM, Pearson RB, Hannan RD (2014) Targeting the nucleolus for cancer intervention. Biochim Biophys Acta 1842:802-816. http://dx.doi.org/10.1016/j.bbadis.2013.12.009.

Rabl J, Leibundgut M, Ataide SF, Haag A, Ban N (2011) Crystal structure of the eukaryotic 40S ribosomal subunit in complex with initiation factor 1. Science 331:730-736. http://dx.doi.org/10.1126/science.1198308.

Rashid R, Liang B, Baker DL, Youssef OA, He Y, Phipps K, et al. (2006) Crystal structure of a Cbf5-Nop10-Gar1 complex and implications in RNA-guided pseudouridylation and dyskeratosis congenita. Mol Cell 21:249-260. http://dx.doi.org/10.1016/j.molcel.2005.11.017.

Rickards B, Flint SJ, Cole MD, LeRoy G (2007) Nucleolin is required for RNA polymerase I transcription *in vivo*. Mol Cell Biol 27:937-948. http://dx.doi.org/10.1128/MCB.01584-06.

Ritossa F (1976) The *bobbed* locus. In Ashburner M, Novitski E (eds) The Genetics and Biology of *Drosophila.* Academic Press, London, pp 1b:801-846.

Ritossa FM, Atwood K, Lindsley D, Spiegelman S (1966) On the chromosomal distribution of DNA complementary to ribosomal and soluble RNA. Nat Cancer Inst Monogr 23:449-472.

Ritossa FM, Spiegelman S (1965) Localization of DNA complementary to ribosomal RNA in the nucleolus organizer region of *Drosophila melanogaster*. Proc Natl Acad Sci USA 53: 737-745. http://dx.doi.org/10.1073/pnas.53.4.737.

Roger B, Moisand A, Amalric F, Bouvet, P (2003) Nucleolin provides a link between Pol I transcription and pre-ribosome assembly. Chromosoma 111:399-407. http://dx.doi.org/10.1007/s00412-002-0221-5.

Romanova L, Grand A, Zhang L, Rayner S, Katoku-Kikyo N, Kellner S, et al. (2009) Critical role of nucleostemin in pre-rRNA processing. J Biol Chem 284:4968-4977. http://dx.doi.org/10.1074/jbc.M804594200.

Rosby R, Cui Z, Rogers E, deLivron MA, Robinson VA, DiMario PJ (2009) Knockdown of the *Drosophila* GTPase Nucleostemin 1 impairs large ribosomal subunit biogenesis, cell growth, and midgut precursor cell maintenance. Mol Biol Cell 20:4424-4434. http://dx.doi.org/10.1091/mbc.E08-06-0592.

Rubbi CP, Milner J (2003) Disruption of the nucleolus mediates stabilization of p53 in response to DNA damage and other stresses. EMBO J 22:6068-6077. http://dx.doi.org/10.1093/emboj/cdg579.

Ruggero D, Grisendi S, Piazza F, Rego E, Mari F, Rao PH, Cordon-Cardo C, Pandolfi PP (2003) Dyskeratosis congenita and cancer in mice deficient in ribosomal RNA modification. Science 299:259-62. http://dx.doi.org/10.1126/science.1079447.

Rujkijyanont P, Adams S-L, Beyene J, Dror Y (2009) Bone marrow cells from patients with Shwachman-Diamond syndrome abnormally express genes involved in ribosome biogenesis and RNA processing. Br J Haematol 145:806-815. http://dx.doi.org/10.1111/j.1365-2141.2009.07692.x.

Russo A, Catillo M, Esposito D, Briata P, Pietropaolo C, Russo G (2011) Autoregulatory circuit of human rpL3 expression requires hnRNP H1, NPM and KHSRP. Nucleic Acids Res 39:7576-85. http://dx.doi.org/10.1093/nar/gkr461.

Russo A, Esposito D, Catillo M, Piettopaolo C, Crescenzi E, Russo G (2013) Human rpL3 induces G_1/S arrest or apoptosis by modulating $p21^{waf1/cip1}$ levels in a p53-independent manner. Cell Cycle 12:76-87. http://dx.doi.org/10.4161/cc.22963.

Sakai D, Trainor PA (2009) Treacher Collins syndrome: unmasking the role of *Tcof1*/treacle. Int J Biochem Cell Bio 41:1229-1232. http://dx.doi.org/10.1016/j.biocel.2008.10.026.

Saporita AJ, Chang HC, Winkeler CL, Apicelli AJ, Kladney RD, Wang J, Townsend RR, Michel LS, Weber JD (2011) RNA helicase DDX5 is a p53-independent target of ARF that participates in ribosome biogenesis. Cancer research 71:6708-17.

Savkur RS, Olson MOJ (1998) Preferential cleavage in pre-ribosomal RNA by protein B23 endoribonuclease. Nucleic Acids Res 26:4508-4515. http://dx.doi.org/10.1093/nar/26.19.4508.

Schneider DA (2012) RNA polymerase I activity is regulated at multiple steps in the transcription cycle: recent insights into factors that influence transcription elongation. Gene 493:176-184. http://dx.doi.org/10.1016/j.gene.2011.08.006.

Sekelsky JJ, Brodsky MH, Burtis KC (2000) DNA repair in *Drosophila*: insights from the *Drosophila* genome sequence. J Cell Biol 150:31F-36F. http://dx.doi.org/10.1083/jcb.150.2.F31.

Sengupta J, Bussiere C, Pallesen J, West M, Johnson AW, Frank J (2010) Characterization of the nuclear export adaptor protein Nmd3 in association with the 60S ribosomal subunit. J Cell Biol 189:1079-1086. http://dx.doi.org/10.1083/jcb.201001124.

Sherr CJ (2006) Divorcing ARF and p53: an unsettled case. Nat Rev Cancer 6:663-673. http://dx.doi.org/10.1038/nrc1954.

Sloan KE, Bohnsack MT, Watkins NJ (2013) The 5S RNP couples p53 homeostasis to ribosome biogenesis and nucleolar stress. Cell Rep 5:237-247. http://dx.doi.org/10.1016/j.celrep.2013.08.049.

Soussi T, Dehouche K, Béroud C (2000) p53 website and analysis of p53gene mutations in human cancer: forging a link between epidemiology and carcinogenesis. Hum Mutat 15:105-113. http://dx.doi.org/10.1002/(SICI)1098-1004(200001)15:1%3C105::AID-HUMU19%3E3.0.CO;2-G.

Staley JP, Woolford JL Jr. (2009) Assembly of ribosomes and spliceosomes: complex ribonucleoprotein machines. Curr Opin Cell Biol 21:109-118. http://dx.doi.org/10.1016/j.ceb.2009.01.003.

Stevens C, Smith L, La Thangue NB (2003) Chk2 activates E2F-1 in response to DNA damage. Nat. Cell Biol 5:401-409. http://dx.doi.org/10.1038/ncb974.

Stiewe T (2007) The p53 family in differentiation and tumorigenesis. Nat Rev Cancer 7:165-168. http://dx.doi.org/10.1038/nrc2072.

Sugimoto M, Kuo ML, Roussel MF, Sherr CJ (2003) Nucleolar Arf tumor suppressor inhibits ribosomal RNA processing. Molecular Cell 11:415-24. http://dx.doi.org/10.1016/s1097-2765(03)00057-1.

Sun XX, Dai MS, Lu H (2008) Mycophenolic acid activation of p53 requires ribosomal proteins L5 and L11. J Biol Chem 283(18):12387-12392. http://dx.doi.org/10.1074/jbc.M801387200.

Tafforeau L, Zorbas C, Langhendries J-L, Mullineux S-T, Stamatopoulou V, Mullier R, Wacheul L, Lafontaine DLJ (2013) The complexity of human ribosome biogenesis revealed by systematic nucleolar screening of pre-rRNA processing factors. Mol Cell 51:539-551. http://dx.doi.org/10.1016/j.molcel.2013.08.011.

Takada S, Kelkar A, Theurkauf WE (2003) *Drosophila* checkpoint kinase 2 couples centrosome function and spindle assembly to genomic integrity. Cell 113:87-99. http://dx.doi.org/10.1016/S0092-8674(03)00202-2.

Takagi M, Absalon MJ, McLure KG, Kastan MB (2005) Regulation of p53 translation and induction after DNA damage by ribosomal protein L26 and nucleolin. Cell 123:49-63; http://dx.doi.org/10.1016/j.cell.2005.07.034.

Taylor AM, Humphries JM, White RM, Murphey RD, Burns CE, Zon LI (2012) Hematopoietic defects in rps29 mutant zebrafish depend upon p53 activation. Exp Hematol 40:228-237. http://dx.doi.org/10.1016/j.exphem.2011.11.007.

Thumati NR, Zeng X-L, Au HHT, Jang CJ, Jan E, Wong JMY (2013) Severity of X-linked dyskeratosis congenita (DKCX) cellular defects is not directly related to dyskerin (*DKC1*) activity in ribosomal RNA biogenesis or mRNA translation. Hum Mutat 34:1698-1707. http://dx.doi.org/10.1002/humu.22447.

Titen SW, Golic KG (2008) Telomere loss provokes multiple pathways to apoptosis and produces genomic instability in *Drosophila melanogaster*. Genetics 180:1821-1832. http://dx.doi.org/10.1534/genetics.108.093625.

Torihara H, Uechi T, Chakraborty A, Shinya M, Sahai N, Kenmochi N (2011) Erythropoiesis failure due to RPS19 deficiency is independent of an activated Tp53 response in a zebrafish model of Diamond-Blackfan anaemia. Br J Haematol 152:648-654. http://dx.doi.org/10.1111/j.1365-2141.2010.08535.x.

Tortoriello G, de Celis JF, Furia M (2010) Linking pseudouridine synthases to growth, development and cell competition. FEBS J 277:3249-3263. http://dx.doi.org/10.1111/j.1742-4658.2010.07731.x.

Tsai RYL, McKay RDG (2005) A multistep, GTP-driven mechanism controlling the dynamic cycling of nucleostemin. J Cell Biol 168:179-184. http://dx.doi.org/10.1083/jcb.200409053.

Tsai RYL, McKay RDG (2002) A nucleolar mechanism controlling cell proliferation in stem cells and cancer cells. Genes Dev 16:2991-3003. http://dx.doi.org/10.1101/gad.55671.

Tsai RYL, Pederson T (2014) Connecting the nucleolus to the cell cycle and human disease. FASEB J. http://dx.doi.org/10.1096/fj.14-254680.

Tsai, RYL (2011) New frontiers in nucleolar research: nucleostemin and related proteins. In: Olson MOJ (ed) The Nucleolus, Protein Reviews. Springer, New York, NY, pp 301-320 http://dx.doi.org/10.1007/978-1-4614-0514-6_13.

Tsang CK, Bertram PG, Ai W, Drenan R, Zheng XFS (2003). Chromatin-mediated regulation of nucleolar structure and RNA Pol I localization by TOR. EMBO J 22:6045-6056. http://dx.doi.org/10.1093/emboj/cdg578.

Tyler DM, Li W, Zhuo N, Pellock B, Baker NE (2007) Genes affecting cell competition in *Drosophila*. Genetics 175:643-657. http://dx.doi.org/10.1534/genetics.106.061929.

van Riggelen J, Yetil A, Felsher DW (2010) MYC as a regulator of ribosome biogenesis and protein synthesis. Nat Rev Cancer 10:301-309. http://dx.doi.org/10.1038/nrc2819.

Vlachos A, Dahl N, Dianzani I, Lipton JM (2013) Clinical utility gene card for: Diamond-Blackfan anemia – update 2013. Eur J Human Genet 2. http://dx.doi.org/10.1038/ejhg.2013.34.

Vlatković N, Boyd MT, Rubbi CP (2013) Nucleolar control of p53: a cellular Achilles' heel and a target for cancer therapy. Cell Mol Life Sci .http://dx.doi.org/10.1007/s00018-013-1361-x.

Voit R, Grummt I (2011) The RNA polymerase I transcription machinery. In: Olson MOJ (ed) The Nucleolus, Protein Reviews. Springer, New York, NY, pp 107-134 http://dx.doi.org/10.1007%2F978-1-4614-0514-6_6.

Vulliamy T, Marrone A, Goldman F, Dearlove A, Bessler M, Mason PJ, Dokal I (2001) The RNA component of telomerase is mutated in autosomal dominant dyskeratosis congenita. Nature 413:432-435. http://dx.doi.org/10.1038/35096585.

Wang Z, Bhattacharya N, Weaver M, Petersen K, Meyer M, Gapter L et al. (2001) Pim-1: a serine/threonine kinase with a role in cell survival, proliferation, differentiation and tumorigenesis. J Vet Sci 2:167-179.

Wang Y, Dimario P (submitted) Loss of Drosophila Nucleostemin 2 blocks nucleolar release of the 60S subunit, alters nucleolar ultrastructure, and induces stress responses. Chromosoma.

Warner JR, McIntosh KB (2009) How common are extrachromosomal functions of ribosomal proteins? Mol Cell 24:437-440. http://dx.doi.org/10.1016/j.molcel.2009.03.006.

Warner JR, Soeiro R (1967) Nascent ribosomes from HeLa cells. Proc Nat Acad Sci USA 58:1984-1990. http://dx.doi.org/10.1073/pnas.58.5.1984.

Warner JR (1977) In the absence of ribosomal RNA synthesis, the ribosomal proteins of HeLa cells are synthesized normally and degraded rapidly. J Mol Biol 115:315-333. http://dx.doi.org/10.1016/0022-2836(77)90157-7.

Weber JD, Taylor LJ, Roussel MF, Sherr CJ, Bar-Sagi D (1999) Nucleolar Arf sequesters Mdm2 and activates p53. Nat Cell Biol 1:20-26. http://dx.doi.org/10.1038/8991.

Welch WJ, Suhan JP (1985) Morphological study of the mammalian stress response: characterization of changes in cytoplasmic organelles, cytoskeleton, and nucleoli, and appearance of intranuclear actin filaments in rat fibroblasts after heat-shock treatment. J Cell Biol 101:1198-2011. http://dx.doi.org/10.1083/jcb.101.4.1198.

Wilson DN, Doudna Cate JH (2012) The structure and function of the eukaryotic ribosome. Cold Spring Harb Perspect Biol 4:a011536. http://dx.doi.org/10.1101/cshperspect.a011536.

Xiao L, Grove A (2009) Coordination of Ribosomal Protein and Ribosomal RNA Gene Expression in Response to TOR Signaling. Current Genomics 10:198-205.

Yadav GV, Chakraborty A, Uechi T, Kenmochi N (2014) Ribosomal protein deficiency causes Tp53-independent erythropoiesis failure in zebrafish. Int J Biochem Cell Biol 49:1-7. http://dx.doi.org/10.1016/j.biocel.2014.01.006.

Yadavilli S, Mayo LD, Higgins M, Lain S, Hegde V, Deutsch WA (2009) Ribosomal protein S3: a multi-functional protein that interacts with both p53 and MDM2 through its KH domain. DNA Repair 8:1215-1224. http://dx.doi.org/10.1016/j.dnarep.2009.07.003.

Yamada Y, Davis KD, Coffman CR (2008) Programmed cell death of primordial germ cells in *Drosophila* is regulated by p53 and the Outsiders monocarboxylate transporter. Development 135:207-216. http://dx.doi.org/10.1242/dev.010389.

Yamaguchi, H, Calado RT, Ly H, Kajigaya S, Baerlocher GM, Chanock SJ, Lansdorp PM, Young NS (2005) Mutations in *TERT*, the gene for telomerase reverse transcriptase, in aplastic anemia. N Engl J Med 352:1413-1424. http://dx.doi.org/10.1056/NEJMoa042980.

Yip SP, Siu PM, Leung PHM, Zhao Y, Yung BYM (2011) The multifunctional nucleolar protein nucleophosmin/NPM/B23 and the nucleoplasmin family of proteins. In: Olson MOJ (ed) The Nucleolus, Protein Reviews. Springer, New York, NY, pp 213-252 http://dx.doi.org/10.1007/978-1-4614-0514-6_10.

Yuan, X, Zhou Y, Casanova E, Chai M, Kiss E, Gröne H-J, et al. (2005) Genetic inactivation of the transcription factor TIF-IA leads to nucleolar disruption, cell cycle arrest, and p53-mediated apoptosis. Mol Cell 19:77–87. http://dx.doi.org/10.1016/j.molcel.2005.05.023.

Zaffran S, Chartier A, Gallant P, Astier M, Arquier N, Doherty D, Gratecos D, Semeriva M (1998) A *Drosophila* RNA helicase gene, pitchoune, is required for cell growth and proliferation and is a potential target of d-Myc. Development 125:3571-84.

Zatsepina OV, Dudnic OA, Todorov IT, Thiry M, Spring H, Trendelenburg MF (1997) Experimental induction of prenucleolar bodies (PNBs) in interphase cells: interphase PNBs show similar characteristics as those typically observed at telophase of mitosis in untreated cells. Chromosoma 105:418-430. http://dx.doi.org/10.1007/BF02510478.

Zemp I, Kutay U (2007) Nuclear export and cytoplasmic maturation of ribosomal subunits, FEBS Letters 581:2783-2793. http://dx.doi.org/10.1016/j.febslet.2007.05.013.

Zhang H, Shertok S, Miller K, Taylor L, Martin-Deleon PA (2005) Sperm dysfunction in the Rb(6.16)- and Rb(6.15)-bearing mice revisited: involvement of Hyalp1 and Hyal5. Molecular reproduction and development 72:404-10. http://dx.doi.org/10.1002/mrd.20360.

Zhang Y, Lu H (2009) Signaling to p53: Ribosomal Proteins Find Their Way. Cancer Cell16:369-77.

Zhang Y, White Wolf G, Bhat K, Jin A, Allio T, Burkhart WA, Xiong Y (2003) Ribosomal protein L11 negatively regulates oncoprotein MDM2 and mediates

a p53-dependent ribosomal-stress checkpoint pathway. Mol Cell Biol 23:8902-8912. http://dx.doi.org/10.1128/MCB.23.23.8902-8912.2003.

Zhang Z, Wang H, Li M, Agrawal S, Chen X, Zhang R (2004) MDM2 is a negative regulator of p21WAF1/CIP1, independent of p53. The Journal of Biological Chemistry 279:16000-6. http://dx.doi.org/10.1074/jbc.m312264200.

Zhao J, Yuan X, Frodin M, Grummt I (2003) ERK-dependent phosphorylation of the transcription initiation factor TIF-IA is required for RNA polymerase I transcription and cell growth. Molecular Cell 11:405-13.

Zhu YH, Zhang CW, Lu L, Demidov ON, Sun L, Yang L, Bulavin DV, Xiao ZC (2009) Wip1 regulates the generation of new neural cells in the adult olfactory bulb through p53-dependent cell cycle control. Stem Cells 27:1433-42.

CHAPTER 2. RNAi-MEDIATED DEPLETION OF NOPP140*

2.1 Introduction

The nucleolar phosphoprotein Nopp140 (Meier et al. 1996; Isaac et al. 1998) likely functions as a molecular chaperone for small nucleolar ribonucleoprotein particles (snoRNPs), either in their assembly, transport to the nucleolus from Cajal bodies, or in their association with pre-rRNA, as these snoRNPs mediate site-specific 2'-*O*-methylation (box C/D snoRNPs) or pseudouridylation (box H/ACA snoRNPs) (Yang et al., 2000; reviewed in He and DiMario 2011). *Drosophila melanogaster* expresses two isoforms of Nopp140 by alternative slicing (Waggener and DiMario 2002). The isoforms are identical up to amino acid residue 584, but then differ in their carboxy termini; one (Nopp140-True) is the canonical ortholog of mammalian Nopp140, while the other (Nopp140-RGG) has a Gly and Arg rich domain common to many RNA-associated proteins. Previously, we used RNAi to target the common 5' end of both splice variant transcripts. *Nopp140* mRNA levels depleted organism-wide by ≥50% caused larval and pupal lethality, while depletions by only ~30% produced viable adults, but with defective legs, wings, thoracic bristles, and abdominal cuticles (Cui and DiMario 2007). These adult structures normally derive from larval imaginal discs and histoblasts which presumably maintain high demands for ribosome biogenesis, and thus protein synthesis.

*This chapter previously appeared as James et al. (2013) Nucleolar stress in *Drosophila melanogaster*: RNAi-mediated depletion of Nopp140. *Nucleus* 4:2, 1–11; March/April. http://dx.doi.org/10.4161/nucl.23944. It is reprinted by permission of Taylor and Francis – see the permission letter for proper acknowledgement phrase in Appendix A of this thesis.

Related to Nopp140 in structure and function is Treacle, a nucleolar protein found thus far in vertebrates along with Nopp140. *TCOF1* is the gene on human chromosome 5 that encodes Treacle. Haplo-insufficiencies in *TCOF1* are closely associated with the Treacher Collins-Franceschetti syndrome (TCS), which is marked by craniofacial malformations during fetus development (Dixon 1996; Trainor et al. 2009). TCS arises from the loss of neural crest cells that normally migrate to populate branchial arches I and II on about day 24 of human embryogenesis (Dixon et al. 2006). Loss of Treacle in these particular neural crest cells results in abnormal ribosome biogenesis (referred to as nucleolar stress) and thus a loss in protein synthesis leading ultimately to cellular stress and p53-dependent apoptosis (Jones et al. 2008). Using the murine system, Jones et al. (2008) showed that depleting p53 or blocking p53 function prevented apoptosis in these neural crest cells; they were thus able to rescue the craniofacial abnormalities normally associated with the TCS.

Malformations in adult flies resulting from the partial loss of Nopp140 in *Drosophila* larval progenitor tissues were reminiscent of the human TCS. The first goal of this study was to determine what cell stress responses resulted from the depletion of Nopp140 by RNAi expression in *Drosophila* larval cells leading either to lethality or to malformations in adult structures. Apoptosis in larval imaginal disc cells and histoblasts could well explain the morphological defects observed in adult structures. The second goal was to determine if p53 is required for the *Drosophila* nucleolar stress response as it is in the mammalian system.

The third goal was to identify principal stress effectors that respond to nucleolar stress responses in *Drosophila*.

2.2 Results

2.2.1 Nucleolar Stress Caused by the Loss of Nopp140

We previously used the GAL4 system in *Drosophila* to express RNAi that targeted mRNAs encoding both Nopp140 isoforms (Figure 1.5) (Cui and DiMario 2007). Essentially two RNAi-expressing transgenes, *UAS-C3* and *UAS-C4.2*, were used in the following studies. Both effectively reduce Nopp140 levels when induced by GAL4. *UAS-C4.2* maps on the second chromosome, and *UAS-C3* maps on the third chromosome; both transgenes reside in the original *UAS-C4* line (Cui and DiMario 2007). For the sake of simplicity, we refer to *UAS-C4.2*, *UAS-C3,* or the original *UAS-C4* as *Nopp140-RNAi* in the text, but figure legends differentiate which transgene was actually used in the respective experiments.

Heterozygous *Act5C-GAL4>UAS-Nopp140-RNAi* lacked Nopp140 within most, but not all of their imaginal diploid cells (Figure 2.1, A and B) and polyploid cells (Figure 2.1, C and D). Polyploid cells lacking Nopp140 have condensed chromatin (Figure 2.1, C) (Cui and DiMario 2007). These larvae died in the late larval and early pupal stages when reared at 27-28^{o}C. While we used w^{1118} as our wild type control in Figure 2.1 (E-H), homozygous parental larvae develop normally (they are viable and fertile) with no detectable loss of Nopp140 in their tissues.

We compared tissues from *Act5C-GAL4>UAS-Nopp140-RNAi* larvae to the same tissues from wild type (w^{1118}) or parental type larvae by transmission

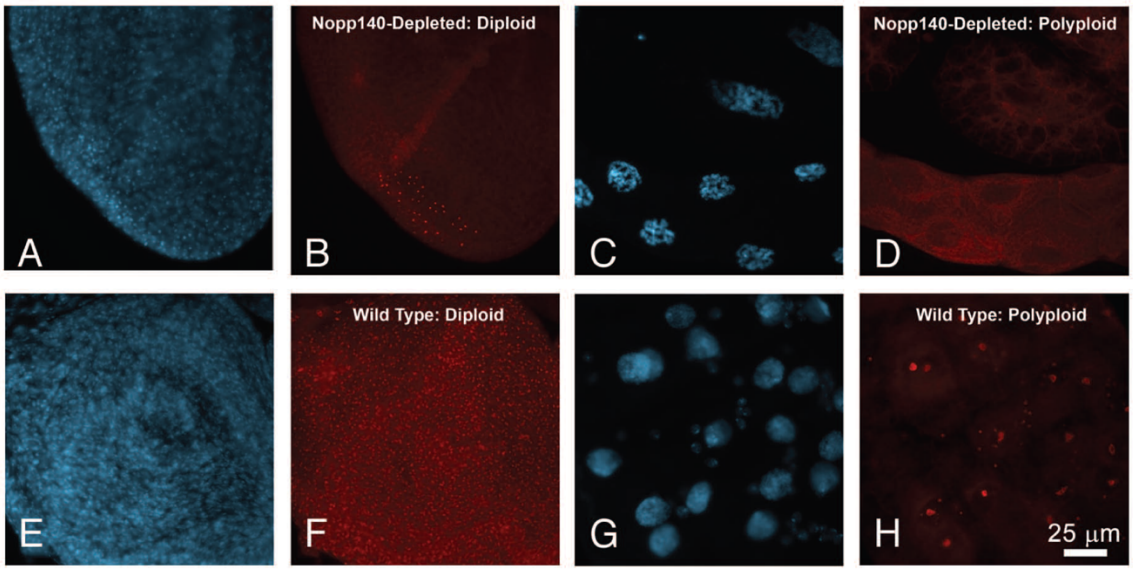

FIGURE 2.1. Selective loss of Nopp140 in *Act5C-GAL4>UAS-C4.2* Larvae. Expression of RNAi targeting *Nopp140* transcripts caused depletion of Nopp140 in most tissues as shown by DAPI staining and immuno-fluorescence microscopy using an antibody directed against a unique sequence within the carboxy terminal domain of Nopp140-RGG (Cui and DiMario 2007). (A and B) Nucleoli in most small diploid imaginal disc cells from *Act5C-GAL4>UAS-C4.2* larvae lacked Nopp140-RGG. A few cells retained detectable Nopp140-RGG in their nucleoli (B), due presumably to insufficient RNAi expression in these particular cells. (C and D) Nucleoli in giant polyploid cells from *Act5C-GAL4>UAS-C4.2* larvae also lacked Nopp140-RGG. Polyploid cells lacking Nopp140 contained condensed chromatin (Cui and DiMario 2007). (E and F) Nucleoli in most imaginal disc cells from wild type larvae stained with anti-Nopp140-RGG. (G and H) Nucleoli in polyploid midgut cells and the smaller imaginal island cells from wild type larvae stained well with the anti-Nopp140-RGG antibody. Scale bar: 25 μm for all images.

electron microscopy, immuno-blot analysis, and metabolic protein labeling to confirm that ribosome synthesis was disrupted due to Nopp140 depletion (*i.e.* nucleolar stress). A diploid cell from an *Act5C-GAL4>UAS-Nopp140-RNAi* larval wing disc (Figure 2.2, A) contained some rough endoplasmic reticulum, but the number of free ribosomes in the cytosol was greatly reduced compared to that in the wild type disc cell (Figure 2.2, B). In addition, the nuclei (Nu) in the

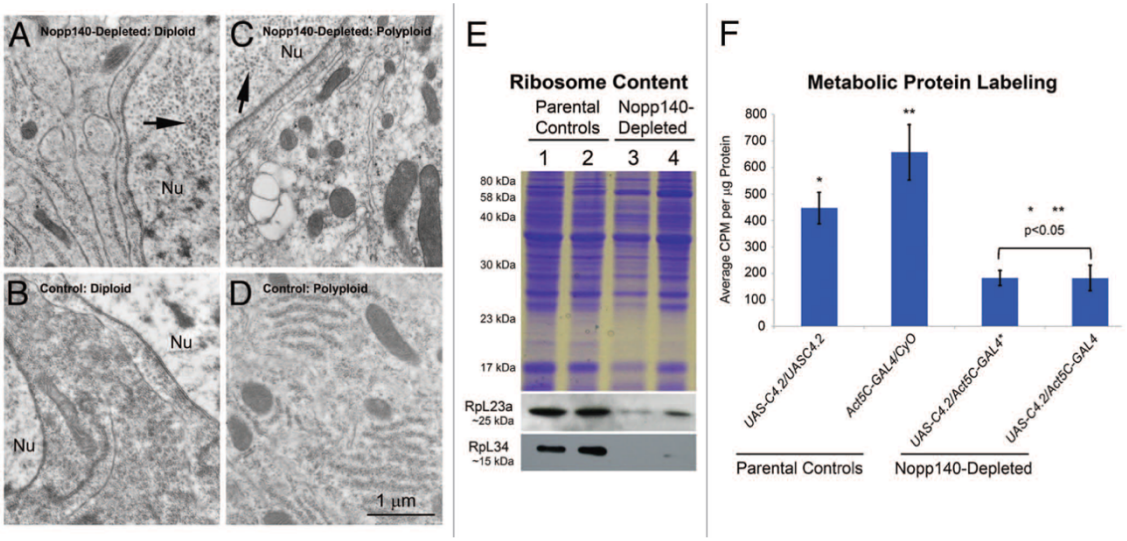

FIGURE 2.2. TEM, Immuno-blot Analysis, and Metabolic Protein Labeling Demonstrate Loss of Ribosomes and Protein Synthesis. (A–D) Separate tissues were isolated by hand and prepared for TEM analysis. Imaginal wing disc cells from *Act5C-GAL4>UAS-C4.2* larvae (A) contained fewer ribosomes as compared with similar cells from wild type control (w^{1118}) larvae (B). Polyploid midgut cells from *Act5C-GAL4>UAS-C4.2* larvae (C) contained far fewer ribosomes than did similar cells from wild type (w^{1118}) larvae (D). Nuclei (Nu) in *Act5C-GAL4>UAS-C4.2* larvae (panels A and C) contained numerous copia virus-like particles (arrows) indicating stress. Scale bar: 1 µm for all TEM images. (E) Upper gel: Coomassie-stained companion gel. Lower panels: specific antibodies showed a loss of RpL23a and RpL34 in lysates from *Act5C-GAL4> UAS-C4.2* larvae compared with parental type larvae. Lane 1: homozygous *UAS-C4.2* parental lysate; Lane 2: heterozygous *Act5C-GAL4/CyO-GFP* parental lysate; Lane 3: *RNAi*-expressing *UAS-C4.2/Act5C-GAL4* lysate; Lane 4: a separate *RNAi*-expressing *UAS-C4.2/Act5C-GAL4* lysate. (F) Metabolic protein labeling was significantly reduced in Nopp140-RNAi-expressing *UAS-C4.2/Act5C-GAL4* larvae compared with larval parental controls. The entire experiment was repeated three times. Absorbance values were determined in triplicate. Two-tailed p values were equated using t-Test analysis (two sample assuming unequal variances). *,** = $p < 0.05$ comparing parental controls and Nopp140-Depleted larvae.

Act5C-GAL4>UAS-Nopp140-RNAi diploid cells contained numerous virus-like particles (arrow in Figure 2.2, A). These particles likely arise from *copia* retrotransposons (Shiba and Saigo 1983) that can be induced by environmental

stress (Strand and McDonald 1985), aging (Gartner and Gartner 1976), or perturbations in poly(ADP-ribose) polymerase (Tulin et al. 2002). In preparing tissues for TEM analysis, we noted the small size of the imaginal discs isolated from *Act5C-GAL4>-UAS-Nopp140-RNAi* larvae. We have yet to determine if reduced disc size is due to smaller cells or failure to produce sufficient cell numbers. A polyploid midgut cell from an *Act5C-GAL4>UAS-Nopp140-RNAi* larva (Figure 2.2, C) contained relatively few ribosomes as compared to the same cell type from a wild type larva (Figure 2.2, D).

Again, the presence of virus-like bodies the nucleus (arrow in Figure 2.2, C) indicated these Nopp140-depleted polyploid cells were under stress. While *Act5C-GAL4>UAS-Nopp140-RNAi* imaginal discs failed to grow, brains from these larvae appeared normal in size; the brain cells showed normal levels of cytoplasmic ribosomes, and their nuclei were clear of virus-like bodies (image not shown). This was surprising since the endogenous *Act5C* gene is normally expressed at high levels in the larval central nervous system, and we expected the *Act5C-GAL4* transgene would be similarly expressed (Figure 1.5). One possibility is that Nopp140 expression levels may be sufficiently high in the larval central nervous system (Chintapalli et al. 2007) such that Nopp140-RNAi expression cannot effectively deplete enough Nopp140 to disrupt ribosome synthesis (http://flybase.org/reports/FBgn0037137.html).

By immuno-blot analysis (Figure 2.2, E), we saw a loss of ribosomal proteins RpL23A and RpL32 in third instar *Act5C-GAL4>UAS-Nopp140-RNAi* larvae (lanes 3 and 4) compared to the two respective parental larval types

(lanes 1 and 2). We note, however, that younger *Act5C-GAL4>UAS-Nopp140-RNAi* larvae that had yet to show obvious defects such as melanotic tumors (see below) contained near normal levels of ribosomal proteins (lane not shown). These younger larvae likely maintained sufficient quantities of maternal Nopp140 and ribosomes that dwindle as these larvae advanced further into the third instar stage.

To verify the effects of ribosome loss in third instar larvae, we compared metabolic protein labeling in parental control larvae versus *Act5C-GAL4>UAS-Nopp140-RNAi* larvae depleted for Nopp140. The loss of Nopp140, leading to the loss of ribosomes, caused a reduction in protein synthesis to ≤40% (Figure 2.2, F). In this assay, we analyzed two separate samples of *Act5C-GAL4>UAS-Nopp140-RNAi*. One sample (*) was older with a greater number of melanotic masses compared to the other, yet we saw similar protein labeling profiles in the two samples. We conclude from the various assays in Figure 2.2 that third instar *Act5C-GAL4>UAS-Nopp140-RNAi* larvae had a pronounced loss of ribosomes and thus protein synthesis, and this resulted in lethality by the late third larval instar to early pupal stages.

2.2.2 Selective Depletion of Nopp140 in Larval Wing Discs

To assess the loss of Nopp140 without inducing lethality, we used the larval wing disc driver, *A9-GAL4,* on the *X* chromosome to induce the *Nopp140-RNAi* gene (*UAS-C4.2* on the second chromosome) (*A9-GAL4>UAS-C4.2*). We set up the cross such that all male progeny displayed normal wings. Conversely, female progeny (*A9-GAL4>UAS-Nopp140-RNAi*) expressed RNAi in their larval

wing discs, which eventually led to malformed adult wings. The wing phenotype in these females varied from a relatively mild upward curl along the anterior and posterior edges of the wing to severely shriveled (vestigial-like) wings (see Figure 2.3). Large fluid-filled blisters were common in the wings of newly eclosed females. Their wings were left badly malformed as the blisters receded over time. Figure 2.3 compares the frequency of the severe wing phenotype to that of the less severe curled wing phenotype. While all the male progeny had normal wings, 47% of the *A9-GAL4>UAS-Nopp140-RNAi* females showed wings with the mild defect, and the remaining 53% showed the severe defect. None of the females had normal wings. We conclude that *A9-GAL4>UAS-Nopp140-RNAi* provides a non-lethal phenotype that we can score to access nucleolar stress in diploid imaginal (progenitor) wing disc cells.

Progeny Genotypes / Progeny Phenotypes	*w⁻/Y; UAS-C4.2/+; +/+* ♂♂	*A9/w⁻; UAS-C4.2/+; +/+* ♀♀	*w⁻/Y; UAS-C4.2/+; Δp53/Δp53* ♂♂	*A9/w⁻; UAS-C4.2/+; Δp53/Δp53* ♀♀
Normal wings 	100%	0%	100%	0%
Mild wing edge curl 	0%	47%	0%	42%
Severe wing malformation 	0%	53%	0%	58%
Number of Flies Scored	270	172	143	178

FIGURE 2.3. Expression of Nopp140-RNAi in Wing Discs With or Without p53 Present. The X and/or Y chromosome, second chromosome, and third chromosome designations are separated by semi-colons. Male larvae (w^{1118}/Y) lacked the *A9-GAL4* driver and therefore did not express *RNAi* from *UAS-C4.2* on their second chromosome. Female larvae ($A9/w^{1118}$) expressed *RNAi* to deplete Nopp140 in their wing discs. Two crosses were performed, with (+) and without (Δ) the *p53* gene on the third chromosome. Abnormal wing phenotypes appeared in only the females as either a mild wing edge curl or a more severe vestigial-like (shriveled) wing. Phenotype frequencies were comparable with or without the *p53* gene.

TCS arises in mammals when specialized embryonic neural crest cells undergo apoptosis due to the loss of Treacle (Jones et al. 2008). To determine if nucleolar stress caused by the loss of Nopp140 in *Drosophila* wing discs also induces apoptosis, we reversed the original cross for Figure 2.3 such that homozygous *A9-GAL4* driver females were crossed to males homozygous for *Nopp140-RNAi.* All larval progeny from this cross expressed Nopp140-RNAi in their wing discs. We probed these wing discs with anti-cleaved Caspase 3 (Asp175) from Cell Signaling Technology. Although the precise antigen remains unknown, this particular antibody provides a good marker for Caspase-9-like DRONC activity in apoptotic *Drosophila* cells (Fan and Bergmann 2010). A wing disc from an *A9-GAL4>UAS-Nopp140-RNAi* larva was heavily labeled by anti-Caspase (Figure 2.4, A-C). Higher magnification showed that the apoptotic cells contained condensed chromatin within their nuclei (Figure 2.4, D), and that anti-Caspase 3 labeled the cytoplasm (Figure 2.4, E) as expected. Wing discs from wild type larvae (w^{1118}) showed minimal anti-caspase labeling (Figure 2.4, F-H). Therefore, as with the loss of Treacle in mammalian neural crest cells, selective loss of Nopp140 in *Drosophila* imaginal wing disc cells induced apoptosis leading to malformed wings in adult flies.

2.2.3 Apoptosis Induced by Nucleolar Stress is p53 Independent

Jones et al. (2008) showed that apoptosis induced by nucleolar stress in mouse embryonic neural crest cells was p53-dependent. The deletion of the mouse *p53* gene or chemical inactivation of p53 suppressed this apoptosis, reducing the severity of phenotypes typically associated with TCS. To test if

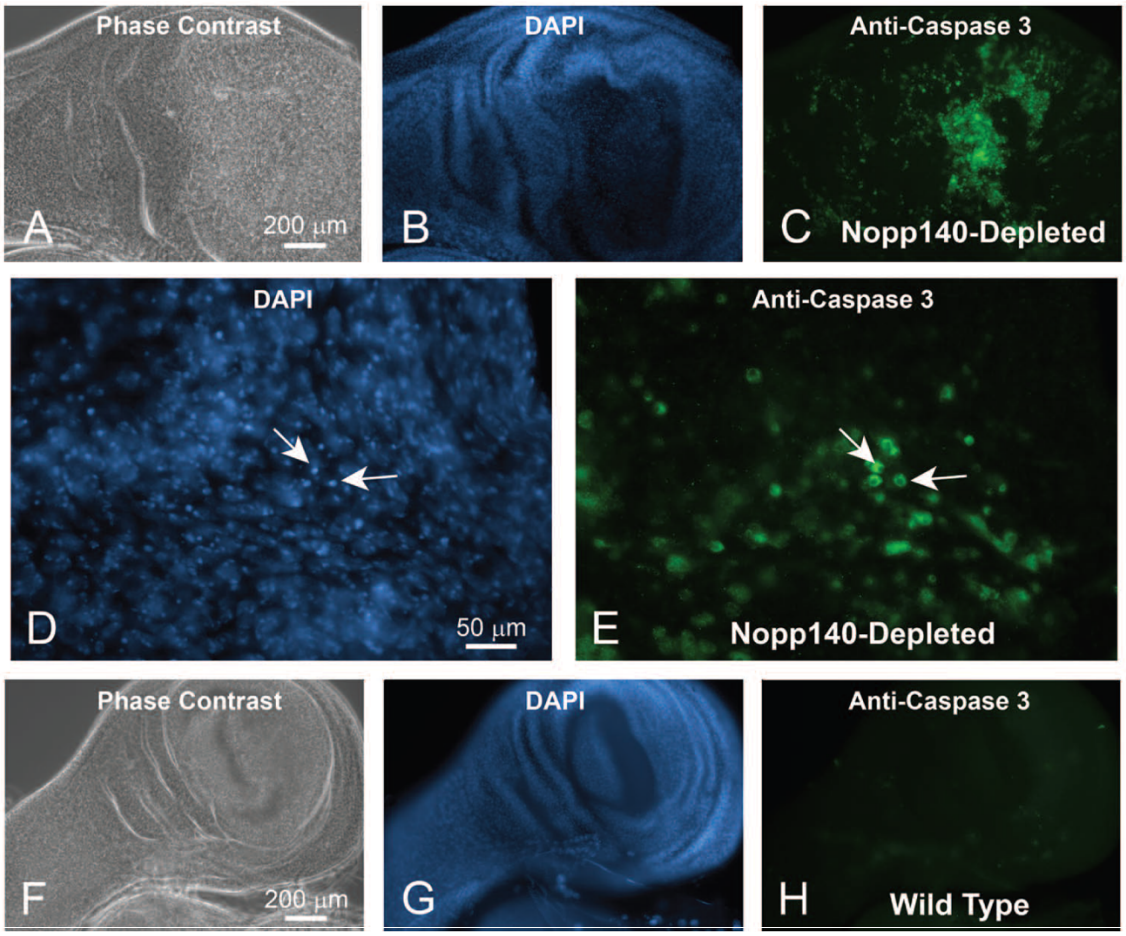

FIGURE 2.4. Loss of Nopp140 in Imaginal Wing Discs of *A9-GAL4>UAS-C4.2* Larvae Resulted in Apoptosis. Phase contrast (A) and DAPI staining (B) of a wing disc isolated from an *A9-GAL4>UAS-C4.2* larva. (C) The wing disc stained heavily with anti-Caspase 3 indicating apoptosis. (D,E) Higher magnification of panels B and C showed anti-Caspase 3 staining in the cytoplasm as expected. Cells with copious anti-Caspase 3 labeling showed condensed chromatin by DAPI staining (arrows). (F–H) Wing discs from control (w^{1118}) larvae were probed with anti-Caspase 3 antibody. They showed minimal background labeling.

apoptosis in *Drosophila* imaginal wing discs resulting from depletion of Nopp140 is p53-dependent, we repeated the original cross described in Figure 2.3 such that only female progeny would display wing defects, but this time the two parental types (the *A9-GAL4* driver and the Nopp140-RNAi-expressing lines) were homozygous for the *p53* gene deletion ($p53^{[5A-1-4]}$) on the third chromosome

(referred to simply as Δ*p53,* diagrammed in Figure 2.5, A). This deletion was originally described by Rong et al. (2002); homozygous deletion flies are viable and fertile, but they display reduced apoptosis in response to DNA damage caused by ionizing radiation (Jaklevic and Su 2004; Wichmann et al. 2006; Wichmann et al. 2010).

Genomic PCRs verified that the modified parental lines were in fact deleted for *p53* (Figure 2.5, B and C). The wild type *p53* gene in w^{1118} flies produced the expected 7.3 kbp PCR product (Figure 2.5, C, lane 1), while the

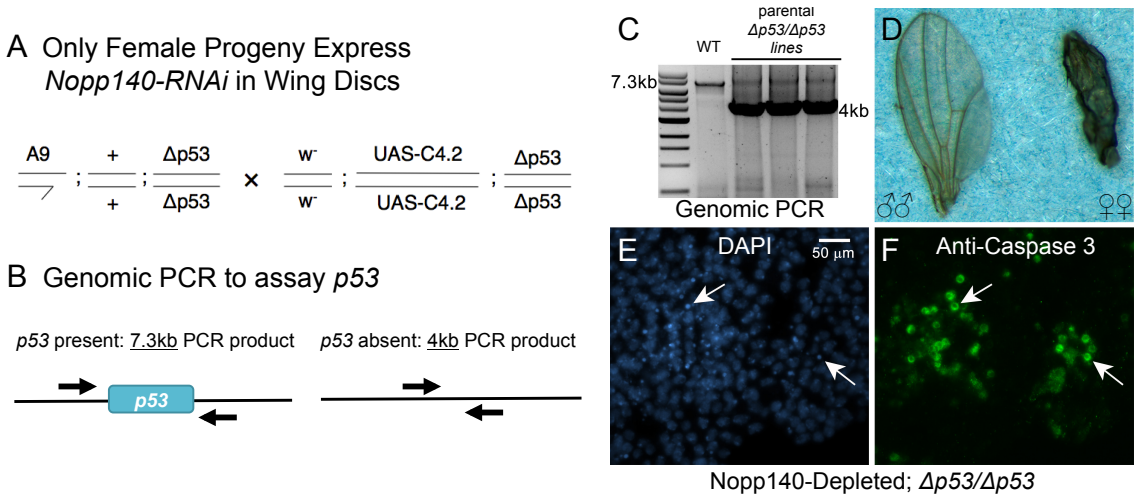

FIGURE 2.5. Verifying the *p53* Gene Deletion in Parental Stocks and Establishing p53-independent Apoptosis in Nopp140-depleted Wing Discs. (A) The cross reported in Figure 2.3 was repeated using the *A9-GAL4* and *UAS-C4.2* lines that were homozygous for *Δp53.* (B and C) The p53 gene deletion was verified using genomic PCR. The 7.3 kb band denotes presence of the wild type p53 gene while the 4.0 kb band denotes its deletion. Tested genotypes were: w^{1118} stock (WT, wild-type) (lane 1), *A9-GAL4/A9-GAL4; +/+; Δp53/Δp53* (the GAL4 driver) (lane 2), the original *Δp53/Δp53* stock (Bloomington 6815) (lane 3), w^{1118}/w^{1118}*; UAS-C4.2/UAS-C4.2; Δp53/Δp53* (RNAi) (lane 4). (D) Adult male progeny (w^{1118}*/Y; UAS-C4.2/+; Δp53/Δp53*) again produced normal wings (left wing), while female progeny (*A9-GAL4/*w^{1118}*; UAS-C4.2/+; Δp53/Δp53*) expressed RNAi to deplete Nopp140 and again displayed malformed wings (right wing). (E and F) Apoptosis was evident in the larval wing discs of *A9-GAL4>UAS-C4.2; Δp53/Δp53* larvae as shown by anti-Caspase 3 labeling within the cytoplasm. White arrows point to corresponding nuclei containing condensed chromatin.

modified *A9-GAL4* driver (Figure 2.5, C, lane 2), the original *p53Δ/p53Δ* stock from the Bloomington Stock Center (Figure 2.5, C, lane 3), and the *Nopp140-RNAi* line (Figure 2.5, C, lane 4) produced the expected 4.0 kbp product indicating homozygous deletion of the *p53* gene (for descriptions of expected PCR products, please see Flybase, http://flybase.org/reports/FBrf0151688.html). Thus, all *A9-GAL4>UAS-Nopp140-RNAi* progeny from this second cross should be homozygous deficient for the *p53* gene. While the male progeny from this cross had normal wings as expected (Figure 2.5, D, left wing), all female progeny again displayed malformed wings (Figure 2.5, D, right wing). Figure 2.3 again summarizes the results: of the female progeny obtained, 42% displayed the less severe curled wing edge phenotype, while 58% showed the more severe shriveled wing phenotype (Figure 2.3). This compares well to 47% and 53%, respectively, for those female progeny that were homozygous for the wild type *p53* gene. We note that variability in wing phenotype in both crosses (with and without *p53*) may be caused by slight temperature fluctuations affecting GAL4-mediated induction of *UAS*-transgenes. To minimize this effect, all crosses were performed at 27-28^{o}C.

We again reversed the cross such that all progeny were *A9-GAL4>UAS-Nopp140-RNAi; Δp53/Δp53*. These larvae also showed apoptosis in wing discs by anti-Caspase 3 labeling (Figure 2.5, E and F). We performed these crosses several times to be certain that the presence or absence of p53 had no effect on wing malformations due to Nopp140 depletion. The combined data in Figure 2.3

indicates that there were no appreciable differences in the abnormal wing phenotypes due to Nopp140 depletion when *p53* was present or deleted. We conclude, therefore, that larvae selectively depleted for Nopp140 in their wing discs, induce apoptosis in these discs, but in a p53-independent manner.

2.2.4 Autophagy in Polyploid Midgut Cells

In earlier studies to examine the loss of Nucleostemin I in *Drosophila* larvae, we observed by TEM premature autophagy in larval polyploid hindgut cells (Rosby et al. 2009). Here, we ectopically co-expressed mCherry-ATG8a (Chang and Neufeld 2009) to determine if excessive autophagy occurred in midgut cells of Nopp140-depleted (*da-GAL4>UAS-C4.2*; *UAS-mCherry-ATG8a*) third instar larvae. We first expressed mCherry-ATG8a in the midgut of a second instar larva using the *da-GAL4* driver, but in an otherwise wild type background; mCherry-ATG8a distributed diffusely throughout these midgut cells (Figure 2.6, A). As a positive control for autophagy, we starved similar second instar larvae to induce autophagy (Wu et al. 2009). As expected, mCherry-ATG8a aggregated into vesicles within the cytoplasm of these midgut polyploid cells (Figure 2.6, B). We interpret the appearance of these vesicles as autophagosomes and lysosomes (Neufeld 2012). Similar vesicles with mCherry-ATG8 appeared prematurely and in great abundance in the midgut of Nopp140-depleted larvae (*da-GAL4>UAS-C4.2; UAS-mCherry-ATG8a*) (Figure 2.6, C). Thus, the loss of Nopp140 and nucleolar function induces premature autophagy in the polyploid midgut cells.

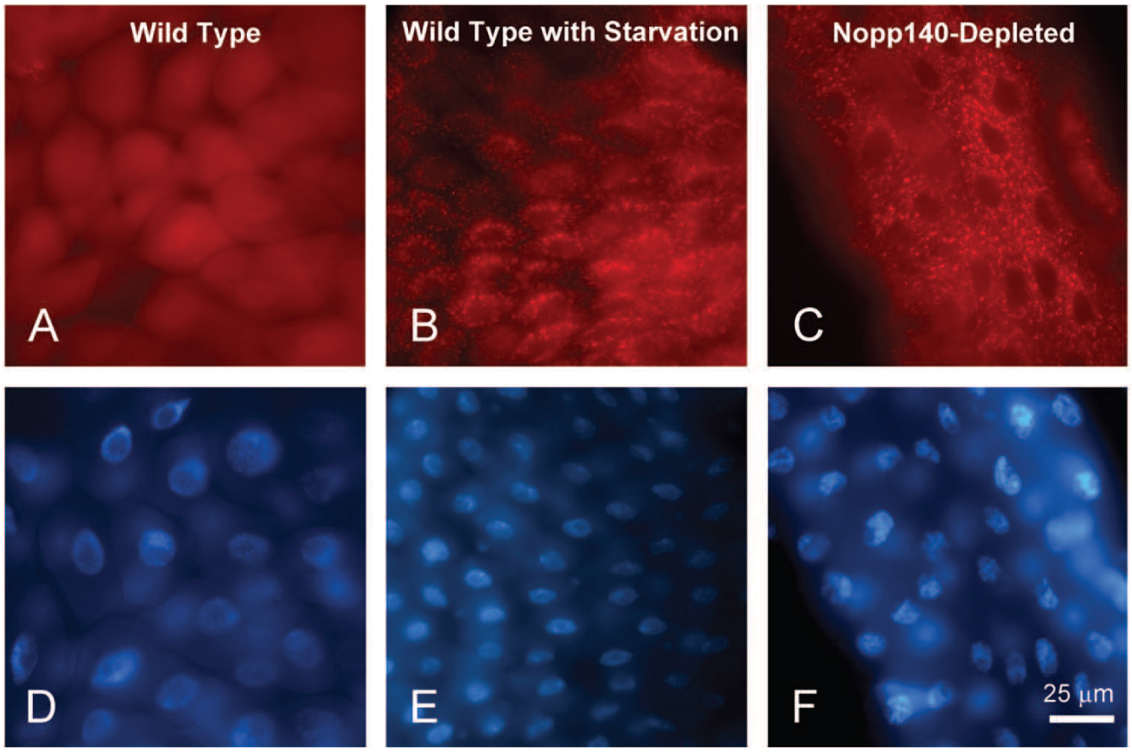

FIGURE 2.6. Autophagy Prominent in Larval Polyploid Cells Depleted for Nopp140. (A and D) *da-GAL4>UAS-mCherry-ATG8* in a wild type background. Labeling remained diffuse throughout the cell. (B and E) As a positive control for autophagy, similar *da-GAL4>UAS-mCherry ATG8a* larvae were starved of amino acids. The accumulation of mCherry-ATG8a into autophagosomes and lysosomes (red speckling in the cytoplasm) indicated autophagy as expected due to starvation. (C and F) Well fed *da-GAL4>UAS-C4.2; UAS-mCherry-ATG8a* larvae displayed similar accumulations of mCherry-ATG8a into cytoplasmic vesicles within their midgut cells indicating premature autophagy in response to the loss of Nopp140.

2.2.5 Accumulation of Phenoloxidase A3

Coomassie-stained SDS-gels showed an abundant 70 kDa protein in whole lysates of *Act5C-GAL4>UAS.C4.2* and *Act5C-GAL4>UAS.C4* larvae (expressing Nopp140-RNAi) versus parental control larvae (Figure 2.7, A). At first, we thought the accumulated protein was a classic heat shock protein (Hsp70), or perhaps a heat shock consensus protein (Hsc70) that was induced

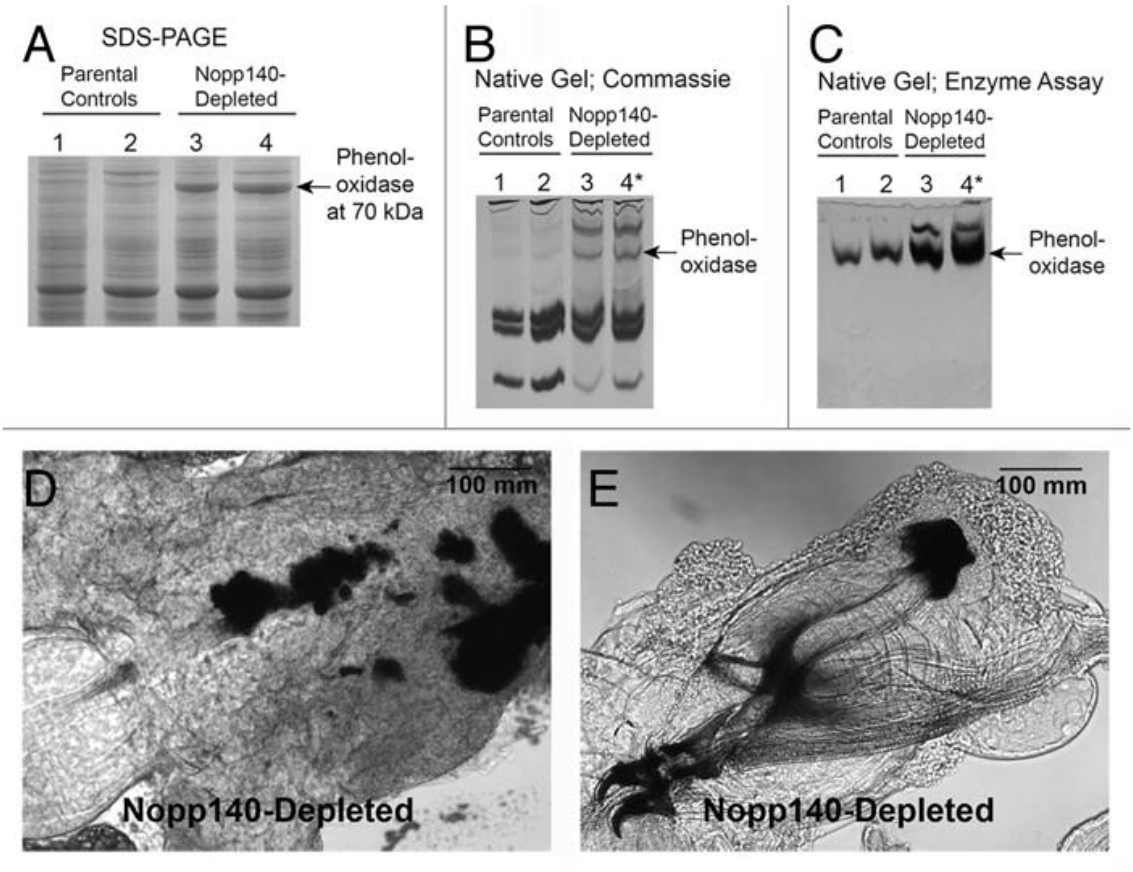

FIGURE 2.7. Phenoloxidase A3 Accumulated in Nopp140-depleted Larvae. (A) Whole larval lysates from parental control larvae (*Act5C-GAL4/CyO*, lane 1; homozygous *UAS-C4.2*, lane 2) were compared with those from Nopp140-depleted larvae (*UAS-C4.2/Act5C-GAL4*, lane 3; *UAS-C4/Act5C-GAL4*, lane 4). *UAS-C4* is the original stock containing *UAS-C4.2* on the 2nd chromosome and *UAS-C3* on the 3rd chromosome. The prominent 70 kDa protein in the lysates of Nopp140-depleted larvae (arrow) was identified by LC-MS/MS as phenoloxidase A3. (B) Hemolymph proteins were resolved on a native polyacrylamide gel and stained with Coomassie Blue. Parental control larvae were homozygous *UAS-C4.2* (lane 1) and *Act5C-GAL4/CyO* (lane 2). *Nopp140-RNAi*-expressing *UAS-C4.2/Act5C-GAL4* larvae (lane 3) with only a few melanotic masses were compared with similar *UAS-C4.2/Act5C-GAL4** larvae (lane 4) that had excess melanotic masses. (C) A native gel similar to that shown in panel B but stained for phenoloxidase activity using tyrosine as substrate. Arrows in B and C mark the position of the most prominent phenoloxidase activity. (D) Melanotic masses were found mostly in the midgut of *Act5C-GAL4> UAS-C4.2* larvae. (E) Melanotic masses also occurred at other sites within *Act5C-GAL4>UAS-C4.2* larvae. This large mass accumulated at the tips of the dorsal arms of the pharyngeal sclerite.

upon nucleolar stress. However, antibodies against Hsp70 and Hsc70 failed to show significant accumulations of either protein in the Nopp140-depleted larvae. LC-MS/MS finally identified the protein as phenoloxidase A3 encoded by *PO45* (conceptual gene *CG8193)* in *Drosophila melanogaster*.

Phenoloxidases in *Drosophila* are released into the hemolymph from circulating crystal cells, usually as part of an innate immune response to parasitic infection. Upon infection, the phenoloxidases convert phenols to quinones that polymerize to form melanin aggregates that then encapsulate the parasite (Tang 2009). To test if phenoloxidases were released to the hemolymph of Nopp140-depleted larvae, we isolated larval serum proteins (Roberts et al. 1977), resolved them on native polyacrylamide gels, and then either stained the gels with Coomassie Blue (Figure 2.7, B) or stained the gels for phenoloxidase activity using tyrosine as substrate (Figure 2.7, C) (Asano and Takebuchi 2009). Compared to parental types, *Act5C-GAL4>UAS-Nopp140-RNAi* larvae showed greater amounts of phenoloxidase in their hemolymph, indicating another phenotype associated with the loss of nucleolar function. In collecting the *Act5C-GAL4>UAS.C4.2* larvae (expressing Nopp140-RNAi), we purposely pooled larvae with numerous melanotic masses. These larvae are designated with an asterisk in Figure 2.7, and they showed more phenoloxidase in their hemolymph than did other *Act5C-GAL4>UAS-C4.2* larvae with only a few melanotic masses.

We noted previously the accumulation of melanotic masses (tumors) in Nopp140-depleted larvae and pupae (Cui and DiMario 2007). These masses

seem to arise preferentially in the midgut (Figure 2.7, D), but we also found melanotic masses scattered throughout the larva; for example, Figure 2.7, E shows melanotic masses at the ends of the dorsal arms of the pharyngeal sclerite. The observed rise in phenoloxidase abundance in whole lysates and its accumulation in the hemolymph correlate well with the appearance of melanotic masses in Nopp140-depleted larvae.

2.2.6 JNK and Pro-apoptotic Hid are Activated

Thus far we have documented three stress response phenotypes that arise due to the loss of nucleolar function: apoptosis in imaginal wing discs, autophagy in polyploid midgut cells, and the formation of melanotic masses due to the release of phenoloxidase from crystal cells. JNK (also known as the stress-activated protein kinase, SAPK) is a principal cell stress response effector (Lin 2003; Weston and Davis 2007) that could link all three phenotypes. Activated *Drosophila* JNK (also referred to as basket) is known to induce apoptosis by activating *Hid* (Bilak and Su 2009) and autophagy by inducing *dFoxo* (Juhász et al. 2007; Chang and Neufeld 2010*)*. Activated JNK also induces the rupture of crystal cells to release phenoloxidases (Bidla et al. 2007). Therefore, we tested if *Drosophila* JNK is activated in Nopp140-depleted larvae (Figure 2.8, B). Activation of human JNK is marked by the phosphorylation of residues Thr183 and Tyr185. These residues are conserved in the one isoform of JNK expressed in *D. melanogaster*. The rabbit monoclonal antibody 81E11 from Cell Signaling cross-reacted well with activated *Drosophila* JNK on immuno-blots (Figure 2.8, B). Whole lysates from *Act5C-GAL4>UAS-Nopp140-RNAi* larvae showed an

elevated level of activated JNK versus lysates from parental controls. We conclude that activated JNK accumulates in Nopp140-depleted larvae.

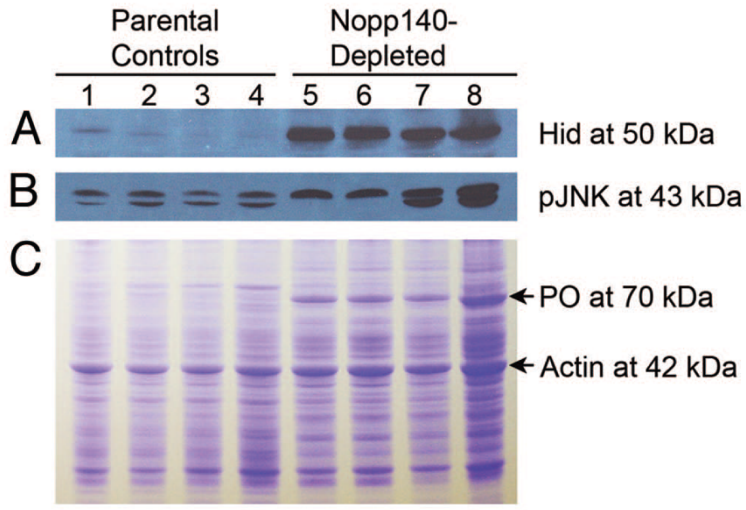

FIGURE 2.8. Pro-apoptotic Hid and Activated JNK Up-regulated in Nopp140-depleted Larvae. (A) An immuno-blot containing lysates from parental control larvae (lanes 1–4) and *Act5C-GAL4>UAS-Nopp140-RNAi* larvae (lanes 5–8) was probed with rabbit anti-Hid (Ryoo et al. 2004). Hid at ~50 kDa was substantially increased in the Nopp140-depleted larvae as compared with parental larvae. Lane 1: homozygous *UAS-C4.2*; Lane 2: *Act5C-GAL4/CyO*; Lane 3: *Act5C-GAL4/+*; Lane 4: *CyO-GFP/+*, Lanes 5 and 7: *UAS-C4.2/Act5C-GAL4*; Lanes 6 and 8: *UAS-C4/Act5C-GAL4*. *UAS-C4* is the original transgenic stock that contains *UAS-C4.2* on the 2nd chromosome and *UAS-C3* on the 3rd chromosome. (B) A companion blot with the same lysates was probed with rabbit monoclonal antibody 81E11 (Cell Signaling #4668) directed against phospho-JNK at 43 kDa. (C) Equal amounts of the same lysates as used in panels A and B were resolved on a Coomassie-stained SDS-gel. Phenoloxidase A3 (PO) is at 70 kDa.

The anti-pJNK immuno-blot (Figure 2.8, B) showed two bands in some lysate preparations from both parental types and from the Nopp140-depleted larvae, while we saw only the higher molecular weight band in other separately prepared lysates. At this time, we have no clear explanation for the appearance of the bottom band other than partial proteolysis.

In their model of p53-independent apoptosis in *Drosophila*, McNamee and Brodsky (2009) proposed that JNK induces Hid protein expression that then induces apoptosis. To test if *Hid* was induced, we probed the same lysates used in Figure 2.8, B with a rabbit polyclonal antibody directed against *Drosophila* Hid (Ryoo et al. 2004). We found Hid levels notably increased in *Actin5C-GAL4>UAS-Nopp140-RNAi* larvae versus parental controls (Figure 2.8, A).

2.3 Discussion

The human TCS results from mutations in the *TCOF1* gene that encodes the nucleolar phosphoprotein, Treacle. Subsets of embryonic neural crest cells are particularly sensitive to the loss of Treacle, a nucleolar chaperone for ribosome biosynthesis. These cells normally migrate to populate embryonic branchial arches I and II that then give rise to adult craniofacial structures. Without Treacle, these neural crest cells fail to meet a relatively high threshold requirement for functional ribosomes. As a result, these cells are stressed and undergo p53-dependent apoptosis. Their loss ultimately leads to the craniofacial malformations associated with the TCS. Jones et al. (2008) could alleviate the syndrome by blocking p53 function either by a *p53* gene deletion or by a specific p53 protein inhibitor.

Vertebrate Nopp140 and Treacle are related in structure and function (He and DiMario 2011). Both proteins are over 100 kDa in size, both contain LisH dimerization motifs in their amino terminal region, and both proteins contain a large central domain consisting of alternating acidic and basic motifs with similar amino acid compositions; the acidic motifs are rich in Glu, Asp, and phospho-Ser,

while the basic motifs are rich in Lys and Pro. Both proteins are believed to function as chaperones for snoRNP complexes, which direct site-specific methylation and pseudouridylation of pre-rRNA within the dense fibrillar regions of eukaryotic nucleoli. While most snoRNAs appear to be non-essential when individually deleted, failure to collectively modify pre-rRNA by the loss of a snoRNP chaperone would likely produce defective or partially functional ribosomes in all cells. Embryonic progenitor cells with high demands for protein synthesis would be most susceptible to the loss of functional ribosomes. Loss of these cells would lead to lethality or developmental defects. Thus, Treacle and Nopp140 are required for normal development. Despite their multiple similarities, Nopp140 and Treacle differ in their carboxy termini, suggesting that each protein maintains its own unique interactions and functions. Interestingly, while *Drosophila* expresses two isoforms of Nopp140 by alternative splicing (Waggener and DiMario 2002), *Drosophila* lacks a Treacle ortholog.

We showed that larval cells depleted for Nopp140 undergo a disruption in ribosome biosynthesis (nucleolar stress). Larval tissues expressing Nopp140-RNAi, both diploid and polyploid, have fewer ribosomes than wild type (Figure 2.2, A-D). These larvae also have reduced amounts of ribosomal proteins RpL23a and RpL32 (Figure 2.2, E). Metabolic labeling verified these findings, revealing that Nopp140-depleted larvae synthesize significantly reduced amounts of protein (≤40%) compared to parental controls (Figure 2.2, F). As larval tissues develop, maternally supplied ribosomes and Nopp140 diminish, and cells expressing Nopp140-RNAi are unable to supply either functional ribosomes and

or sufficient protein synthesis. This nucleolar stress leads to distinctive cell death pathways.

Here we showed that the loss of *Drosophila* Nopp140 specifically in imaginal wing disc cells lead to apoptosis and impaired wing development, analogous to the loss of Treacle in embryonic neural crest cells. However, while Jones et al. (2008) rescued the TCS in mice by employing a *p53* gene deletion, the similar rescue failed in *Drosophila* as apoptosis occurred in the absence of the *p53* gene (Figure 2.4). Induction of apoptosis in the absence of p53 has been well documented in *Drosophila* (Wichmann et al. 2006; McNamee and Brodsky 2009).

Besides apoptosis, we documented a strong and premature induction of autophagy in larval midgut polyploid cells that were depleted for Nopp140 (Figure 2.6, C). As with apoptosis, JNK activation (phosphorylation) is reportedly linked to autophagy induction (Wu et al. 2009) by way of the downstream activation of dFoxo (Juhász et al. 2007). We note, however, that this stress-induced autophagy is in contrast to a JNK-independent induction of autophagy that normally occurs during development or in response to starvation resulting in the inhibition of Tor signaling (Wu et al. 2009; Neufeld 2012).

We also showed that formation of excess melanotic masses in Nopp140-depleted larvae was coincident with the accumulation of phenoloxidase A3 both in whole larval lysates (Figure 2.7, A) and in the larval hemolymph (Figure 2.7, B and C). While phenoloxidases are normally synthesized and stored in crystal cells, they are not secreted in a typical secretory pathway; rather, crystal cells

rupture in a JNK-dependent manner releasing the phenoloxidases to the hemolymph (Tang 2009; Bidla et al. 2007). How Nopp140-depleted larvae synthesize excess amounts of phenoloxidase when nucleolar function (ribosome biosynthesis) is impaired remains a perplexing question. Since the Nopp140-depleted larvae are developmentally delayed, we speculate that phenoloxidase A3 may simply amass in abundance over time despite a slow rate of protein synthesis as compared to wild type larvae. This could explain the excess accumulations of phenoloxidase in whole larval lysates as shown by Coomassie-stained gels (Figure 2.7, A). The activation of JNK in the Nopp140-depeleted larvae may then release the phenoloxidase to the hemolymph as shown in the hemolymph enrichments (Figure 2.7, B and C).

Many of the melanotic masses we saw seemed to reside within non-hematopoietic tissues such as the midgut, trachea, and salivary glands (Minakhina and Steward 2006). One possibility suggested by Bidla et al. (2007) is that apoptosis followed by secondary necrosis triggers formation of melanotic masses. If so, we would expect to see the formation of multiple melanotic masses at non-hematopoietic sites undergoing heavy apoptosis and secondary necrosis.

2.3.1 Nucleolar stress in *Drosophila* versus mammals

Our working hypothesis is that depletion of Nopp140 in *Drosophila* cells disrupts normal ribosome biogenesis, a term now referred to as “nucleolar stress” (Mayer and Grummt 2005; Tollini et al. 2011). Studies on nucleolar stress in mammalian cells have focused primarily on the nucleolar protein Arf ($p19^{Arf}$ in

mice, $p14^{Arf}$ in humans), its interactions with MDM2, which is the E3 ubiquitin ligase for p53, and the role that nucleolar protein B23 (Nucleophosmin) plays in sequestering Arf to the nucleolus (Tollini et al. 2011). Upon stress in mammalian cells, Arf indirectly activates p53 by interacting with MDM2 to suppress its ubiquitination of p53. Under these conditions, p53 accumulates and activates genes necessary for cell cycle arrest, senescence, or apoptosis. Interestingly, *Drosophila* lacks identifiable Arf, MDM2, and B23. Hence, nucleolar stress in *Drosophila* likely plays out by an alternative mechanism.

From our work, JNK appears to be a common link between *Hid* (apoptosis), *dFoxo* (autophagy) (Wu et al. 2009; Juhász et al. 2007), and the release of phenoloxidases from crystal cells as these cells rupture in JNK-dependent manner (Bidla et al. 2007). We showed by immuno-blot analysis that Hid levels rise (Figure 2.8, A), coincidently with activated JNK (Figure 2.8, B) in Nopp140-depleted larvae. While JNK activation has been reported to be delayed in the p53-independent mechanism (Wichmann et al. 2006; Gowda et al. 2012), once activated, JNK is thought to induce *Hid* expression and thus apoptosis (McNamee et al. 2009). While we have yet to assess the abundance and activities of dFoxo and dFos in the Nopp140-depleted larvae, others have shown that Hid induction results from JNK activation via these two transcription factors (Bilak and Su 2009; Luo et al. 2007). From the combined evidence, we propose that JNK is a central effector activated in response to perturbations in *Drosophila* ribosome biogenesis.

JNK is a member of the MAP kinase superfamily, and while mammals express multiple forms of JNK, *Drosophila melanogaster* expresses only one version of JNK (basket). Precisely how *Drosophila* JNK is activated in response to nucleolar failure remains unknown. As a clue, Moreno et al. (2002) showed that JNK signaling is required for the apoptotic elimination of slowly proliferating *Minute*$^{-/+}$ cells in larval wing discs where *Minute*$^{-}$ is a dominant, haplo-insufficient mutation in a gene encoding a ribosomal protein (Marygold et al. 2007). McNamee and Brodsky (2009) proposed that gene haplo-insufficiencies in these same ribosomal protein genes could induce expression of *brinker* (*brk*) which encodes a transcription factor in larval wing discs, and that brk is sufficient to activate JNK, thus leading to apoptosis. Also upstream of *Drosophila* JNK are at least two JNKKs (Hemipterous and MKK4) and several JNKKKs. Puckered is the *Drosophila* protein phosphatase that is also induced by JNK to deactivate JNK in a negative feedback loop. How Hemipterous and Puckered are regulated upon nucleolar stress in *Drosophila* remains unknown. Our future efforts in linking nucleolar stress to JNK activation will examine the expression levels of *brk*, *hemipterous* and *puckered*.

Finally, JNK signaling has been implicated in direct nucleolar function. For example, mammalian JNK2 phosphorylates the RNA polymerase I transcription factor, TIF-IA, to down-regulate rRNA synthesis (Mayer et al. 2005). JNK activity was also required for the release of B23 and p19^{Arf} from mammalian nucleoli upon UV radiation (DNA-damage) (Yogev et al. 2008). Conversely, Mialon et al. (2008) showed that upon genetic or chemical inhibition of JNK signaling, the

mammalian nucleolar RNA helicase, DDX21, is partially redistributed to the nucleoplasm and that rRNA processing is inhibited. Their observation suggests that besides stress-induced JNK-activation, JNK signaling maintains homeostasis for the nucleolus in non-stressed cells. Thus the effects of activated JNK on the localization of *Drosophila* nucleolar components during normal cell growth and upon stress remain largely unknown, but subject for future investigation.

2.4 Materials and Methods

2.4.1 Fly lines

Fly lines expressing short hairpin RNA specific for the common 5' end of mRNAs that encode the two Nopp140 isoforms were *P{w[+mC]=UAS-Nopp140.dsRNA}*^{C3} and *P{w[+mC]=UAS-Nopp140.dsRNA}*$^{C4.2}$ as described previously (Cui and DiMario 2007). Here we refer to them simply as *UAS-C3* and *UAS-C4.2*. *UAS-C3* resides on the third chromosome. The original *UAS-C4* line contained two RNAi-expressing transgenes: one on the second chromosome and the other on the third chromosome. The transgene on the third chromosome is *UAS-C3*. We isolated the second chromosome from *UAS-C4*, and refer to the resulting line as *UAS-C4.2*. Both *UAS-C3* and *UAS-C4.2* lines are homozygous viable and fertile. The *P{UAS-mCherry-Atg8a}* line, D169 (third chromosome), was a kind gift from Thomas Neufeld (Chang and Neufeld 2009). Four additional lines came from the Bloomington *Drosophila* Stock Center; stock 6815 is a deletion for the *p53* gene (*p53*$^{[5A-1-4]}$) (Rong et al. 2002). We refer to this deletion simply as *p53*Δ throughout this report. GAL4 driver lines included

P{w[+mC]=Actin5C-GAL4}25FO1/CyO (stock 4414, referred to simply as *Act5C-GAL4*), the homozygous *daughterless-GAL4* line on the third chromosome (stock 8641, referred to as da-GAL4), and the wing disc-specific *P{w[+m*]=GAL4}A9* on the *X* chromosome (stock 8761, referred to here as *A9-GAL4*). A9-GAL4 expresses GAL4 strongly in larval wing and haltere discs (Haerry et al. 1998). We previously used the w^{1118} line (Bloomington stock 3605) to construct our RNAi-expressing transgenic lines (Cui and Dimario, 2007), and we use it here as our "wild type" control. All stocks were reared at 22-24°C on standard *Drosophila* medium. Genetic crosses using GAL4 drivers were kept at 27-28°C.

2.4.2 Genomic PCR to verify p53Δ

Genomic DNA from adult flies was prepared according to E. Jay Rehm of the Berkeley *Drosophila* Genome Project (http://www.fruitfly.org/about/methods/inverse.pcr.html). Primers for verifying the *p53* gene deletion ($p53^{[5A-1-4]}$) were described by K. Golic in a reference report to FlyBase (http://flybase.org/reports/FBrf0151688.html). The forward primer is P53-C1: 5'-AGCTAATGTGACTTCGCATTGAACAAA-3', and the reverse primer is P53-C2: 5'-TCGATAAACATTGGCTACGGCGATTGT. These primers were prepared by Integrated DNA Technologies (Coralville, IA, USA). The deletion should produce a 4.0 kbp product, while the wild type allele should produce a 7.3 kbp product. We used i-MAX™ II from iNtRON Biotechnology (South Korea, available from Boca Raton Scientific) for the long distance genomic PCRs.

2.4.3 Immuno-fluorescence and transmission electron microscopy

For immuno-fluorescence microscopy, larval tissues were fixed in a phosphate buffered solution containing freshly prepared paraformaldehyde (2% final concentration), washed, blocked, and incubated with antibodies as described (de Cuevas et al. 1996). We used a previously characterized isoform-specific guinea pig antiserum (Cui and DiMario 2007) at 1/100 and an Alexa Fluor® 546-conjugated goat anti-guinea pig antibody (A11074, Molecular Probes, Eugene, OR, USA) at 1/250 to demonstrate the loss of Nopp140-RGG in RNAi-expressing larvae. To demonstrate apoptosis in imaginal wing discs, we used rabbit anti-cleaved Caspase-3 (Asp175) (#9661, Cell Signaling Technology, Danvers, MA, USA) at 1/200. This particular antibody has been well described as a marker for Caspase-9-like DRONC activity in apoptotic *Drosophila* cells (Fan et al. 2010). The secondary antibody was the Alexa Fluor® 488-conjugated goat anti-rabbit from Molecular Probes (A11034) at 1/250. Tissues were stained with DAPI at 1 µg/mL in the final wash buffer and viewed with a Zeiss Axioskop equipped with a SPOT RT/SE CCD camera (Diagnostic Instruments, Sterling Heights, MI, USA).

Transmission electron microscopy of wild type and Nopp140-RNAi-expressing larval tissues was performed as described (Rosby et al. 2009). Diploid tissues (imaginal discs and brains) and polyploid tissues (mid-gut and Malpighian tubules) were hand isolated, fixed, and flat-embedded separately so we could section and analyze one known tissue at a time. From Nopp140-RNAi-expressing larvae, we captured 16 images of polyploid cells and 20 images of diploid cells. About half as many images were captured from the same wild type

tissues. We used a JEOL 100CX operating at 80 KV and a magnification of 16,000 X. Negatives (8 X 10 cm) were scanned at 1200 dpi. Resulting positive images were prepared using Photoshop.

2.4.4 Immuno-blots

Third instar larval lysates were prepared by using small plastic tissue grinders designed for Eppendorf tubes. Larvae were homogenized in 267 µL of Laemmli sample buffer to which we added 3 µL of 0.1 M PMSF dissolved in isopropanol, 15 µL of a protease inhibitor cocktail (P-8340, Sigma-Aldrich Corp. St. Louis, MO, USA), and 15 µL of 2-mercaptoethanol. The homogenate was then sonicated by 5 bursts using a Branson Digital Sonifier; each burst was for 5 seconds at 40% maximum power. The resulting lysates were centrifuged for 30 min. The supernatant was boiled for 5 min. and re-centrifuged for an additional 30 min. Lysate proteins were resolved by standard SDS-PAGE and blotted to nitrocellulose using a Bio-Rad Trans-Blot semi-dry transfer cell. Blots were blocked with 5% non-fat dry milk in TTBS. We used rabbit antibodies against ribosomal proteins RpL34 (center) and RpL23A (C-terminus) (Abgent, San Diego, CA; catalog numbers AP13207c-ev20 and AP1939b, respectively) at 1/2000 in 5% non-fat dry milk. We used the 81E11 rabbit monoclonal antibody directed against phospho-JNK (Thr183/Tyr185; Cell Signaling Technologies, #4668) and a rabbit anti-Hid antibody that was kindly provided by Hyung Don Ryoo (Ryoo et al. 2004) at New York University Medical School diluted to 1/1000 in TTBS.

2.4.5 Mass spectroscopy

Proteins resolved on SDS-polyacrylamide gels were identified by mass spectroscopy at Louisiana State University's Pennington Biomedical Research Center, Baton Rouge, LA, USA. Briefly, 2 mm gel plugs were automatically excised using a ProteomeWorks spot cutter (Bio-Rad) and deposited in a 96-well plate. In-gel tryptic digestion was performed using an automated robotic workstation (MassPrep, Waters Corp., Milford, MA, USA). Gel plugs were washed with NH_4HCO_3 and CH_3CN followed by reduction and alkylation using 10 mM DTT and 55 mM iodoacetamide, respectively. Proteins were cleaved by sequencing grade trypsin (150 ng/gel plug) at 37°C overnight. The peptide fragments were extracted with 2% CH_3CN, 1% HCOOH in water and directly analyzed using liquid chromatography (LC) – tandem mass spectrometry (MS/MS). The peptides from each digested band were separated and analyzed using a capillary LC system coupled on-line with a nanospray quadrupole time-of-flight (Q-TOF) MS (Waters Corp.) as described (Zvonic et al. 2007). Tandem mass spectra were analyzed using the ProteinLynx Global Server 2.5 software (Waters Corp.) against a Swiss Prot database. The database search settings included one missed tryptic cleavage and fixed carbamidomethylation of cysteine residues.

2.4.6 Hemolymph phenoloxidase assays

Relative hemolymph phenoloxidase levels were determined using native gels and staining techniques with tyrosine as substrate as described previously (Asano and Takebuchi 2009).

2.4.7 Metabolic labeling

Twenty third-instar larvae, either parental controls or progeny expressing RNAi to deplete Nopp140, were added to ~300 µL of Robb's A + B solution (Robb 1969) in disposable plastic depression slides and gently torn open to expose internal tissues. Excess fluid was removed leaving approximately 50 µL to which we added 10 µL of EXPRE^{35}S^{35}S Protein Labeling Mix, [^{35}S]-EasyTag™ (Perkin-Elmer, NEG772002M, 10.0 mCi/ml). The depression slides were placed in a moist chamber, and the tissues were incubated for 30 min at room temperature. Tissues were then washed once with Robb's A + B solution. Lysates were prepared by adding 25 µL of a protease inhibitor cocktail (Sigma-Aldrich, P-8340), 445 µL of Laemmli sample buffer, 25 µL 2-mercaptoethanol, and 5 µL 0.1 M PMSF dissolved in isopropanol. Tissues were homogenized in Eppendorf tubes with disposal plastic tissue grinders, boiled for five minutes, and centrifuged for one hour. Protein concentrations were determined in triplicate using a modified Lowry assay (Peterson 1983). Absorbance values were determined using a Perkin-Elmer Lambda 3B spectrophotometer. To determine incorporated CPM, 200 µL of larval lysate was combined with 100 µL of ddH_2O, 100 µL BSA (2 mg/ml), and 80 µL 100% TCA (16.7% final concentration). Samples were mixed and incubated on ice for 30 min. Each sample was passed through a vacuum filter assembly (Sigma-Aldrich, Z290475) containing a Whatman 25 mm GFC glass microfiber filter which was then rinsed with cold 10% TCA and 100% EtOH. Filters were air dried, and placed separately into 10 mL of Scintiverse (TM) BD Cocktail (Fisher Scientific). CPM was determined

using a Beckman LS 6000IC scintillation counter. Ratios of CPM per microgram of protein were determined for each sample. The entire experiment was repeated three times. We also verified the relative protein concentrations and CPM values for each sample by resolving lysate proteins on SDS-10% polyacrylamide gels; Coomassie blue staining verified the relative protein concentrations. The gels were dried and exposed to Kodak X-OMAT LS film; resulting autoradiograms verified the relative scintillation counts.

2.5 References

Asano T, Takebuchi K (2009) Identification of the gene encoding pro-phenoloxidase A_3 in the fruitfly, *Drosophila melanogaster*. Insect Mol Biol 18:223-232.

Bidla G, Dushay MS, Theopold U (2007) Crystal cell rupture after injury in *Drosophila* requires the JNK pathway, small GTPases and the TNF homolog Eiger. J Cell Sci 120:1209-1215.

Bilak A, Su TT (2009) Regulation of *Drosophila melanogaster* pro-apoptotic *hid*. Apoptosis 14: 943-949.

Chang Y-Y, Neufeld TP (2009) An Atg1/Atg13 complex with multiple roles in TOR-mediated autophagy regulation. Mol Biol Cell 20:2004-2014.

Chang Y-Y, Neufeld TP (2010) Autophagy takes flight in *Drosophila*. FEBS Lett. 584:1342-1349.

Chintapalli VR, Wang J, Dow JAT (2007) Using FlyAtlas to identify better *Drosophila melanogaster* models of human disease. Nat Genet. 39:715-720.

Cui Z, DiMario PJ (2007) RNAi knockdown of Nopp140 induces *Minute*-like phenotypes in *Drosophila.* Mol Biol Cell 18:2179-2191.

de Cuevas M, Lee JK, Spradling AC (1996) Alpha-spectrin is required for germline cell division and differentiation in the *Drosophila* ovary. Development 122:3959-3968.

Dixon J, Jones NC, Sandell LL, Jayasinghe SM, Crane J, Rey J-P, et al. (2006) *Tcof1*/treacle is required for neural crest cell formation and proliferation

deficiencies that cause craniofacial abnormalities. Proc Natl Acad Sci USA 130:13403-13408.

Dixon MJ (1996) Treacher Collins syndrome. Hum. Mol. Genet. 5:1391-1396.

Fan Y, Bergmann A (2010) The cleaved-Caspase-3 antibody is a marker of Caspase-9-like DRONC activity in *Drosophila*. Cell Death Differ 17:534-539.

Gartner LP, Gartner RC (1976) Nuclear inclusions: a study of aging in *Drosophila*. J. Gerontology 31:396-404.

Gowda P, Zhou F, Chadwell LV, McEwen DG (2012) p53 binding prevents phosphatase-mediated inactivation of diphosphorylated c-Jun N-terminal kinase. J Biol Chem 287:17554-17567.

Haerry TE, Khalsa O, O'Connor MB, Wharton KA (1998) Synergistic signaling by two BMP ligands through the SAX and TKV receptors controls wing growth in *Drosophila*. Development 125:3977-3987.

He F, DiMario P (2011) Structure and function of Nopp140 and Treacle. In: Olson MOJ (ed) The Nucleolus, Protein Reviews. Springer, New York, NY, pp 253-278.

Isaac C, Yang Y, Meier UT (1998) Nopp140 functions as a molecular link between the nucleolus and the coiled bodies. J Cell Biol 142:319-329.

Jaklevic BR, Su TT (2004) Relative contribution of DNA repair, cell cycle checkpoints, and cell death to survival after DNA damage in *Drosophila* larvae. Curr Biol 14:23-32.

Jones NC, Lynn ML, Gaudenz K, Sakai D, Aoto, K, Rey J-P, et al. (2008) Prevention of the neurocristopathy Treacher Collins syndrome through inhibition of p53 function. Nat Med 14:125–133.

Juhász G, Puskás LG, Komonyi O, Érdi B, Maróy P, Neufeld TP, et al. (2007) Gene expression profiling identifies FKBP39 as an inhibitor of autophagy in larval *Drosophila* fat body. Cell Death Differ 14:1181-1190.

Lin A (2003) Activation of the JNK signaling pathway: breaking the brake on apoptosis. Bioessays 25:17–24.

Luo X, Puig O, Hyun J, Bohmann D, Jasper H (2007) Foxo and Fos regulate the decision between cell death and survival in response to UV irradiation. EMBO J 26:380-390.

Marygold SJ, Roote J, Reuter G, Lambertsson A, Ashburner M, Millburn GH, et al. (2007) The ribosomal protein genes and *Minute* loci of *Drosophila melanogaster*. Genome Biol. 8:R216.

Mayer C, Bierhoff H, Grummt I (2005) The nucleolus as a stress sensor: JNK2 inactivates the transcription factor TIF-IA and down-regulates rRNA synthesis. Genes Dev 19:933-941.

Mayer C, Grummt I (2005) Cellular stress and nucleolar function. Cell Cycle 4:1036-1038.

McNamee LM, Brodsky MH (2009) p53-independent apoptosis limits DNA damage-induced aneuploidy. Genetics 182:423-435.

Meier UT (1996) Comparison of the rat nucleolar protein Nopp140 with its yeast homologue SRP40. J Biol Chem 271:19376-19384.

Mialon A, Thastrup J, Kallunki T, Mannermaa L, Westermarck J, Holmström TH (2008) Identification of nucleolar effects in JNK-deficient cells. FEBS Lett 582:3145-3151.

Minakhina S, Steward R (2006) Melanotic mutants in *Drosophila*: pathways and phenotypes. Genetics 174:253-263.

Moreno E, Basler K, Morata G (2002) Cells compete for Decapentaplegic survival factor to prevent apoptosis in *Drosophila* wing development. Nature 416:755-759.

Neufeld TP (2012) Autophagy and cell growth – the yin and yang of nutrient responses. J Cell Sci 125:2359-2368.

Peterson GL (1983) Determination of total protein. Method Enzymol 9:95-119.

Robb JA (1969) Maintenance of imaginal discs of *Drosophila melanogaster* in chemically defined media. J Cell Biol 41:876-885.

Roberts DB, Wolfe J, Akam ME (1977) The developmental profiles of two major haemolymph proteins from *Drosophila melanogaster*. J Insect Physiol 23:871-878.

Rong YS, Titen SW, Xie HB, Golic MM, Bastiani M, Bandyopadhyay P, et al. (2002) Targeted mutagenesis by homologous recombination in *D. melanogaster*. Genes Dev 16:1568-1581.

Rosby R, Cui Z, Rogers E, deLivron MA, Robinson VL, DiMario PJ (2009) Knockdown of the *Drosophila* GTPase Nucleostemin 1 impairs large

ribosomal subunit biogenesis, cell growth, and midgut precursor cell maintenance. Mol Biol Cell 20:4424-4434.

Ryoo HD, Gorenc T, Steller H (2004) Apoptotic cells can induce compensatory cell proliferation through the JNK and the Wingless signaling pathways. Dev Cell 7:491–501.

Shiba T, Saigo K (1983) Retrovirus-like particles containing RNA homologous to the transposable element *copia* in *Drosophila melanogaster*. Nature 302:119-124.

Strand DJ, McDonald JF (1985) *Copia* is transcriptionally responsive to environmental stress. Nucleic Acids Res 13:4401-4410.

Tang H (2009) Regulation and function of the melanization reaction in *Drosophila*. Fly 3:105-111.

Tollini LA, Frum RA, Zhang Y (2011) The role of the nucleolus in the stress response. In: Olson MOJ (ed) The Nucleolus, Protein Reviews. Springer, New York, NY, pp 281-299.

Trainor PA, Dixon J, Dixon MJ (2009) Treacher Collins syndrome: etiology, pathogenesis and prevention. Eur J Hum Genet 17:275-283.

Tulin A, Stewart D, Spradling AC (2002) The *Drosophila* heterochromatin gene encoding poly(ADP-ribose) polymerase (PARP) is required to modulate chromatin structure during development. Genes Dev 16:2108-2119.

Waggener JM, DiMario PJ (2002) Two splice variants of Nopp140 in *Drosophila melanogaster*. Mol Biol Cell 13:362-381.

Weston CR, Davis RJ (2007) The JNK signal transduction pathway. Curr Opin Cell Biol 19:142–149.

Wichmann A, Jaklevic B, Su TT (2006) Ionizing radiation induces caspase-dependent but Chk2- and p53-independent cell death in *Drosophila melanogaster*. Proc Natl Acad Sci 103:9952-9957.

Wichmann A, Uyetake L, Su TT (2010) E2F1 and E2F2 have opposite effects on radiation-induced p53-independent apoptosis in *Drosophila*. Dev Biol 346:80-89.

Wu H, Wang MC, Bohmann D (2009) JNK protects *Drosophila* from oxidative stress by transcriptionally activating autophagy. Mech Dev 126:624-637.

Yang Y, Isaac C, Wang C, Dragon F, Pogačić V, Meier UT (2000) Conserved composition of mammalian box H/ACA and box C/D small nucleolar ribonucleoprotein particles and their interaction with the common factor Nopp140. Mol Biol Cell 11:567-577.

Yogev O, Saadon K, Anzi S, Inoue K, Shaulian E (2008) DNA damage-dependent translocation of B23 and $p19^{ARF}$ is regulated by the Jun N-terminal kinase pathway. Cancer Res 68:1398-1406.

Zvonic S, Lefevre M, Kilroy K, Floyd ZE, DeLany JP, Kheterpal I, et al. (2007) Secretome of primary cultures of human adipose-derived stem cells (ASCs): modulation of serpins by adipogenesis. Mol Cell Proteomics 6:18-28.

CHAPTER 3. DELETION OF *NOPP140**

3.1 Introduction

Ribosome biogenesis is an intricate choreography of interactions and reactions between large numbers of protein and RNA molecules (Granneman and Baserga 2004; Kressler et al. 2010). In eukaryotes, ribosome assembly occurs within the nucleolus where RNA polymerase I (Pol I) synthesizes pre-ribosomal RNA (pre-rRNA) from multiple genes arranged in tandem. These genes (rDNA) reside at defined genetic loci referred to as nucleolar organizers. The pre-rRNA (47S in mammals, 38S in *Drosophila,* 35S in yeast) is chemically modified by nucleotide-specific 2'-*O*-methylation via box C/D small nucleolar ribonucleoprotein (snoRNP) complexes and by site-specific pseudouridylation via box H/ACA snoRNPs. The pre-rRNA is concomitantly cleaved by endo- and exo-nucleolytic events to generate the mature 18S rRNA that assembles with 33 proteins into the small ribosomal subunit and mature 5.8S and 28S rRNAs that assemble with 46 proteins into the large ribosomal subunit. The large subunit also contains a copy of the 5S rRNA that is transcribed from its own set of repeated genes by RNA Pol III.

The nucleolar and Cajal body phosphoprotein of 140 kDa (Nopp140 in metazoans, SRP40 in yeast) is one of many non-ribosomal nucleolar proteins (Andersen et al. 2002; Tafforeau et al. 2013) that participate in ribosome

This chapter previously appeared as He F, James A*, Raje H, Ghaffari H, DiMario P. (2014). Deletion of *Drosophila* Nopp140 induces subcellular ribosomopathies. *Chromosoma*. *co-first authors http://dx.doi.org/10.1007/s00412-014-0490-9. It is reprinted by permission of Springer – see the permission letter for proper acknowledgement phrase in Appendix B of this thesis.

assembly. Vertebrate Nopp140 consists of three distinct peptide regions: the amino terminal domain contains a Lissencephaly type-1-like homology (LisH) dimerization motif (Kim et al. 2004), the large central domain consists of several alternating acidic and basic motifs, and the conserved carboxy domain contains a protein kinase A phosphorylation site (Ser_{685} in rat Nopp140), suggesting that signaling pathways mediate Nopp140 interactions and functions in nucleoli or Cajal bodies (Meier 1996; Chiu et al. 2002; Kim et al. 2006). While the three dimensional structure of Nopp140 has not been determined, its compositional bias toward hydrophilic amino acids suggests that it presents a natively unfolded structure which correlates well with its many putative functions in ribosome assembly (Fink 2005; Kim et al. 2006).

The functions of vertebrate Nopp140 are largely inferred from its co-localizations and interactions with other nuclear and nucleolar components. During interphase, Nopp140 enriches within the dense fibrillar component of nucleoli and within extra-nucleolar Cajal bodies (Isaac et al. 1998; Vandelaer and Thiry 1998). Reports indicate that Nopp140 interacts with C/D and H/ACA snoRNPs, perhaps in their assembly within Cajal bodies, their transport to the nucleolus, or in their interactions with target sites within the pre-rRNA (Isaac et al. 1998; Yang et al. 2000). Nopp140 in Cajal bodies may also participate in the modification of small Cajal body RNAs (scaRNAs) (Isaac et al. 1998). Besides associating with snoRNPs, Nopp140 has been reported to interact with RNA Pol I (Chen et al. 1999) and rDNA (Tsai et al. 2008), suggesting a regulatory role in rDNA transcription. For instance, over-expression of either full length Nopp140 or

a dominant negative Nopp140-carboxyl truncation leads to mis-localization of Pol I and altered nucleolar structure (Chen et al. 1999). While suggestive, the precise roles of Nopp140 in Pol I transcription or post-transcriptional modification of the pre-rRNA remain unknown.

Our past work on Nopp140 has been at the organismal level. We showed that a substantial (≥50%) depletion of *Nopp140* transcripts by RNAi expression in *Drosophila* larvae caused late larval and pupal lethality, while a moderate decrease (30%) caused developmental deformities in adult legs, wings, and cuticle (Cui and DiMario 2007). Recently, we showed that the more substantial loss of Nopp140 induced p53-independent apoptosis in larval imaginal diploid cells, premature autophagy in polyploid gut cells, and a significant accumulation of phenoloxidase A3 in the hemolymph, which likely explains the formation of melanotic masses prior to lethality. The apoptosis, autophagy, and release of phenoloxidase can all be linked to the activation of Jun amino-terminal kinase (JNK), the stress-response kinase (Chapter 2, James et al. 2013).

To examine intracellular phenotypes (ribosomopathies) resulting from the loss of Nopp140, we induced inter-chromosomal recombination between *piggyBac* (*pBac*) transposable elements that flanked the *Nopp140* gene, thus deleting the gene. The *Nopp140* gene in *Drosophila melanogaster* resides within the centromere-proximal region 87F4 on the left arm of chromosome 3. The gene produces two experimentally confirmed splice variants that are identical in their first 583 amino acid residues, after which their carboxyl domains differ (Waggener and DiMario 2002). Nopp140-True is the canonical orthologue of

vertebrate Nopp140; its carboxyl domain is well conserved (64% identical) with the carboxyl domain of human Nopp140. Conversely, *Drosophila* Nopp140-RGG contains a carboxyl terminal domain rich in RGG tri-peptide repeats. Similar RGG-rich domains are common to several RNA-associated proteins (Thandapani et al. 2013) such as the nucleolar methyl-transferase, fibrillarin (Ochs et al. 1985), and the vertebrate pre-rRNA binding protein, nucleolin (Ginisty et al. 1999). A similar Nopp140 isoform with a carboxyl RGG-rich domain has been described in Trypanosomes (Kelly et al. 2006). Complete deletion of the *Drosophila* Nopp140 isoforms induced novel intracellular phenotypes (ribosomopathies) that are reported here.

3.2 Results

3.2.1 Deleting the *Nopp140* Gene

We deleted the *Nopp140* gene in *Drosophila melanogaster* using FLP-FRT recombination between upstream and downstream FRT-bearing *pBac* elements on homologous third chromosomes. The *pBac*-bearing parental fly line, $Nopp140^{e01407}$, contained an *RB*+ element 440 base pairs (bp) upstream of the *Nopp140* transcription start site, while fly line $P5CDh1^{f04633}$ contained the *WH*- element downstream of *Nopp140* (Figure 3.1, A). Appropriate orientations of *RB*+ and *WH*- elements were necessary to initiate flippase-mediated inter-homologue recombination that deleted the intervening sequences (see Parks et al. 2004). While the particular *WH*- element used here is the closest to the *RB*+ element, it resides within the last coding exon of the downstream gene, *P5CDh1* (previously *CG7145*), which transcribes in the convergent direction relative to *Nopp140*. We

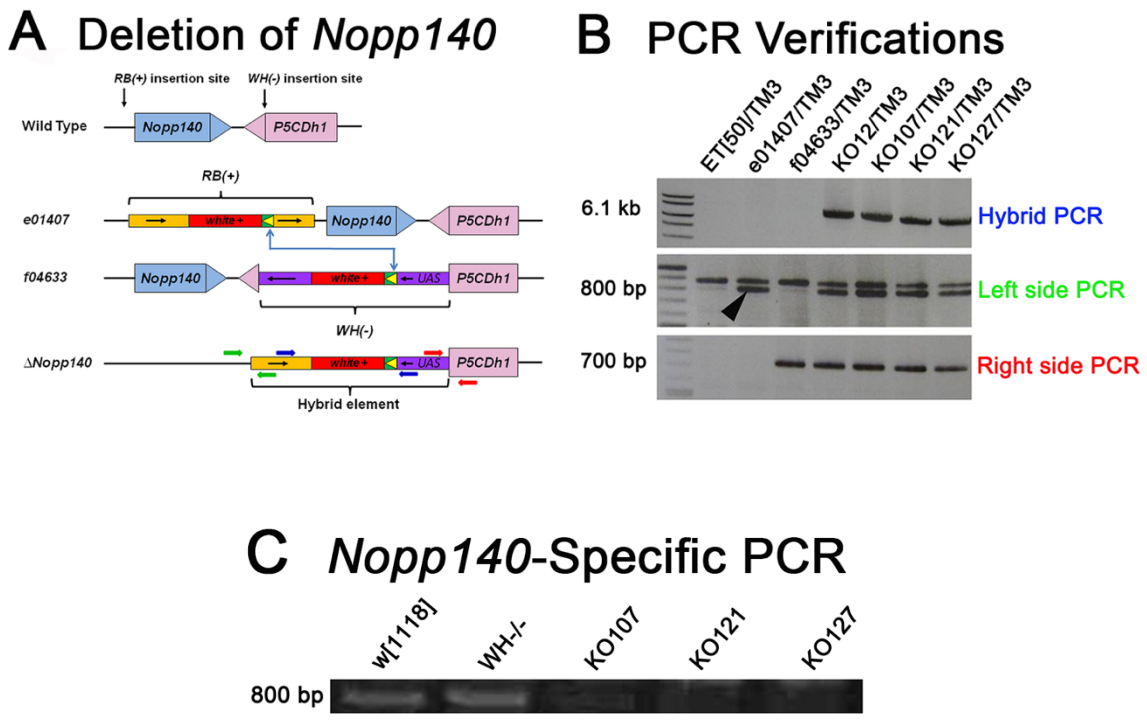

FIGURE 3.1. FLP-FRT-mediated Deletion of the *Nopp140* Gene in *Drosophila melanogaster.* (A) The *Nopp140* gene resides within cytological region 78F4 of the left arm of chromosome 3. *P5CDh1* is downstream such that transcription of the two genes is convergent as shown. The *RB(+)* pBac element resides approximately 440 bp upstream of the *Nopp140* gene in fly strain *e01407*. The *WH(−)* pBac element resides within the last exon of *P5CDh1* in fly strain *f04633*. The *Flippase* gene was introduced on the *X* chromosome and induced by heat shock. Flippase-mediated recombination between the *FRT* sequences within *RB(+)* and *WH(−)* deleted *Nopp140* and the 3′ end of *P5CDh1*. Oligonucleotide pairs for diagnostic PCRs are shown as green, blue, and red arrows. (B) The hybrid PCR produced a 6.1 kbp product diagnostic of recombination between *RB(+)* and *WH(−)* elements only in those lines heterozygous for the *Nopp140* gene deletion (see Parks et al. 2004). The left-side PCR product (lower band; arrow head) was produced from the *e01407* line and the *Nopp140* deletion lines. The higher band obtained from the left-side PCR was unexpected but it served as an internal control. The right-side PCR product was produced from the *f04633* line and the *Nopp140* deletion lines. (C) Primers specific for the *Nopp140* gene were used to verify the *Nopp140* gene deletion in homozygous larvae hand selected from three of the deletion stocks, *KO107, KO121, and KO127*. He (2011).

characterized the phenotype of larvae homozygous for the *WH*- element (referred to as *WH*-/-) (He and DiMario 2011b), and in the work described below we consistently compared *WH*-/- phenotypes to those caused by the homozygous deletion (*Nopp140*-/-).

We recovered approximately 75 chromosomes that potentially carried the *Nopp140* gene deletion. These chromosomes were initially balanced over *TM3* as we examined these viable heterozygous larvae by genomic PCR for the presence of the hybrid *pBac* element that arises from recombination between the original *RB*+ and *WH*- elements (Figure 3.1, B). Of the 75 chromosomes, 10 appeared to have undergone recombination that deleted the *Nopp140* gene as predicted (Figure 3.1, A). Four representative lines (*KO12*, *KO107*, *KO121*, and *KO127*) are described initially (Figure 3.1, B). The expected hybrid PCR product of 6.1 kbp could originate only from recombination between the *RB*+ and *WH*- *pBac* elements (see Parks et al. 2004); we found this product only in the deletion lines, and not in our *TM3/Et*^{50} balancer stock, the *Nopp140*^{e01407}*/TM3* stock (*RB*+), or in the *P5CDh1*^{f04633}*/TM3* stock (*WH*-).

Genomic PCRs on either side of the hybrid elements verified the extent of the deletion (Figure 3.1, B). The left sided PCR (Figure 3.1, B, green primers) generated the expected 800 bp band (Figure 3.1, B, green arrowhead) that confirmed the left boarder. We obtained an unexpected PCR product of 850 bp from all the stocks including the *TM3/Et*^{50} stock, indicating this band had nothing to do with the *pBac* elements or the recombination events; this product essentially served as an internal PCR control. The right sided PCR (Figure 3.1,

A, red primers) generated the expected 700 bp band, thus confirming the right side of the deletion. The parental *pBac* fly lines *e01407* and *f04633* produced the respective left and right PCR products as expected for their role as positive controls.

To further verify the loss of the *Nopp140* gene, we again performed genomic PCRs but on larvae that were now homozygous for the *Nopp140* gene deletion. To obtain these larvae, which die in the second instar stage, we balanced the particular deletion chromosome (*Nopp140*-) over *TM3-GFP,* and after *inter se* crosses, hand-selected homozygous (*Nopp140*-/-) progeny larvae that lacked GFP. Genomic PCRs with primers specific for the *Nopp140* gene promoter and 5' coding sequences failed to produce the expected 800 bp PCR product in three representative knock out lines (*KO107*, *KO121*, and *KO127*), while control w^{1118} (wild type) and *WH*-/- larvae produced the expected 800 bp PCR product (Figure 3.1, C).

3.2.2 Loss of *Nopp140* Gene Products

Since the three *Nopp140* deletion lines (Figure 3.1, C, *KO107*, *KO121*, and *KO127*) displayed similar growth arrest phenotypes (see below), subsequent analyses were performed using only the *KO121* line. To demonstrate the loss of *Nopp140* transcripts, we performed reverse transcriptase-PCR using homozygous *KO121* larvae (*Nopp140*-/-) that were aged for 3 days post egg laying (PEL). *Nopp140* mRNA levels were absent in the *Nopp140*-/- larvae (Figure 3.2, A).

We next examined *Nopp140*-/- larvae at day 4-6 PEL for the presence of the Nopp140-RGG protein, using an isoform-specific polyclonal antibody that had been raised previously against a unique peptide sequence within the carboxyl domain of Nopp140-RGG (Cui and DiMario 2007). As expected, the antibody labeled nucleoli in polyploid cells of wild type (Figure 3.2, B-D) and *WH*-/- (Figure 3.2, E-G) larval midgut, but it failed to label nucleoli in the midgut of *Nopp140*-/- larvae (Figure 3.2, H-J), and in other polyploid *Nopp140*-/- cells including fat body

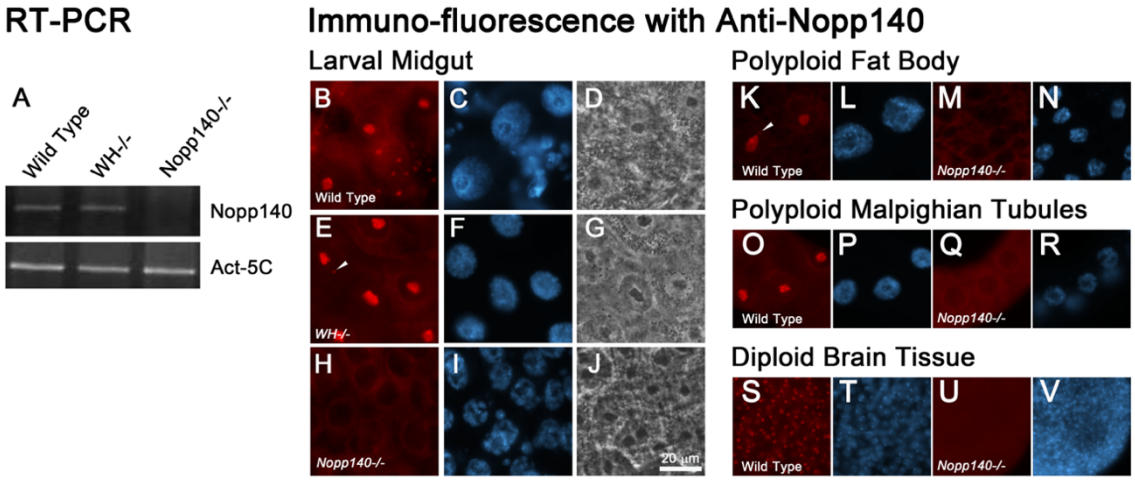

FIGURE 3.2. Loss of the *Nopp140* Gene Products. (A) RT-PCR showed the loss of *Nopp140* mRNAs in *Nopp140-/-* larvae versus wild-type (w^{1118}) and *WH-/-* larvae. Actin-5C transcripts served as a control. (B-V) Phase contrast, DAPI, and immunofluorescence micrographs showed that tissues from wild-type and *WH-/-* larvae contained Nopp140-RGG as detected by a peptide-specific antibody developed by Cui and DiMario (2007), while tissues from *Nopp140-/-* lacked Nopp140-RGG. (B-D) Wild-type polyploid midgut (MG) cells. (E-G) *WH-/-* midgut cells. (H-J) *Nopp140-/-* midgut cells. Other tissues included: (K and L) wild-type polyploid fat body (FB), (M and N) *Nopp140-/-* fat body, (O and P) wild-type polyploid Malpighian tubules (MT), (Q and R) *Nopp140-/-* Malpighian tubules, (S and T) wild-type diploid (2n) imaginal tissue, (U and V) *Nopp140-/-* diploid brain tissue. While nucleoli in various polyploid tissues from *Nopp140-/-* larvae were apparent by phase contrast microscopy, the antibody directed against Nopp140-RGG failed to stain nucleoli. Nopp140 localizes to Cajal bodies; white arrow heads point to Cajal bodies that were apparent in some wild-type and *WH-/-* nuclei. Bar, 20 μm for all images. He (2011).

(Figure 3.2, M and N), Malpighian tubules (Figure 3.2, Q and R), and in the diploid brain cells (Figure 3.2, U and V). Phase-dark nucleoli in the polyploid *Nopp140*-/- cells were present, but in general they appeared somewhat smaller (Figure 3.2, J). Taken together, inter-chromosomal recombination between *pBac* elements upstream and downstream of the *Nopp140* gene successfully deleted the *Nopp140* gene (Figure 3.1), which resulted in the loss of the *Nopp140* mRNA, the Nopp140-RGG isoform (Figure 3.2), and presumably the Nopp140-True isoform as both isoforms are encoded by the single copy *Nopp140* gene (Waggener and DiMario 2002). Besides nucleoli, Nopp140 also localizes to Cajal bodies, and this is evident in Figure 3.2, E and K (white arrowheads).

3.2.3 Phenotypes Associated with Homozygous *WH-/-* Versus *Nopp140-/-* Larvae

The *pBac WH-* element used to delete the *Nopp140* gene lies within the 3' coding region of *P5CDh1*, the gene immediately downstream of *Nopp140*, but transcribed in a convergent manner. *P5CDh1* encodes the highly conserved delta-1-pyrroline-5-carboxylate dehydrogenase (Hu et al. 1996; Inagaki et al. 2006), a mitochondrial matrix enzyme (Small and Jones 1990; Haslett et al. 2004) required for normal proline breakdown (Valle et al. 1974, 1979). Mutations in human *ALDH4A1,* which encodes P5CDh cause type II hyperprolinemia, a syndrome marked by mental retardation and seizures, perhaps due to excess proline (Geraghty et al. 1998). The *WH-* element used here disrupts the last exon of *P5CDh1* such that the carboxyl 83 amino acids are missing. This deleted segment normally forms a homo-dimerization domain in the *T. themophilus* enzyme (Inagaki et al. 2006, 2007). Previously, we showed that *WH-/-* larvae

displayed elevated proline levels twice that of wild type levels, and that their mitochondria were swollen by 1.5- to 2-fold as compared to mitochondria in wild type larvae. While cristae were apparent in these swollen mitochondria, their inner matrices appeared empty (He and DiMario 2011b).

To differentiate phenotypes caused by the loss of Nopp140 versus the truncation of P5CDh1 alone, we first examined the lethality phases of *WH*-/- and *Nopp140*-/- larvae. We again used *inter se* crosses between heterozygous *Nopp140*-/*TM3-GFP* flies to hand select homozygous *Nopp140*-/- embryos. We did the same to generate homozygous *WH*-/- embryos. Wild type (w^{1118}) embryos were also collected from stock females. All three genotypic larvae were allowed to develop on yeasted agar plates for up to six days PEL, or longer in some experiments. The survival ratios for *WH*-/- and *Nopp140*-/- at different developmental stages were recorded and normalized to w^{1118} (Figure 3.3, A). *WH*-/- and *Nopp140*-/- embryos had similar hatching rates (39.3% vs. 35.4%, respectively), and both genotypes had similar ratios of first-instar larvae developing to the second-instar stage (85.5% vs. 82.8%, respectively). Wild type w^{1118} larvae and *WH*-/- larvae continued to grow within the six day PEL period, while *Nopp140*-/- larvae stopped growing by day 3 PEL (Figure 3.3, B). We counted the number of "teeth" on the mouth hooks of day six larvae to confirm their developmental stage; w^{1118} and *WH*-/- larvae had 8-10 teeth, indicating they had reached the third larval instar stage (Bodenstein 1950). *Nopp140*-/- larvae, however, had only 2-3 teeth by day 6 PEL indicating they arrested in the second larval instar stage. A few *Nopp140*-/- larvae lingered to day 8 PEL, but they too

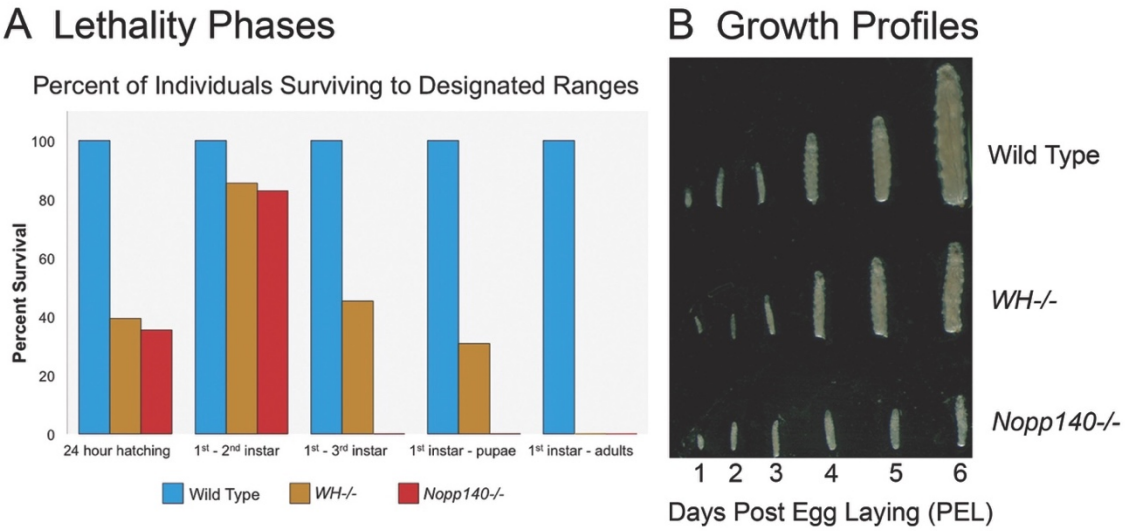

FIGURE 3.3. Lethality Phases and Growth Profiles of Wild-type (w^{1118}), *WH-/-*, and *Nopp140-/-* Larvae. (A) Hatching rates for *WH-/-* and *Nopp140-/-* embryos were similar at approximately 37%. The majority (84%) of first instar *WH-/-* and *Nopp140-/-* larvae survived to the second instar. While 42% of the *WH-/-* first instar larvae survived to the third instar stage, none of the *Nopp140-/-* survived beyond the second instar stage. None of the *WH-/-* or *Nopp140-/-* larvae survived to eclose as adults. (B) Growth profiles of wild-type, *WH-/-*, and *Nopp140-/-* larvae over time expressed as days post-egg laying (PEL). He (2011).

displayed only 2-3 teeth. Approximately 42% of *WH*-/- first instar larvae developed to the third instar stage. Less than one-third of the *WH*-/- first instar larvae survived to the pupal stage (Figure 3.3, A). All *WH*-/- pupae failed to eclose as adults.

In summary, the growth and lethality profiles suggest that the *Nopp140* gene deletion (which includes the *Nopp140* gene and the 3' coding region of the *P5CDh1* gene) induced lethality earlier than did the *P5CDh1* gene disruption alone (*WH*-/-). All experiments described below compare intracellular phenotypes in both *Nopp140*-/- and *WH*-/- larvae aged to day 5-6 PEL.

3.2.4 Nopp140 is Required for 2'-*O*-methylation of rRNA

Fibrillarin is the methyl-transferase associated with C/D snoRNPs; it catalyzes nucleotide-specific 2'-*O*-methylation of rRNA within the dense fibrillar component of nucleoli. Nopp140 has been reported to associate with C/D snoRNPs, perhaps acting as a chaperone to assist their delivery to nucleoli, or perhaps in targeting the snoRNPs to their respective methylation sites within the pre-rRNA (Isaac et al. 1998; Yang et al. 2000). To investigate the possible impact of Nopp140 loss on C/D snoRNPs, we first examined the location of fibrillarin by immuno-fluorescence microscopy using the mouse mAb72B9 originally directed against mammalian fibrillarin (Reimer et al. 1987). Fibrillarin is highly conserved, and this antibody efficiently labels *Drosophila* nucleoli (*e.g.* McCain et al. 2006). The antibody labeled nucleoli of midgut cells from control larvae (wild type and *WH*-/-), and as expected, there was little to no labeling in the nucleoplasm (Figure 3.4, A and D). The antibody, however, labeled the nucleoplasm in *Nopp140*-/- midgut cells (Figure 3.4, G) despite the fairly normal appearance of nucleoli in these cells (Figure 3.4, I). While fibrillarin remained within nucleoli of wild type (Figure 3.4, J) and *WH*-/- fat body cells (Figure 3.4, M), fibrillarin redistributed to the nucleoplasm almost completely in many of the Nopp140-/- fat body cells (Figure 3.4, P). Again, nucleoli in *Nopp140*-/- fat body cells were present and they appeared normal by phase contrast microscopy. We conclude at this point that Nopp140 is not required for general nucleolar integrity, but it is required for the efficient localization of C/D snoRNPs (fibrillarin) to nucleoli, or perhaps their retention within nucleoli.

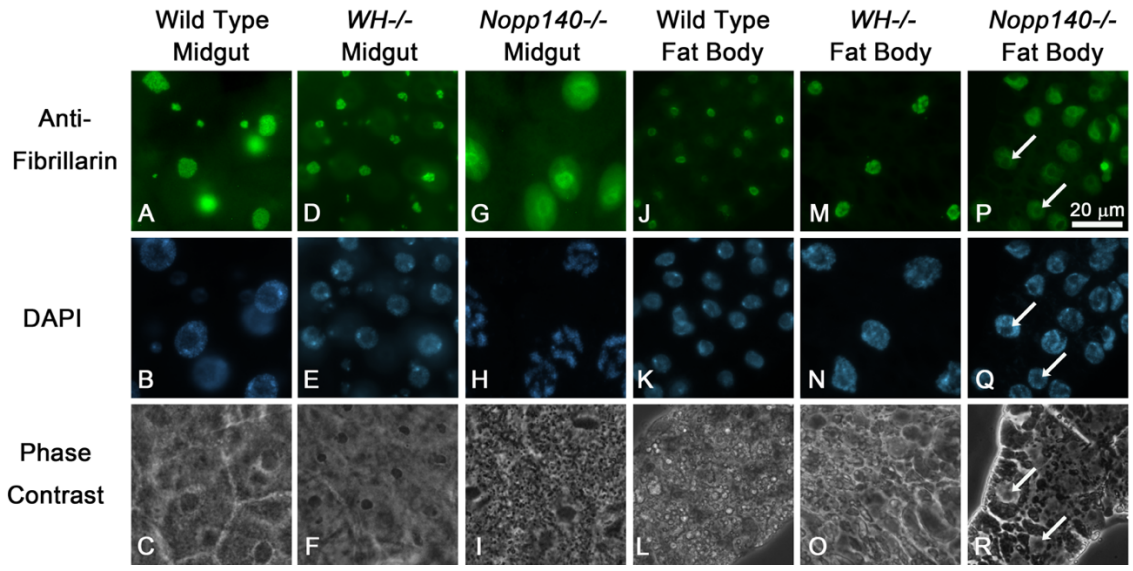

FIGURE 3.4. Anti-fibrillarin mAb 72B9 Labeling, DAPI Staining, and Phase Contrast Microscopy. Midgut cells from (A-C) wild-type, (D-F) *WH-/-*, (G-I) *Nopp140-/-* larvae and of fat body cells from (J-L) wild-type, (M-O) *WH-/-*, and (P-R) *Nopp140-/-* larvae. Midgut cells from *Nopp140-/-* larvae contained nucleoli that appeared smaller and denser (f). Fibrillarin localized exclusively to nucleoli in wild-type (A and J) and *WH-/-* cells (D and M), while fibrillarin redistributed to the nucleoplasm in *Nopp140-/-* midgut (G) and fat body (P) cells. Nucleoli appeared as dark holes in DAPI stained nuclei; arrows in (P-R) show nucleoli. Bar, 20 μm for all images.

Treacle is a vertebrate-specific nucleolar protein related to Nopp140 in structure (Isaac et al. 2000, reviewed by He and DiMario 2011a). An earlier report showed that the loss of treacle inhibited 2'-*O*-methylation of rRNA (Gonzales et al. 2005). To test if the loss of Nopp140 in *Drosophila* also affected 2'-*O*-methylation in pre-rRNA, we used a reverse transcriptase PCR (RT-PCR) assay (Dong et al. 2012) with reduced dNTPs (0.5 or 1.0 μM) during reverse transcription. We chose three closely spaced ribonucleotides in the *Drosophila* 18S rRNA (U_{1356}, G_{1358}, and C_{1367}) and in the 28S rRNA (A_{2634}, C_{2645} and A_{2653}) that were previously determined to undergo 2'-*O*-methylation (Yuan et al. 2003; Huang et al. 2005). We analyzed these sites in rRNA isolated from *Nopp140-/-,*

WH-/-, and w^{1118} larvae. The technique (Figure 3.5, A) uses a reverse primer complementary to rRNA sequence downstream of the clustered methylation site for first strand cDNA synthesis. Two forward primers are then used for PCR amplification; one forward primer is upstream (Forward Upstream or FU) of the methylation sites, and the second is downstream (Forward Downstream or FD) of the methylation sites (Figure 3.5, A). The FD primer controls for the amount of cDNA generated by RT, while the FU primer is used to indirectly measure the degree of methylation. Representative triplicate RT-PCRs for *Nopp140*-/-, *WH*-/-, and wild type (w^{1118}) larvae are shown for the 18S and 28S sites (Figure 3.5, B and C, respectively). The ratios of FU product to FD product are presented as a bar graph (Figure 3.5, D). At low dNTP concentrations, the methylated residues caused reverse transcriptase to pause, resulting in a shorter cDNA product. Hence, the amount of FU product obtained under low dNTP concentrations was inversely related to the amount of 2'-*O*-methylation present within the selected rRNA sites. Averages with standard errors from three biological experiments are shown for the 18S and 28S sites. Loss of Nopp140 generated approximately four times as much FU product, thus indicating that methylation at the 18S and 28S sites was suppressed by approximately four-fold in *Nopp140*-/- larvae as compared to the same sites within rRNA isolated from wild type or *WH*-/- larvae. A slight accumulation of RT-PCR product from *WH*-/- 28S rRNA, however, suggests that defective mitochondria may contribute partially to block 2'-*O*-methylation.

FIGURE 3.5. Loss of Nopp140 Impairs 2′-*O*-methylation of 18S and 28S rRNA. (A) Schematic describing the RT-PCR methodology in assessing methylation of clustered nucleotides within *Drosophila* rRNA. First-strand cDNA synthesis by RT should be impaired at 2′-*O*-methylated nucleotides when dNTPs are in low concentrations (0.5 or 1.0 μM). The PCR forward downstream (FD) primer served as a control to measure the amount of first-strand cDNA produced in the RT reaction. The PCR forward upstream (FU) primer measured how much first-strand cDNA was produced as RT attempted to pass through the potentially methylated ribonucleotides. Subsequent PCRs were run in triplicate. (B) Representative gels from one of three biological replicates that measured the degree of 2′-*O*-methylation at clustered methylation sites within the 18S rRNAs from wild-type (w^{1118}), *WH-/-*, and *Nopp140-/-* larvae. (C) Representative gels from one of three biological replicates that measured 2′-*O*-methylation of the 28S rRNA from wild-type (w^{1118}), *WH-/-*, and *Nopp140-/-* larvae. RT reactions used 1.0 μM dNTPs. (D) Gel bands were scanned and quantified using ImageJ. Values for the FU-primed product were normalized to values for FD-primed products and expressed as a bar graph below the respective gels. The FD-primed control PCR product for all three genotypes remained constant, while reduced FU-primed PCR product indicated methylation in rRNA isolated from wild-type (w^{1118}) and *WH-/-* larvae. Accumulation of FU-primed product indicated a significant loss of methylation in rRNA from *Nopp140-/-* larvae compared to both wild type and *WH-/-* ($p<0.05$). Error bars are ± standard errors, calculated from combining the three biological replicates with their respective PCR outputs.

A Scheme of RT-PCR

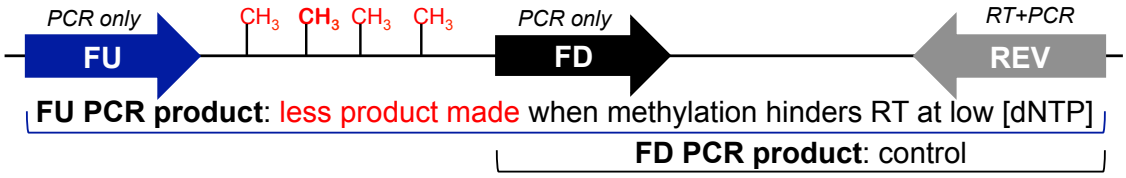

B Representative gel for 18S
0.5 µM dNTPs for RT reaction

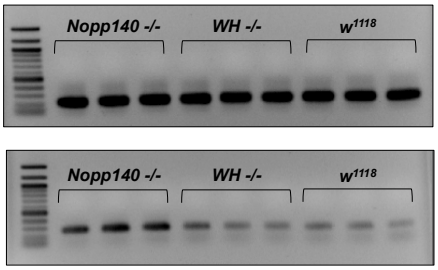

C Representative gel for 28S
1.0 µM dNTPs for RT reaction

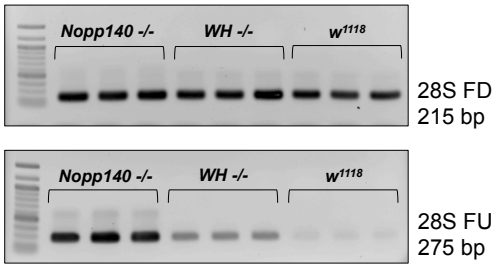

D Relative Abundance of RT-PCR Products for 18S and 28S

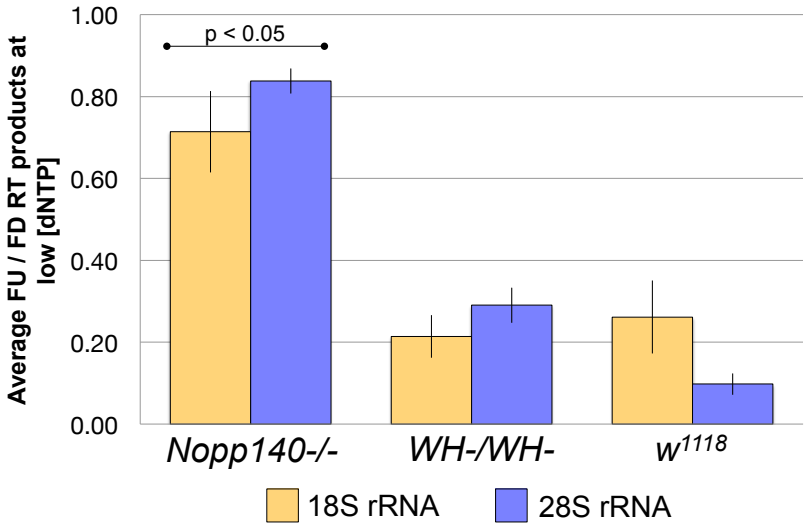

Overall, we conclude that loss of Nopp140 inhibits 2'-*O*-methylation within rRNA, perhaps due to the redistribution of fibrillarin (box C/D snoRNPs) to the nucleoplasm.

3.2.5 Loss of Nopp140 Induced Formation of Aberrant Cytoplasmic Granules

We used toluidine blue staining with bright field light microscopy and transmission electron microscopy (TEM) to determine if ribosome abundance changed due to the loss of Nopp140. We concentrated on polyploid cells of the midgut isolated from *Nopp140*-/-, *WH*-/-, and w^{1118} larvae (Figure 3.6) since this was the most abundant tissue available in *Nopp140*-/- larvae. In preparing thin sections for TEM we routinely prepare thick sections (0.5 µm) first and examine them by bright field light microscopy after routine toluidine blue staining, a basic dye used to stain ribosomes and RNA (Feder and Wolf 1965; Easton et al. 2010). Toluidine blue stained the cytoplasm and nucleoli of wild type midgut cells metachromatically (dark purple) as expected (Figure 3.6, A). The cytoplasm in *Nopp140*-/- midgut cells, however, was only weakly stained by the dye (Figure 3.6, B) suggesting a lack of rRNA (ribosomes) in the cytoplasm. Nucleoli in these *Nopp140*-/- cells maintained intense metachromatic staining, and in general appeared no different than the nucleoli in wild type cells.

At the TEM level, wild type cells showed abundant cytoplasmic ribosomes (Figure 3.6, C), both free and associated with the endoplasmic reticulum (rER). Mitochondrial matrices in these cells typically appeared dark with cristae apparent based upon the orientation of the mitochondria relative to the plane of sectioning. Conversely, *Nopp140*-/- cells were deficient in free cytoplasmic

FIGURE 3.6. Bright Field Light Microscopy and TEM analysis of *Nopp140-/-* Cells Compared to Wild-type and *WH-/-* Cells. (A) A thick section (0.5 µm) of midgut taken from a second instar wild-type larva was stained with toluidine blue. The cytoplasm and nucleoli stained intensely, while the brush boarder remained unstained. (B) A thick section of midgut taken from a second instar *Nopp140-/-* larva stained with toluidine blue. While nucleoli stained intensely, the cytoplasm was essentially devoid of stain. (C) Two polyploid wild-type (w^{1118}) cells separated by their adjacent plasma membranes running diagonally through the image showed numerous ribosomes in their cytoplasm. Mitochondria stained darkly, but their cristae were discernible. The nucleus (the lower left) lacked virus-like particles. (D) A polyploid cell from a *Nopp140-/-* larva appeared deficient in cytoplasmic ribosomes, but instead contained numerous dark cytoplasmic granules. Mitochondria appeared normal. The nucleus (left) contained many scattered virus-like particles (white arrows). (E) A polyploid cell from a *Nopp140-/-* larva under higher magnification. The cytoplasmic granules appeared to have a dense spherical core with ribosomes attached to their surfaces. A small patch of rER indicates some functional ribosomes were still present. (F) A polyploid cell from a *WH-/-* larva contained substantial free ribosomes and rER within the cytoplasm. Conversely, the mitochondria appeared swollen with depleted matrices (see He and DiMario 2011b).

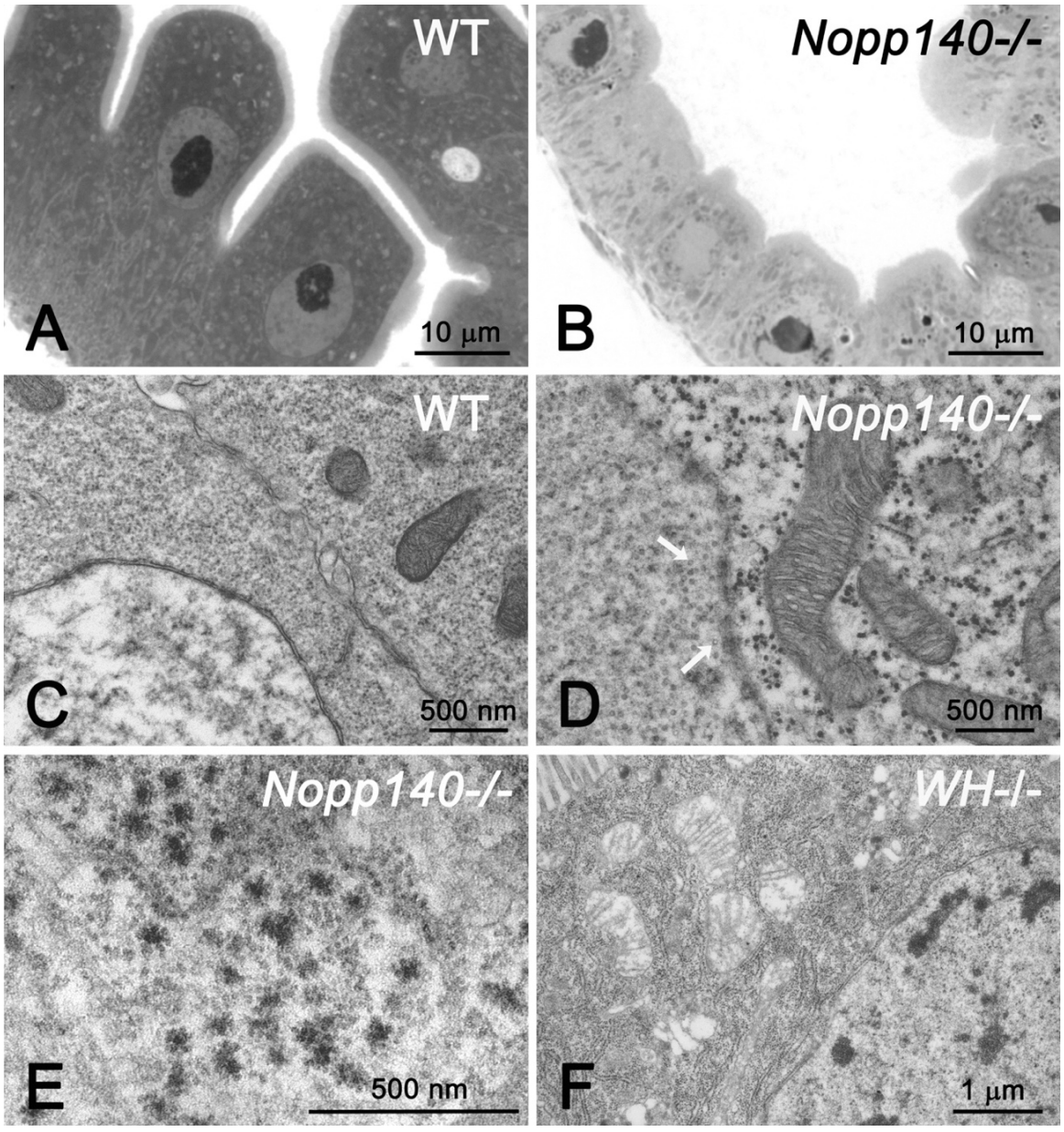
WT
A
10 μm
Nopp140-/-
B
10 μm
WT
C
500 nm
Nopp140-/-
D
500 nm
Nopp140-/-
E
500 nm
WH-/-
F
1 μm

ribosomes (Figure 3.6, D). Instead, the cytoplasm of *Nopp140*-/- cells contained numerous electron dense granules that measured 40-50 nm in diameter. Under higher magnification (Figure 3.6, E), the granules appeared to consist of a central electron dense core and what appear to be aggregated ribosomes on their surfaces. Most importantly, the granules were specific to *Nopp140*-/- cells, as neither wild type cells (Figure 3.6, C) nor *WH*-/- cells (Figure 3.6, F) contained these granules. We have yet to identify these granules with certainty, but we consider possibilities in the *Discussion*.

Besides the cytoplasmic granules, *Nopp140*-/- cells contained unusually high numbers of virus-like particles in their nuclei (white arrows in Figure 3.6, D). These particles are likely derived from the expression of *copia*-like retrotransposon elements (Akai et al. 1967; Rubin 1983; Finnegan 1985; Miyake et al. 1987). The virus-like particles can appear dispersed as they do in the nucleus of Figure 2.2, D, but they usually appeared in tightly aligned clusters in most *Nopp140*-/- nuclei (not shown). The occurrence of a few virus-like particles is common in the nuclei of wild type laboratory stocks, so the unusually high numbers observed in the *Nopp140*-/- cells suggested cell stress (Strand and McDonald 1985). The morphology of the virus-like particles apparent in *Nopp140*-/- nuclei is distinctly different from the morphology of the electron dense granules found exclusively in the cytoplasm of *Nopp140*-/- cells, but at this time we do not believe the nuclear particles are directly related to the cytoplasmic granules. While virus-like particles have been observed in the cytoplasm of *Drosophila* cells, their morphology remains unchanged from that of the nuclear

particles; both nuclear and cytoplasmic virus-like particles show an electron dense coat surrounding a less dense interior (Felluga et al. 1971).

As expected, homozygous *WH*-/- cells were enriched with cytoplasmic ribosomes, both free and ER-bound (Figure 3.6, F). However, their mitochondria were abnormally swollen, and while cristae remained visible, their matrices appeared empty. These mitochondrial phenotypes were previously attributed to the *pBac WH*- insertion in *P5CDh1* (He and DiMario 2011b). Interestingly, these abnormal mitochondrial phenotypes did not appear in *Nopp140*-/- cells (Figure 3.6, D) (see *Discussion*).

3.2.6 Metabolic Labeling to Assay Ribosome Function

Thus far we have shown that *Nopp140*-/- cells contain reduced amounts of cytoplasmic rRNA by toluidine blue staining and reduced amounts of cytoplasmic ribosomes by TEM analysis. To pursue this further we first showed that the relative abundance of ribosomal protein RpL34 in day 5-7 PEL *Nopp140*-/- second instar larvae (Figure 3.7, A, lane 1) was reduced compared to wild type second instar larvae and third instar larvae (lanes 3 and 4, respectively), and to *WH*-/- third instar larvae (lane 2). A companion SDS-polyacrylamide gel showed fairly equal loads of larval lysate; in particular, the actin band at 42 kDa was comparable in each lane. The loss of RpL34 agrees well with previously published results on the RNAi-mediated depletion of Nopp140 (Chapter 2, James et al. 2013).

We next used metabolic labeling as described (Chapter 2, James et al. 2013) to test the functionality of the ribosomes that remain in *Nopp140*-/- cells

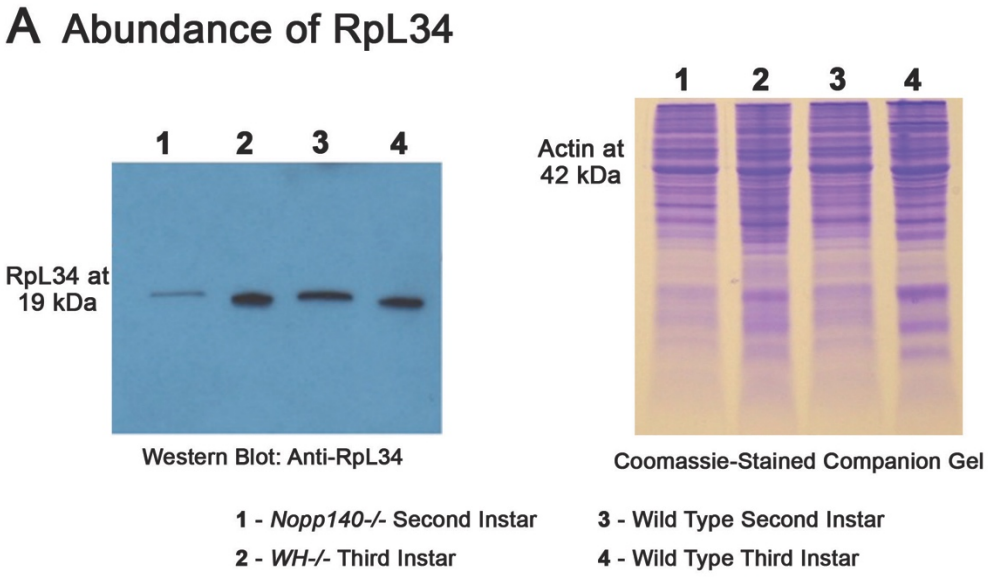

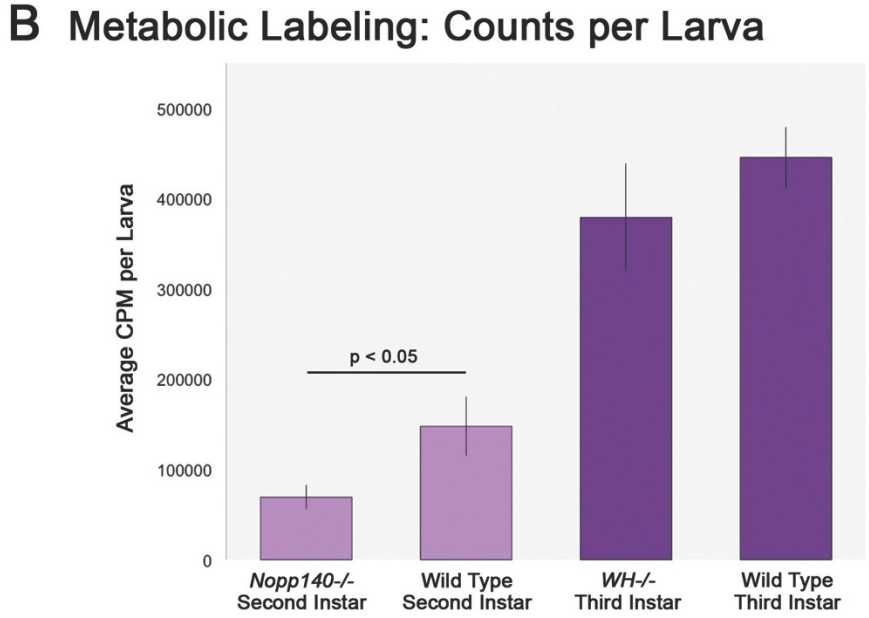

FIGURE 3.7. Immunoblot Analysis of RpL34 and Metabolic Labeling. (A) A specific antibody showed a loss of RpL34 in *Nopp140-/-* compared to *WH-/-* and wild-type lysates (Abgent, AP13207cev20). The band migrating at 42 kDa, which corresponds to actin, was used from the companion Coomassie-stained gel to determine equal loading of protein lysates. (B) Metabolic protein labeling was significantly reduced in second instar *Nopp140-/-* larvae compared to second instar wild-type (w^{1118}) larvae. Conversely, metabolic protein labeling was similar between third instar *WH-/-* and wild-type (w^{1118}) larvae. The entire experiment was performed three times. Two-tailed p values were equated using t test analysis (paired two sample for means). Error bars are ± standard error.

compared to wild type and *WH-/-* larvae (Figure 3.7). Metabolic protein labeling was performed by measuring the incorporation of ^{35}S-labeled amino acids into newly synthesized proteins during a 30 minute pulse. The amount of newly synthesized protein, reported as TCA-precipitable CPM per larva (Figure 3.7, B), was significantly reduced in *Nopp140-/-* larvae compared to similarly sized second instar wild type (w^{1118}) larvae. The complete loss of Nopp140 led to a 50% reduction of protein synthesis compared to wild type. We also compared TCA-precipitable CPM per third instar *WH-/-* larva and per third instar wild type (w^{1118}) larva, but we found no significant difference. We conclude that a total loss of Nopp140 leads to depletion of functional ribosomes, resulting in a 50% reduction in protein synthesis.

3.3 Discussion

We know that ribosomal RNA is produced in *Nopp140*-/- cells and that normal processing rRNA intermediates are present (Figure 3.6, B; He et al. 2014). This suggests that nucleoli in *Nopp140*-/- larvae are working at least partially, despite the general loss of cytoplasmic ribosomes. Ribosomal subunits may be assembled improperly in the absence of Nopp140; for example insufficient rRNA methylation (Figure 3.5) may disrupt proper assembly or function. Defective cytoplasmic ribosomes would then be degraded by P bodies for the small ribosomal subunits and by proteasomes for the large ribosomal subunits (Lafontaine, 2009). The electron dense cytoplasmic granules that we see in *Nopp140*-/- cells (Figure 3.6, D and E) (discussed below) may be the key

in explaining how the ribosomes are lost in these cells, leading to reduced protein synthesis (Figure 3.7).

3.3.1 *Nopp140* gene deletion versus P5CDh1 gene disruption

We previously described the organismal phenotypes caused by RNAi-depletion of Nopp140 in *Drosophila* (Cui and DiMario 2007; James et al. 2013). Here we focused on intracellular phenotypes caused by deleting the *Nopp140* gene. We necessarily had to delete the 3' exon of the down-stream gene, *P5CDh1,* to generate the deletion. Therefore, we differentiated phenotypes caused by the *WH- pBac* disruption in *P5CDh1* alone versus phenotypes caused by the deletion that eliminated *Nopp140* and the 3' end of *P5CDh1*. Briefly, *Nopp140*-/- larvae arrested in the second instar, while most *WH*-/- larvae developed further; *Nopp140*-/- larvae were severely deficient in cytoplasmic ribosomes compared to *WH*-/- larvae, and unlike *WH*-/- larvae, *Nopp140*-/- larvae displayed abnormal cytoplasmic granules. Conversely, mitochondria in *Nopp140*-/- larvae appeared normal at the ultra-structural level, suggesting that abnormal mitochondrial phenotypes had yet to display in *Nopp140*-/- larvae by day 6 PEL. Although not tested, maternal full length P5CDh1 enzyme may have persisted long enough to maintain normal mitochondrial morphology in the *Nopp140*-/- larvae. Alternatively, the predicted P5CDh1 truncation may have been under produced in *Nopp140*-/- larvae due to the loss of ribosomes and protein synthesis.

3.3.2 Pre-rRNA modifications

Nopp140 has been described as a chaperone for the initial delivery of C/D snoRNPs to nucleoli or for their proper interactions with target methylation sites within the pre-rRNA. We showed that fibrillarin localized variably to the nucleoplasm of *Nopp140*-/- midgut and fat body cells. Variable redistributions of nucleolar proteins like fibrillarin upon nucleolar stress may partially explain why human ribosomopathies affect select cells (*e.g.* bone marrow cells), while many other cell types seem to remain unaffected (Narla and Ebert, 2010). Preliminary results show that other nucleolar and nuclear proteins (nucleostemin 1 and 2, coilin) also redistribute upon complete loss of Nopp140 (Wang and DiMario, in preparation).

With fibrillarin redistributed in *Nopp140*-/- cells, we tested for proper 2'-*O*-methylation of clustered nucleotides within 18S and 28S rRNA regions. Loss of Nopp140 led to at least a three-fold and as much as eight-fold reduction in methylation at these sites compared to wild type and *WH*-/- controls. However, the half-life of ribosomes is several days (Liebhaber et al. 1978), and maternal ribosomes derived from *Nopp140-/TM3-GFP* mothers may still be present in their *Nopp140*-/- progeny. Since the balanced stock is healthy, these maternal ribosomes should be functional; therefore, we expect any remaining maternal ribosomes to have normal rRNA methylation patterns. If these maternal ribosomes can endure to day 5-6 PEL, our measured reductions in the methylation of *Nopp140*-/- rRNA would be under-estimated. To our knowledge,

this is the first report showing that Nopp140 is required for 2'-*O*-methylation of pre-rRNA.

Treacle is the vertebrate nucleolar phosphoprotein related to Nopp140 (Isaac et al. 2000); it too is required for 2'-*O*-methylation of C_{427} in the *Xenopus* 18S rRNA (Gonzales et al. 2005). Mutations in *Tcof1* which encodes treacle, lead to the Treacher Collins-Franceschetti Syndrome (Dixon 1996; Dixon et al. 2006; Trainor et al. 2009). Interestingly, *Tcof1*+/- mouse embryos with either a *CBA* or a *C57BL/6* genetic background are deficient in pre-rRNA methylation, and these embryos die. Conversely, *Tcof*+/- embryos with a BALB/c background maintain normal pre-rRNA methylation, and these embryos develop normally. Thus, unknown genetic factors within the *BALB/c* genome likely contribute to rRNA 2'-*O*-methylation.

Nopp140 has also been described as a chaperone for H/ACA snoRNPs (Meier and Blobel 1994; Yang et al. 2000; Wang et al. 2002). We tried several times to measure the degree of pseudouridylation at clustered sites in both the 18S and 28S rRNAs from *Nopp140*-/- larvae using established techniques (Ofengand and Bakin 1997; Wilkinson et al. 2006), but we consistently observed normal pseudouridylation in the absence of Nopp140. Wang et al. (2002) showed that *in vitro* pseudouridylation by H/ACA snoRNPs occurred normally in the absence of Nopp140. Gonzales et al. (2005) also showed that while 2'-*O*-methylation was impaired in *Tcof1*+/- mouse embryos with a *CBA* genetic background, pseudouridylation of U_{1642} in the 18S region was unaffected by

treacle haplo-insufficiency. Thus Nopp140 and treacle appear to function in 2'-*O*-methylation rather than in pseudouridylation.

3.3.3 Aberrant cytoplasmic granules in *Nopp140*-/- cells

The electron dense granules that appear in the cytoplasm of *Nopp140-/-* cells could be P bodies, neuronal-like RNA granules, stress granules, hybrids of these granules (Buchan and Parker 2009), or even proteasomes. P bodies are cytoplasmic foci that participate in 5'→3' exonuclease digestion of un-capped mRNAs, in nonsense-mediated decay of mRNAs, and in micro-RNA-induced translation silencing (Eulalio et al. 2007). P bodies normally recycle small ribosomal subunits (LaFontaine 2009). The granules in *Nopp140*-/- cells measured 40-50 nm in diameter, and they appear to have ribosomes bound to their surfaces (Figure 3.6, E). P bodies measure about 100-300 nm in HeLa cells (Eystathioy et al. 2002; Yang et al. 2004), and they lack large ribosomal subunits. Neuronal granules on the other hand, contain ribosomes, but they range in size from 150 to 1000 nm (Krichevsky and Kosik 2001). Stress granules contain small ribosomal subunits (Anderson and Kedersha 2008; Buchan and Parker 2009), but they too are much larger in size (*e.g.* Souquere et al. 2009). Granules that come closest in size and morphology to those we see in *Nopp140*-/- cells are heat shock (stress) granules found in tomato cells (Nover et al. 1983, 1989).

We continue our efforts at identifying these electron dense cytoplasmic granules in *Nopp140*-/- cells. Preliminary immuno-fluorescence data (not shown) suggests that an antibody directed against the *Drosophila* decapping protein 1 (DCP-1, Barbee et al. 2006), a marker for processing (P) bodies, labels granules

in the cytoplasm of *Nopp140*-/- midgut cells preferentially compared to wild type midgut cells, but this same antibody failed to completely label the electron dense granules in *Nopp140*-/- cells by immuno-gold labeling. Compounding the problem in identifying the electron dense granules, other tissues (Malpighian tubules, fat body) in *Nopp140*-/- larvae failed to show convincing immuno-fluorescence labeling with the anti-DCP-1. We also tried antibodies against FMR1, a marker protein for stress granules (Sheth and Parker 2003), but these antibodies failed to show a convincing signal above background. We are currently exploring the possibility that the granules in *Nopp140*-/- cells are related to proteasomes that are known to recycle the large ribosomal subunit (LaFontaine 2009). Despite the uncertainty, we propose that formation of these granules is related to nucleolar stress, and that their formation be ascribed as an intracellular ribosomopathy (Narla and Ebert 2010), or a defective ribostasis (Ramaswami et al. 2013).

3.4 Materials and Methods

3.4.1 Fly stocks

Strains used in this study included the w^{1118} line (Bloomington stock #3605) which we use as a wild type control, the second chromosome balancer stock *w*/w**; Sp^{1}/*CyO* originally from W. M. Saxton (Indiana University), the second chromosome GFP-balancer stock w^{-}/w^{-}; Pin^{1}/*CyO, P{Gal4-Kr.C},P{UAS-GFP.S65T}* (Bloomington stock #5194, abbreviated here simply as *CyO-GFP*), the third chromosome balancer stock w^{-}/w^{-}; Scm^{Et50} *e*/*TM3* Sb^{1}, *Ser* originally from J. A. Simon (University of Minnesota) and abbreviated here as $TM3/Et^{50}$, the third chromosome balancer stock w^{-}/w^{-}; *Sb/Tm3, Ser, Act-GFP* (Bloomington

stock #4534, abbreviated here simply as *TM3-GFP*), the flippase-encoding stock *P{hsFLP}*^{1}, *y*^{1}, *w*^{1118}, *Dr*^{Mio}*/TM3*, *ry** *Sb*^{1} (Bloomington stock #7), and the homozygous *daughterless-GAL4* driver line (Bloomington stock #8641). The two *PiggyBac* (*pBac*) lines used for recombination were *Nopp140*$^{e01407/e01407}$ containing an *RB+ pBac* element and *P5CDh1*^{f04633}*/TM6* containing a *WH- pBac* element. Both lines were obtained from the Exelixis collection at Harvard University. Flies were maintained on standard fly food at room temperature (22-24° C).

3.4.2 Deleting the *Nopp140* gene

We used the FLP/FRT method described by Parks et al. (2004) to delete the *Nopp140* gene (Figure 3.1). The technique used two *pBac* elements that contained Flippase Recognition Target (FRT) elements. Male flies bearing *RB+* were crossed to females from the *hsFLP* (X chromosome) stock. Progeny males carrying both *hsFLP* and *RB+* were then crossed to *P5CDh1*^{f04633}/*TM3* females in bottles. This cross was maintained for an initial 48 hours, after which progeny embryos and larvae with parents still present were subjected to a one hour heat-shock at 37° C to induce flippase expression. The parents were removed after 72 hours of mating, at which time the progeny were again subjected to a one hour heat-shock at 37° C and then identical heat shocks on four subsequent days. Progeny were raised to adults, and newly eclosed females were crossed to the 3rd chromosome balancer stock, *TM3/Et*^{50}.

3.4.3 Genomic PCRs to verify *Nopp140* gene deletion

Genomic DNA was extracted according to the protocol provided by the Berkeley *Drosophila* Genome Project (http://www.fruitfly.org/about/methods/inverse.pcr.html). Two-sided and hybrid PCR strategies detected and verified the *Nopp140* gene deletion (Figure 3.1, A and B). Green forward and reverse PCR primers flanking the left end of the recombinant element were 5'-CAGATCCAGTTGCTCGTAGGCATGG-3' (upstream of *RB*+) and 5'- CATCGCTTTGCAGAAGAGCAGAGAG-3' (within *RB+)*. Red forward and reverse PCR primers flanking the right end of the recombinant element were 5'-TGACAATGTTCAGTGCAGAGACTCG-3' (within *WH-*) and 5'AAACTGGTGCACACCTCTACCAAG-3' (within *P5CDh1)*. The blue primer for the hybrid PCR (Figure 3.1, A) was the same for both forward and reverse directions; the sequence was 5'-GACGCATGATTATCTTTTACGTGAC-3' as described in the Supplementary Methods from Parks et al. (2004). We used Phusion High-Fidelity DNA polymerase (New England BioLabs) for the genomic PCRs.

3.4.4 Hand-selection of homozygous *Nopp140*-/- and *WH*-/- larvae

Chromosomes with known *Nopp140* deletions were re-balanced over *TM3-GFP* to establish permanent stocks. Flies from these stocks were crossed *inter se* to generate homozygous *Nopp140*-/- knock-out progeny embryos and larvae that failed to fluoresce green. Since the *WH-* transposon in parental line $P5CDh1^{f04633}$ resides within the 3' coding region of the downstream *P5CDh1*gene, homozygous larvae from this parental line ($P5CDh1^{f04633/f04633}$,

expressed here simply as *WH*-/-) were hand-selected in the same manner. These larvae were used throughout this study as controls to differentiate phenotypes related to the *P5CDh1* gene disruption versus phenotypes caused by the *Nopp140* deletion. We used w^{1118} larvae as 'wild type' controls.

3.4.5 Immuno-fluorescence microscopy

Tissues from staged larvae were prepared for immuno-fluorescence microscopy using buffered 2% paraformaldehyde as described (de Cuevas et al., 1996). Primary antibodies included a guinea pig polyclonal antibody directed against a unique peptide sequence within the carboxy terminus of Nopp140-RGG (Cui and DiMario 2007) used at 1/100, and the mouse monoclonal anti-fibrillarin mAb72B9 (Reimer et al. 1987; spent hybridoma supernatant used without dilution). Secondary antibodies included the Alexa Fluor 546 conjugated goat anti-guinea pig IgG (Molecular Probes, A11074), an Alexa-Fluor 488 conjugated goat anti-mouse IgG (Molecular Probes, A10667), and a fluorescein conjugated Immuno-Pure® goat anti-mouse IgG (Pierce, 31563). We routinely used these secondary antibodies at 1/250. Tissues were counter-stained with 4',6-diamino-2-phenylindole (DAPI, Polysciences) at 1 µg/ml and examined by conventional fluorescence microscopy using a Zeiss Axioskop equipped with a SPOT RTSE digital camera.

3.4.6 Transmission Electron Microscopy

Larval tissues were dissected and fixed in EM-grade 2% glutaraldehyde, 1% formaldehyde in 0.1 M cacodylate buffer, pH 7 for 1 hr, and then rinsed overnight in 0.1 M cacodylate buffer, pH 7, containing 4 mM glycine. Tissues

were post-fixed with 2% osmium tetroxide for 1 hr, rinsed twice with water 5 min each, and then stained with 0.5% uranyl acetate in the dark for 1 hr. Tissues were dehydrated through 100% ethanol and embedded in LR White plastic. Sections were prepared using a Leica EM UC7 ultra-microtome. Thick sections (0.5 μm) were mounted on glass slides, stained with 0.5% toluidine blue in 2.0% Na+ borate using a warm heating plate, washed with water, air dried, and viewed with a Zeiss Axioskop. Thin sections for TEM were stained with Reynold's lead citrate and viewed with either a JEOL 100CX TEM operating at 80 kv or a JEOL JEM-1400 TEM operating at 120 kv. We used standard 3 X 4 inch Kodak film with the 100CX, and Gatan's Orius side-mount or Ultra-scan bottom-mount digital cameras with the JEM-1400. The 3 X 4 inch negatives were scanned at 1200 dpi and the images were inverted. All digital images were prepared for publication using Adobe Photoshop.

3.4.7 Assessing 2'-*O*-methylation

We used the reverse transcriptase-PCR technique of Dong et al. (2012) to determine the extent of 2'-*O*-methylation on clustered nucleotides within the 18S and 28S regions of rRNA that were previously determined to undergo 2'-*O*-methylation (Yuan et al. 2003; Huang et al. 2005). Total RNA was isolated from w^{1118}, *WH*-/-, and *Nopp140*-/- larvae using TRIzol (Invitrogen) as described by the manufacturer. RNA concentrations were determined by measuring the absorbance at 260 nm using a NanoDrop spectrophotometer (Thermo Scientific). Total RNA (200 ng) was used for reverse transcription using M-MLV reverse transcriptase (Promega) with dNTPs set at 0.5 μM, 1.0 μM, or 400 μM. Reverse

transcriptase hesitates at 2'-*O*-methylation sites in the presence of reduced dNTPs (0.5 or 1.0 μM) and fails to produce full length cDNAs. First strand cDNAs were amplified using *Taq* polymerase (New England BioLabs) and the same reverse primer used for RT extension and one of two forward primers: one forward primer was downstream of the target methylation site, and the other was upstream of the target methylation site (see Figure 3.5). For the 18S target site, the cluster of methylated nucleotides included U_{1356}, G_{1358}, and C_{1367}. The reverse primer for this site was 5'-CCATTTAAGAAGCTAGTGTCCTTATAATGGG-3', the forward primer upstream (FU) of these methylated nucleotides was 5'-ACAGATTGATAGCTCTTTCTCGAATC-3', and the forward primer downstream (FD) of these methylated nucleotides was 5'-GTTCGTGGAGTGATTTGTCTGG-3'. We used 0.5 μM (and 400 μM as control) dNTPs in the 18S RT reaction. For the 28S target site, the cluster of methylated nucleotides included A_{2634}, C_{2645} and A_{2653}, the reverse primer was 5'-TGGCTAGGAAATGATACACGTTCC-3', the forward primer upstream (FU) of these methylated nucleotides was 5'-TCTAATTAGTGACGCGCATGAATG-3' and the forward primer downstream (FD) of the methylated residues was 5'-AGCGAAACCACAGCCAAG-3'. We used 1.0 μM (and 400 μM as control) dNTPs in the 28S RT reaction. Three biological experiments were performed for both the 18S and 28S sites with all PCRs run in triplicate. PCRs were limited to 25 cycles. PCR products were resolved on agarose gels, stained with ethidium bromide, and quantified using Image Lab (BioRad) and ImageJ software. The bar graphs in Figure 3.5 were assembled

using Microsoft Excel. Two-tailed P values were equated using t-Test analysis (paired two sample for means).

3.4.8 Metabolic labeling

Methods to determine relative protein synthesis rates in wild type, WH-/-, and Nopp140-/- larvae were as described in Chapter 2 (James et al. 2013) with minor modifications. Briefly, 40-60 second instar larvae (*Nopp140-/-* and w^{1118}) and 10-20 third instar larvae (*WH-/-* and w^{1118}) were dissected in Robb's A+B buffer (Robb 1969) in disposable plastic depression slides. All liquid was removed, after which 200 µL of Robb's A+B and 10 µL of EXPRE^{35}S^{35}S Protein Labeling Mix (Perkin-Elmer, NEG772002M, 10.0 mCi/ml) were added. The depression slides were placed in a moist chamber and incubated for 30 minutes at room temperature with gentle shaking to distribute the ^{35}S mix evenly. The number of larvae used per experiment was carefully counted. To determine incorporated CPM, 300 µL of larval lysate was combined with 150 µL dH_2O, 150 µL of 2 mg/mL BSA, and 120 µL 100% TCA. The mixture was incubated on ice for 30 minutes. 200 µL of this precipitation mixture was passed through a vacuum filter assembly (Sigma-Aldrich, Z290475) containing a Whatman 25 mm GFC glass microfiber filter, so that there were three filters per genotype. Filters were air-dried and placed separately into 10 mL of Scintiverse (TM) BD Cocktail (Fisher Scientific). CPM was determined using a Beckman LS 6000IC scintillation counter. The final CPM per sample was determined by taking an average of these three filters. The CPM per larva was then determined. The entire experiment was performed three times.

3.4.9 RT-PCRs

Total RNA was extracted from control and *Nopp140*-/- larvae using TRIzol (Invitrogen) according to the manufacturer's recommendations. The RNA was dissolved in diethyl pyrocarbonate-treated water. First-strand cDNA synthesis was performed using SuperScript III Reverse Transcriptase (Invitrogen) according to the manufacturer's recommendations with either oligo(dT) primers or gene-specific primers.

Specific PCR primer sets included the following: *Nopp140* gene-specific forward and reverse primers were 5'-CTAGCCAAGGTTTTCCAGCAGAAGAC-3' (3' end of exon 1) and 5'-GCTGGCTTAGTCTCCTCATCGGAG-3' (within exon 2). *Actin 5C* gene-specific forward and reverse primers were 5'-CTCACCTATAGAAGACGAAGAAGTTGCTGCTCT-3' and 5'-CTAACTGTTGAATCCTCGTAGGACTTCTCCAACG-3'.

3.5 References

Akai H, Gateff E, Davis LE, Schneiderman, HA (1967). Virus-like particles in normal and tumorous tissues of *Drosophila*. Science 157:810-813.

Andersen JS, Lyon CE, Fox AH, Leung AKL, Lam YW, Steen H, Mann M, Lamond AI (2002) Directed proteomic analysis of the human nucleolus. Curr Biol 12:1-11.

Anderson P, Kedersha N (2007) Stress granules: the Tao of RNA triage. Trends Biochem Sci 33:141-150.

Barbee SA, Estes PS, Cziko A-M, Hillebrand J, Luedeman RA, Coller JM, Johnson N, Howlett IC, Geng C, Ueda R, Brand AH, Newbury SF, Wilhelm JE, Levine RB, Nakamura A, Parker R, Ramaswami M (2006) Staufen- and FMRP-containing neuronal RNPs are structurally and functionally related to somatic P bodies. Neuron 52:997-1009.

Bodenstein D (1950) The postembryonic development of *Drosophila*. In: Demerec M ed) Biology of Drosophila. Wiley, NewYork, pp275–367.

Buchan JR, Parker R (2009) Eukaryotic stress granules: the ins and outs of translation. Mol. Cell 36:932-941.

Chen HK, Pai CY, Huang JY, Yeh NH (1999) Human Nopp140, which interacts with RNA polymerase I: implications for rRNA gene transcription and nucleolar structural organization. Mol. Cell. Biol. 19:8536-8546.

Chiu CM, Tsay YG, Chang CJ, Lee SC (2002) Nopp140 is a mediator of the protein kinase A signaling pathway that activates the acute phase response α_1-acid glycoprotein gene. J. Biol. Chem. 277:39102-39111.

Cui Z, DiMario PJ (2007) RNAi knockdown of Nopp140 induces *Minute*-like phenotypes in *Drosophila*. Mol. Biol. Cell 18:2179-2191.

de Cuevas M, Lee JK, Spradling AC (1996) alpha-spectrin is required for germline cell division and differentiation in the *Drosophila* ovary. Development 122:3959-3968.

Dixon MJ (1996) Treacher Collins syndrome. Hum. Mol. Genet. 5:1391–1396.

Dixon J, Jones NC, Sandell LL, Jayasinghe SM, Crane J, Rey J-P, Dixon MJ, Trainor PA (2006) *Tcof1*/treacle is required for neural crest cell formation and proliferation deficiencies that cause craniofacial abnormalities. Proc. Natl. Acad. Sci. USA 103:13403–13408.

Dong Z-W, Shao P, Diao L-T, Zhou H, Yu C-H, Qu L-H (2012) RTL-P: a senstive approach for detecting sites of 2'-*O*-methylation in RNA molecules. Nucleic Acids Res. 40:e157.

Easton LE, Shibata Y, Lukavsky PJ (2010) Rapid, nondenaturing RNA purification using weak anion-exchange fas performance liquid chromatography. RNA 16:647–653.

Eulalio A, Behm-Ansmant I, Izaurralde E (2007) P bodies: at the crossroads of post-transcriptional pathways. Nat. Rev. Mol. Cell Biol. 8:9-22.

Eystathioy T, Chan EKL, Tenenbaum SA, Keene JD, Griffith K, Fritzler MJ (2002) A phosphorylated cytoplasmic autoantigen, GW182, associates with a unique population of human mRNAs within novel cytoplasmic speckles. Mol. Biol. Cell 13:1338-1351.

Feder N, Wolf MK (1965) Studies on nucleic acid metachromasy II. Metachromatic and orthochromatic staining by toluidine blue of nucleic acids in tissue sections. J Cell Biol 27:327–336.

Felluga F, Jonsson V, Liljeros MR (1971) Ultrastructure of new viruslike particles in *Drosophila*. J Invertebr Pathol 17:339–346.

Finnegan DJ (1985) Transposable elements in eukaryotes. Int. Rev. Cytol. 19:281-326.

Fink AL (2005) Natively unfolded proteins. Curr. Opin. Struc. Biol. 15:35-41.

Geraghty MT, Vaughn D, Nicholson AJ, Lin WW, Jimenez-Sanchez G, Obie C, Flynn MP, Valle D, Hu CA (1998) Mutations in the delta-1-pyrroline 5-carboxylate dehydrogenase gene cause type II hyperprolinemia. Hum. Mol. Genet. 7:1411-1415.

Ginisty H, Sicard H, Roger B, Bouvet P (1999) Structure and functions of nucleolin. J. Cell Sci. 112:761-772.

Gonzales B, Henning D, So RB, Dixon J, Dixon ML, Valdez BC (2005) The Treacher Collins syndrome (*TCOF1*) gene product is involved in pre-rRNA methylation. Hum. Mol. Genet. 14:2035–2043.

Granneman S, Baserga SJ (2004) Ribosome biogenesis: of knobs and RNA processing. Exp. Cell Res. 296:43-50.

Haslett MR, Pink D, Walters B, Brosnan ME (2004) Assay and subcellular localization of pyrroline-5-carboxylate dehydrogenase in rat liver. Biochim. Biophys. Acta 1675:81-86.

He F (2011) Functional analysis of *Nopp140* and *CG7145* in *Drosophila melanogaster*. Doctor of Philosophy, Louisiana State University.

He F, DiMario PJ (2011a) Structure and function of Nopp140 and Treacle. In: Olson MOJ (ed) The Nucleolus, Protein Reviews 15, Springer, New York, pp 253-278.

He F, DiMario PJ (2011b) *Drosophila* delta-1-pyrroline-5-carboxylate dehydrogenase (P5CDh) is required for proline breakdown and mitochondrial integrity - establishing a fly model for human type II hyperprolinemia. Mitochondrion 11:397-404.

He F,* James A*, Raje H, Ghaffari H, DiMario P (2014) Deletion of *Drosophila* Nopp140 induces subcellular ribosomopathies. Chromosoma 124:191-208. *co-first authors http://dx.doi.org/10.1007/s00412-014-0490-9.

Hu CA, Lin WW, Valle D (1996) Cloning, characterization, and expression of cDNAs encoding human delta 1-pyrroline-5-carboxylate dehydrogenase. J. Biol. Chem. 271:9795-9800.

Huang ZP, Zhou H, He HL, Chen CL, Liang D, Qu LH (2005) Genome-wide analyses of two families of snoRNA genes from *Drosophila melanogaster*, demonstrating the extensive utilization of introns for coding of snoRNAs. RNA 11:1303-1316.

Inagaki E, Ohshima N, Takahashi H, Kuroishi C, Yokoyama S, Tahirov TH (2006) Crystal structure of *Thermus thermophilus* Δ^1-pyrroline-5-carboxylate dehydrogenase. J. Mol. Biol. 362:490-501.

Inagaki E, Ohshima N, Sakamoto K, Babayeva ND, Kato H, Yokoyama S, Tahirov TH (2007) New insights into the binding mode of coenzymes: structure of *Thermus thermophilus* Δ^1-pyrroline-5-carboxylate dehydrogenase complexed with $NADP^+$. Acta Cryst. F 63:462-465.

Isaac C, Yang Y, Meier UT (1998) Nopp140 functions as a molecular link between the nucleolus and the coiled bodies. J. Cell Biol. 142:319-329.

Isaac C, Marsh KL, Paznekas WA, Dixon J, Dixon MJ, Jabs EW, Meier UT (2000) Characterization of the nucleolar gene product, treacle, in Treacher Collins syndrome. Mol. Biol Cell 11:3061–3071.

James A, Cindass R Jr, Mayer D, Terhoeve S, Mumphrey C, DiMario P (2013) Nucleolar stress in *Drosophila melanogaster*, RNAi-mediated depletion of Nopp140. Nucleus 4:123-133.

Kelly S, Singleton W, Wickstead B, Ersfeld K, Gull K (2006) Characterization and differential nuclear localization of Nopp140 and a novel Nopp140-like protein in Trypanosomes. Eukaryotic Cell 5:876-879.

Kim MH, Cooper DR, Oleksy A, Devedjiev Y, Derewenda U, Reiner O, Otlewski J, Derewenda ZS (2004) The structure of the N-terminal domain of the product of the lissencephaly gene Lis1 and its functional implications. Structure 12:987-998.

Kim YK, Lee WK, Jin Y, Lee KJ, Jeon H, Yu YG (2006) Doxorubicin binds to un-phosphorylated form of hNopp140 and reduces protein kinase CK2-dependent phosphorylation of hNopp140. J. Biochem. Mol. Biol. 39:774-781.

Kressler D, Hurt E, Baβler J (2010) Driving ribosome assembly. Biochim. Biophys. Acta 1803:673-683.

Krichevshy AM, Kosik KS (2001) Neuronal RNA granules: a link between RNA localization and stimulation-dependent translation. Neuron 32:683-696.

Lafontaine D (2009) A ‘garbage can’ for ribosomes: how eukaryotes degrade their ribosomes. Trends Biochem Sci 35:267–277.

Liebhaber SA, Wolf S, Schlessinger D (1978) Differences in rRNA metabolism of primary and SV40-transformed human fibroblasts. Cell 13:121–127.

McCain J, Danzy L, Hamdi A, Dellafosse O, DiMario P (2006) Tracking nucleolar dynamics with GFP-Nopp140 during *Drosophila* oogenesis and embryogenesis. Cell Tissue Res. 323*:*105-115.

Meier UT (1996) Comparison of the rat nucleolar protein nopp140 with its yeast homolog SRP40. Differential phosphorylation in vertebrates and yeast. J. Biol. Chem. 271:19376-19384.

Meier UT, Blobel G (1994) NAP57, a mammalian nucleolar protein with a putative homolog in yeast and bacteria. J. Cell Biol. 127:1505-1514.

Miyake T, Mae N, Shiba T, Kondo S (1987) Production of virus-like particles by the transposable genetic element, *copia*, of *Drosophila melanogaster*. Mol. Gen. Genet. 207:29-37.

Narla A, Ebert BL (2010) Ribosomopathies: human disorders of ribosome dysfunction. Blood 115:3196-3205.

Nover L, Scharf K-D, Neuman D (1983) Formation of cytoplasmic heat shock granules in tomato cell cultures and leaves. Mol. Cell Biol. 3:1648-1655.

Nover L, Scharf K-D, Neumann D (1989) Cytoplasmic heat shock granules are formed from precursor particles and are associated with a specific set of mRNAs. Mol. Cell. Biol. 9*:*1298-1308.

Ochs RL, Lischwe MA, Spohn WH, Busch H (1985) Fibrillarin: a new protein of the nucleolus identified by autoimmune sera. Biol. Cell 54:123-133.

Ofengand J, Bakin A (1997) Mapping to nucleotide resolution of pseudouridine residues in large subunit ribosomal RNAs from representative eukaryotes, prokaryotes, archaebacteria, mitochondria and chloroplasts. J. Mol. Biol. 266:246-268.

Parks AL, Cook KR, Belvin M, Dompe NA, Fawcett R, Huppert K, Tan LR, Winter CG, Bogart KP, Deal JE, Deal-Herr ME, Grant D, Marcinko M, Miyazaki WY, Robertson S, Shaw KJ, Tabios M, Vysotskaia V, Zhao L, Andrade RS, Edgar KA, Howie E, Killpack K, Milash B, Norton A, Thao D, Whittaker K, Winner MA, Friedman L, Margolis J, Singer MA, Kopczynski C, Curtis D, Kaufman TC, Plowman GD, Duyk G, Francis-Lang HL (2004) Systematic generation of high-resolution deletion coverage of the *Drosophila melanogaster* genome. Nat. Genet. 36:288-292.

Ramaswami M, Taylor JP, Parker R (2013) Altered ribostasis: RNA-protein granules in degenerative disorders. Cell 154:727-736.

Reimer G, Pollard KM, Penning CA, Ochs RL, Lischwe MA, Busch H, Tan EM (1987) Monoclonal autoantibody from a (New Zealand black x New Zealand white) F_1 mouse and some scleroderma sera target an M_r 34,000 nucleolar protein of the U3 RNP particle. Arthritis Rheum. 30:793-800.

Rubin GM (1983) Dispersed repetitive DNAs in *Drosophila*. In: Shapiro JA (ed) Mobile Genetic Elements, Academic Press, New York, pp 329-361.

Sheth U, Parker R (2003) Decapping and decay of messenger RNA occur in cytoplasmic processing bodies. Science 300:805-808.

Small WC, Jones ME (1990) Pyrroline 5-carboxylate dehydrogenase of the mitochondrial matrix of rat liver. Purification, physical and kinetic characteristics. J. Biol. Chem. 265:18668-18672.

Souquere S, Mollet S, Kress M, Dautry F, Pierron G, Weil D (2009) Unravelling the ultrastructure of stress granules and associated P-bodies in human cells. J. Cell Sci. 122:3619-3626.

Strand DJ, McDonald JF (1985) *Copia* is transcriptionally responsive to environmental stress. Nucleic Acids Res. 13:4401-4410.

Tafforeau L, Zorbas C, Langhendries J-L, Mullineux S-T, Stamatopoulou V, Mullier R, Wacheul L, Lafontaine DLJ (2013) The complexity of human ribosome biogenesis revealed by systematic nucleolar screening of pre-rRNA processing factors. Mol. Cell 51:539-551.

Thandaponi P, O'Connor TR, Bailey TL, Richard S (2013) Defining the RGG/RG motif. Mol. Cell 50:613-623.

Trainor PA, Dixon J, Dixon MJ (2009) Treacher Collins syndrome: etiology, pathogenesis and prevention. Eur. J. Hum. Genet. 17:275–283.

Tsai Y-T, Lin C-I, Chen H-K, Lee K-M, Hsu C-Y, Yang S-J, Yeh N-H (2008) Chromatin tethering effects of hNopp140 are involved in the spatial organization of nucleolus and the rRNA gene transcription. J. Biomed. Sci. 15:471-486.

Valle DL, Phang JM, Goodman SI (1974) Type 2 hyperprolinemia: absence of delta1-pyrroline-5-carboxylic acid dehydrogenase activity. Science 185:1053-1054.

Valle D, Goodman SI, Harris SC, Phang JM (1979) Genetic evidence for a common enzyme catalyzing the second step in the degradation of proline and hydroxyproline. J. Clin. Invest. 64:1365-1370.

Vandelaer M, Thiry M (1998) The phosphoprotein pp135 is an essential constituent of the fibrillar components of nucleoli and of coiled bodies. Histochem. Cell Biol. 110:169-177.

Waggener JM, DiMario PJ (2002) Two splice variants of Nopp140 in *Drosophila melanogaster*. Mol. Biol. Cell 13:362-381.

Wang C, Query CC, Meier UT (2002) Immunopurified small nucleolar ribonucleoprotein particles pseudouridylate rRNA independently of their association with phosphorylated Nopp140. Mol. Cell. Biol. 22:8457-8466.

Wilkinson KA, Merino EJ, Weeks KM (2006) Selective 2'-hydroxyl acylation analyzed by primer extension (SHAPE): quantitative RNA structure analysis at single nucleotide resolution. Nat. Protoc. 1:1610-1616.

Yang Y, Isaac C, Wang C, Dragon F, Pogacic V, Meier UT (2000) Conserved composition of mammalian box H/ACA and box C/D small nucleolar ribonucleoprotein particles and their interaction with the common factor Nopp140. Mol. Biol. Cell 11:567-577.

Yang Z, Jakymiw A, Wood MR, Eystathioy T, Rubin RL, Fritzler MJ, Chan EKL (2004) GW182 is critical for the stability of GW bodies expressed during the cell cycle and cell proliferation. J. Cell Science 117:5567-5578.

Yuan G, Klambt C, Bachellerie JP, Brosius J, Huttenhofer A (2003) RNomics in *Drosophila melanogaster*: identification of 66 candidates for novel non-messenger RNAs. Nucleic Acids Res. 31:2495-2507.

CHAPTER 4. CONFIRMATION AND EXTENSION

4.1 Introduction

In Chapters 2 and 3, we utilized loss-of-function approaches to elucidate the role of Nopp140, either by RNAi-mediated knockdown or gene knockout. In Chapter 2, we reported that Nopp140 is required in diploid imaginal cells (wing discs) for cell survival and proper tissue development. To confirm and extend upon that finding, we expressed Nopp140-RNAi in a different precursor cell population: embryonic brain and eye disc cells. Additionally, since we have observed autophagy and JNK activation in larvae expressing Nopp140-RNAi organism-wide, we assayed the activity status of the JNK pathway as well as the activation of autophagy at the gene-level in *Nopp140-/-* larvae.

Most recently, we have conducted gain-of-function experiments involving the expression of individual Nopp140 isoforms. Over-expression of either Nopp140 isoform organism-wide is lethal (Cui and DiMario 2007), so we first utilized the UAS-GAL4 system to over-express GFP-Nopp140-RGG or GFP-Nopp140-True selectively in the larval wing discs, which are progenitor cells for the adult wings. This leads to a non-lethal, scorable phenotype that we may use to assay the consequence of disrupting the balance of Nopp140 expression. We also assayed RNA Polymerase I activity in larvae that over-express either GFP-Nopp140-True or GFP-Nopp140-RGG organism-wide.

4.2 Nopp140 and Eye Development

Expression of Nopp140-RNAi in the wing disc (*A9-GAL4>UAS.C4.2*, Figure 2.4) resulted in a non-lethal phenotype, so we wanted to see if knockdown

of Nopp140 in a different diploid progenitor cell population would induce a similar result. The cross in Figure 4.1, A was designed to express shRNA directed against *Nopp140* mRNA under the control of the *eyeless* (*ey*) promoter. As is the design of the UAS-GAL4 system developed for use in *Drosophila melanogaster* (Figure 1.5) (Brand and Perrimon 1993), our cross allows shRNAs targeting the common 5' end of *Nopp140* mRNAs to be expressed in the same temporal and spatial pattern as the endogenous *ey* gene. *ey* expression varies throughout development of *D. melanogaster*. *ey* is initially expressed in the embryonic ventral nerve cord, primordial cells of the eye imaginal disc, in the optic lobes, and certain regions of the brain (Quiring et al. 1994). *ey* is also expressed in the embryonic progenitor cells that give rise to the mushroom body (MB) (Noveen et al. 2000), which is a part of the brain involved in olfactory learning and memory (Zars et al. 2000). In the larval stages, *ey* is continually expressed in the developing eye discs. However, in the third larval stage, *ey* expression is mostly restricted to the portion of the eye disc that is anterior to the morphogenic furrow (Halder et al. 1995).

From the cross described in Figure 4.1, A, F1 progeny were selected based on wing phenotype: straight-winged progeny express Nopp140-RNAi in the *ey* pattern (*UAS-C4.2/ey-GAL4; UAS-C3/+)* while curly-winged flies were used as sibling controls (*UAS-C4.2/CyO; UAS-C3/+)*. The majority of Nopp140-RNAi expressing flies displayed eyes that were strikingly small and malformed, measuring almost half the size of parental stock flies (*UAS-C4.2/UAS-C4.2; UAS-C3/UAS-C3* and *ey-GAL4/CyO;+/+*) and sibling controls on average (Figure

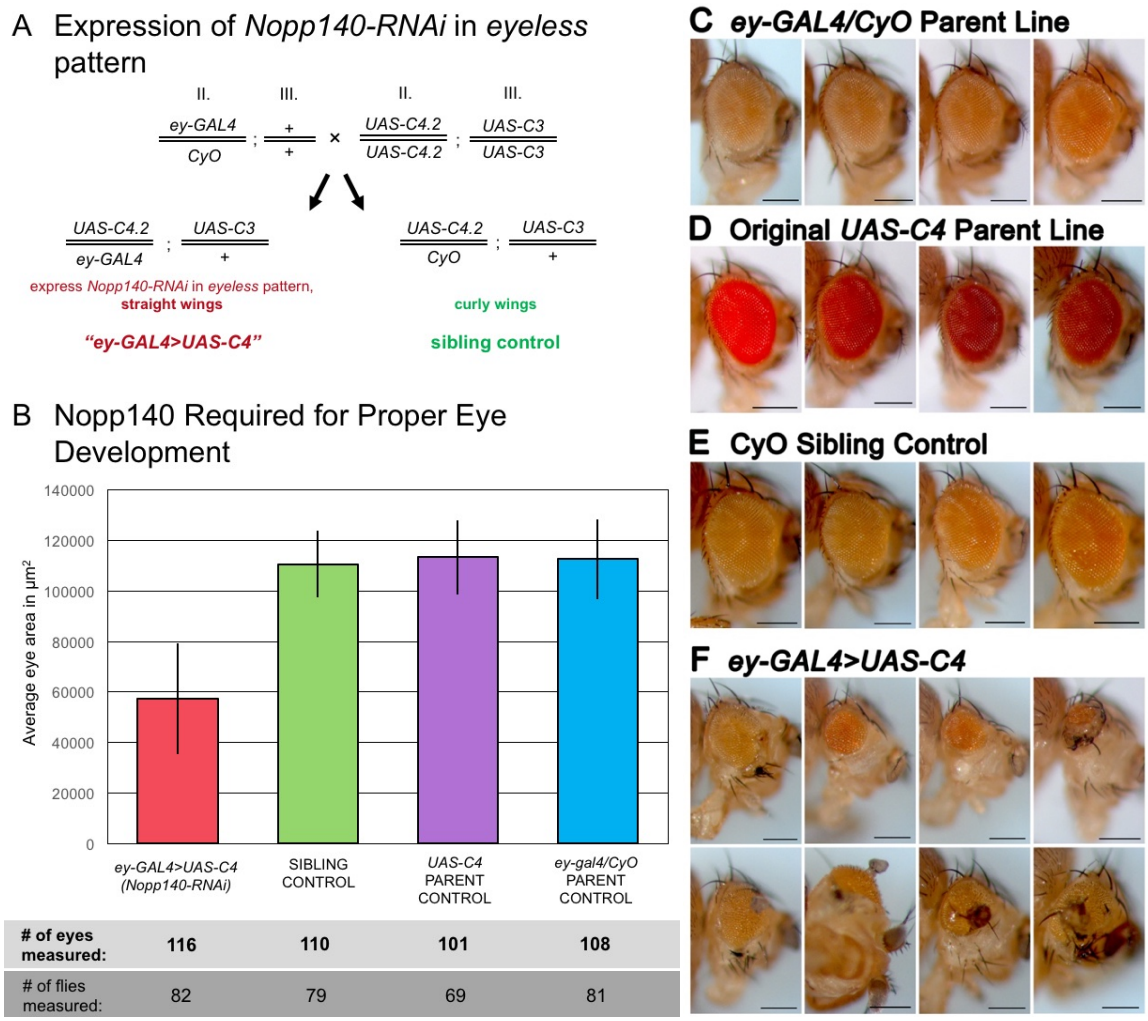

FIGURE 4.1. Expression of Nopp140-RNAi in *eyeless* Pattern.
(A) *ey-GAL4/CyO* flies were crossed to *UAS-C4* homozygous flies at 27-28° C for efficient knockdown of Nopp140. The *Nopp140-RNAi* expressing flies (*ey-GAL4>UAS-C4*) were separated from sibling controls due to the absence of curly wings. *UAS-C4* is the original transgenic stock that expresses short hairpin RNA specific for the common 5' end of *Nopp140* mRNAs from the 2nd and 3rd chromosomes. (B) Knockdown of Nopp140 in the *ey* pattern leads to a striking reduction in adult eye size. Bars represent the average eye area (in μm^2) of all scored flies; the total number of eyes and the number of individual flies scored per genotype are listed at the bottom of the graph. Error bars are ± standard deviation. (C-F) Photos representing eye size and morphology observed per genotype. Bar = 200 µm for all photos.

4.1, B-F). The eye phenotypes of Nopp140-RNAi expressing flies ranged from a mild almost wild-type size, to more severe, displaying very few ommatidia (Figure 4.1, F). In addition to overall smaller eyes in Nopp140-RNAi expressing flies, we often observed a change in the pattern of the bristles that normally protrude between the ommatidia; the bristles were short and not uniform, as they are in wild type flies. Also, hairs that normally surround the eye are misshapen in most Nopp140-RNAi expressing flies (Figure 4.1, F). Additionally, one of the more extreme eye phenotypes we observed had unknown structures protruding from the center of the eye (Figure 4.1, F, bottom panel). We noticed that the severity of the eye phenotype correlated to the age of the culture; earlier-eclosing progeny had a milder phenotype while later flies had more extreme eye malformations. We have observed this change in phenotype severity before (Figure 2.3); we assume that changes in nutrition availability as the culture ages contribute to this difference.

At this time, we have only measured the eye size for adult flies that express Nopp140-RNAi in the *ey* pattern; since shRNAs against Nopp140 express in cell types other than the eye disc using this system (primordial MB cells, embryonic ventral nerve cord) there may be other consequences to disrupting Nopp140, either developmental or behavioral, that we have not yet observed (see Chapter 5).

4.3 Expression of Stress Related genes in *Nopp140-/-* Larvae

Immunoblots probing whole larval lysates with an anti-pJNK antibody indicated that JNK is activated in larvae expressing Nopp140-RNAi organism-

wide (Figure 2.8). To determine if JNK is activated in *Nopp140-/-* larvae as well, RT-PCR experiments were conducted using primers targeting the *JNK*, *puc,* and *Actin5C* gene products. The results reported in Figure 4.2 are represented as a ratio of the gene-specific RT-PCR product to the *Actin5C*-specific product, which is used here as a control for the amount of total RNA used in each RT-PCR experiment. JNK expression levels are near equivalent in all samples (Figure 4.2). This result is consistent with JNK's main regulation mechanism: phosphorylation of JNK already present. Activated JNK (pJNK) phosphorylates the transcription factor AP-1 which activates the expression of the pro-apoptotic *hid* gene (summarized in a figure in Chapter 5) (Riesgo-Escovar 1996, McNamee and Brodsky 2009). Another gene that is activated by pJNK is *puc*, which encodes a phosphatase that affects JNK's activity in a negative feedback loop; measuring the amount of *puc* mRNA present in *Nopp140-/-* larvae is an indirect yet often used assessment of JNK's phosphorylation/activity status (McNamee and Brodsky 2009, Wu et al. 2009). Compared to similarly aged wild type larvae (WT, w^{1118}), *puc* expression in *Nopp140-/-* larvae is significantly increased (Figure 4.2). A less drastic increase in *puc* expression was observed in third instar *WH-/-* larvae compared to similarly aged wild type (WT, w^{1118}) control larvae (*p=0.0005 for *Nopp140-/-* vs. w^{1118} and ■p=0.03 for *WH-/-* vs. w^{1118}, see Figure 4.2). *WH-/-* larvae usually die within the third instar stage and *puc* expression may be in response to stress induced by the presence of swollen, presumably non-functional mitochondria (He and DiMario, 2011b and Figure 3.6). *Puc* overexpression in *Nopp140-/-* larvae is consistent with our hypothesis that

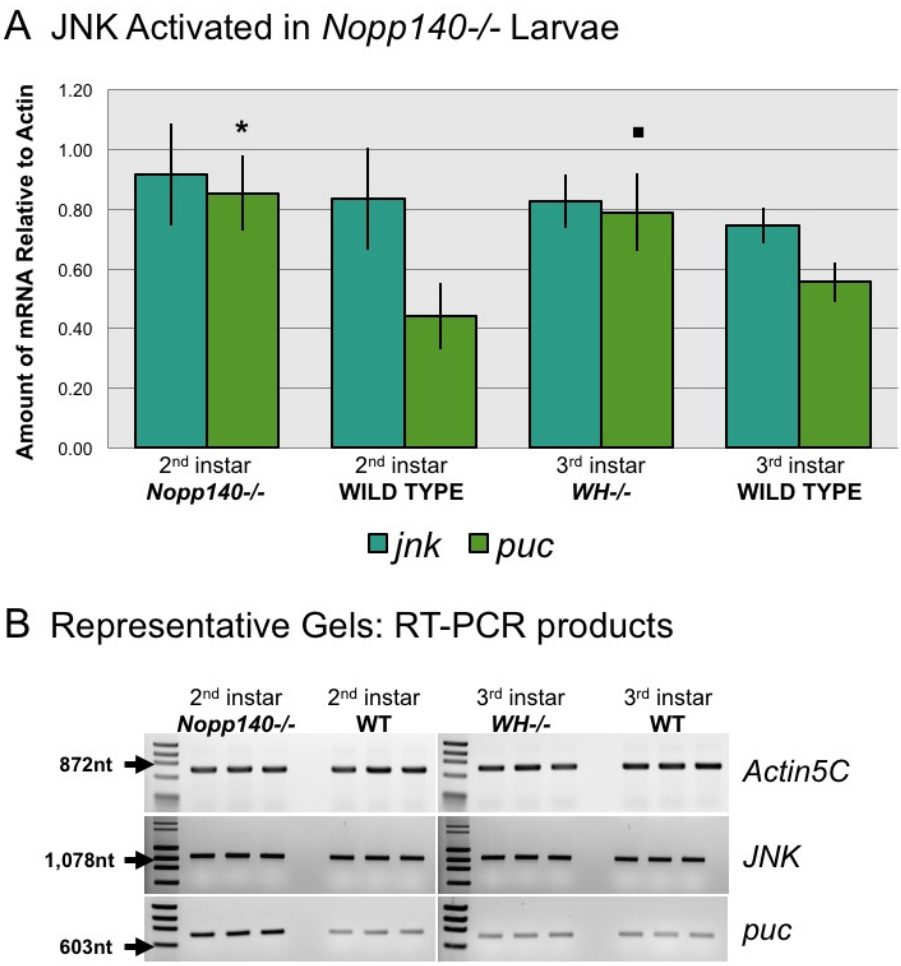

FIGURE 4.2. JNK Pathway Activated in *Nopp140-/-* Larvae. *JNK* expression is constant for all samples tested. JNK activity, however, is increased in *Nopp140-/-* larvae compared to similarly aged wild type (WT, w^{1118}) controls. Expression of *puc* is a commonly used measurement of JNK activity. (A) Bars represent average RT-PCR products of *JNK* or *puc* compared to that of *Actin5C*. Error bars are ± standard error. *p=0.0005 comparing 2nd instar *Nopp140-/-* and wild type (w^{1118}) control. ■p=0.03 comparing 3rd instar *WH-/-* and wild type (w^{1118}) control. p values = one-tailed values from t-Test, paired two sample for means, calculated by Microsoft Excel. (B) Representative agarose gels, with *Actin5C* control, *JNK*, and *puc* RT-PCR products. Four independent experiments were performed per gene and PCR reactions were performed in triplicate.

the nucleolar stress response induced by loss of Nopp140 involves the JNK pathway (diagrammed in the figure in Chapter 5 of this thesis).

In larvae expressing Nopp140-RNAi organism-wide, an mCherry-Atg8a fluorescent reporter was also expressed ectopically to visualize autophagy in the polyploid midgut cells (Figure 2.6). The genetic crosses to introduce the mCherry-Atg8a construct into the *Nopp140-/-* background are currently underway, so we first conducted RT-PCR on whole larval RNA extracts to assay the expression of three genes involved in the autophagy pathway (Wu et al. 2009). Atg1 is a kinase that forms a complex responsible for the initiation of phagophore formation, and Atg18.2 is a member of the Atg18 protein family, which is responsible for further assembly of the phagophore (Nagy et al. 2014). Atg8a is a ubiquitin-like protein, conjugated to phosphatidyl-ethanolamine (PE) to both the inner and outer autophagosome membrane leaflets (Wu et al. 2009, Nagy et al. 2014). Compared to similarly aged wild type controls (w^{1118}), the expression of *atg1*, *atg18.2,* and *atg8a* were significantly increased in *Nopp140-/-* samples (Figure 4.3). Third instar *WH-/-* and w^{1118} samples had mostly comparable expression of the autophagy-related genes. The expression of *atg8a* may be slightly higher in *WH-/-* larvae compared to third instar w^{1118}, due to stress induced by the loss of P5CDh1.

Our results agree with previous observations made by Wu et al. (2009), who showed that expression of several autophagy-related genes (including *atg1, atg18.2*, and *atg8a)* occurs in *D. melanogaster* in response to both oxidative stress (12h paraquat treatment) and increased activation of the JNK pathway (induced by over-expression of Hep, a JNK kinase). JNK-dependent activation of *atg* genes is very likely mediated by d-FOXO (Juhász et al. 2007, Wang et al.

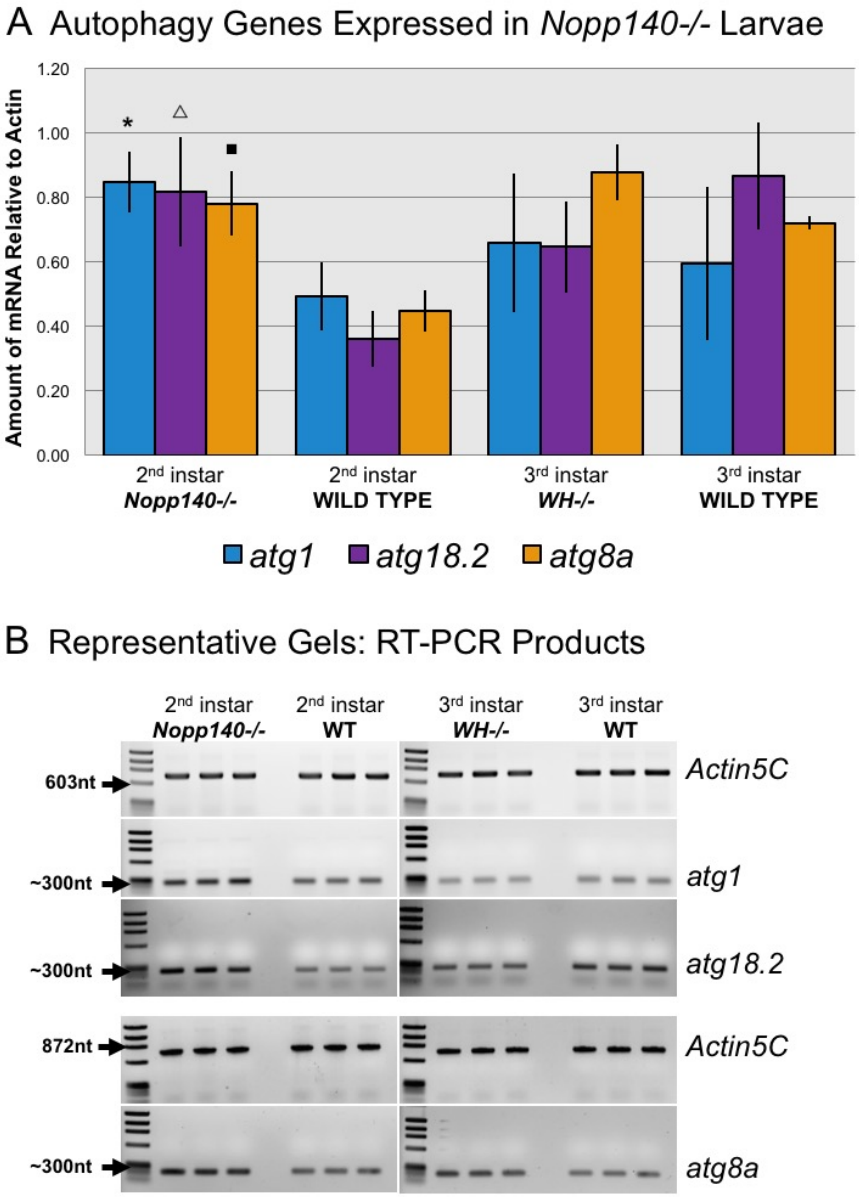

FIGURE 4.3. Autophagy Gene Expression in *Nopp140-/-* Larvae (*atg1*, *atg18.2*, and *atg8a*) is low in 2nd instar wild type (w^{1118}) larvae, as expected. However, expression of these genes is significantly higher in *Nopp140-/-* larvae. Expression is generally comparable between 3rd instar *WH-/-* larvae and wild type (w^{1118}) controls. (A) Bars represent average RT-PCR products using *atg1-, atg18.2-,* or *atg8a*-specific primers compared to that of *Actin5C*. Error bars are ± standard error. *p=0.0017, △p=0.0164, ■p=0.0087 comparing 2nd instar *Nopp140-/-* and w^{1118} control. p values = one-tailed values from t-Test, paired two sample for means, calculated by Microsoft Excel. (B) Representative agarose gels, with *Actin5C* control, *atg1*, *atg18.2*, and *atg8a* RT-PCR products. Between 3 and 5 independent experiments were performed per gene, and PCR reactions were performed in triplicate.

2005, Chang and Neufeld 2010). The results in Figure 4.3 agree with our previously reported results, describing the induction of autophagy in response to loss of Nopp140 (Figure 2.6).

4.4 Over-expression of Nopp140

Since all of the experiments described above involve disrupting the function of Nopp140 and assaying the resultant phenotypes, we wanted to take an opposite approach: how is cell homeostasis disrupted when either isoform of Nopp140 is *over-expressed*? Fly lines that allow the expression of GFP-Nopp140-True or GFP-Nopp140-RGG under UAS-GAL4 control were made previously in our lab (Cui and DiMario 2007). We crossed *A9-GAL4* females (Figure 4.4, B) to either *UAS-GFP-Nopp140-True* (Figure 4.4, C) or the *UAS-GFP-Nopp140-RGG* (Figure 4.4, D) males at 27-28° C to express either Nopp140 isoform selectively in the wing discs of all progeny (crosses diagrammed in Figure 4.4, A). The consequence of Nopp140 over-expression was evident in wing morphology of F1 progeny adults. Surprisingly, the wing phenotypes differed, depending on which Nopp140 isoform was over-expressed. Over-expression of GFP-Nopp140-True induced a severe phenotype (*i.e.* fragile, blistered, crumpled wings with an extreme curl along the long axis, Figure 4.4, E) while GFP-Nopp140-RGG over-expression led to a milder phenotype (*i.e.* smooth wings with a slight to medium curl along the short axis, Figure 4.4, F). The number of progeny scored from the cross described in Figure 4.4, A is listed in Figure 4.5 (grey rows). We also performed reciprocal crosses to those diagrammed in Figure 4.4, A, using *A9-GAL4* males such that only female

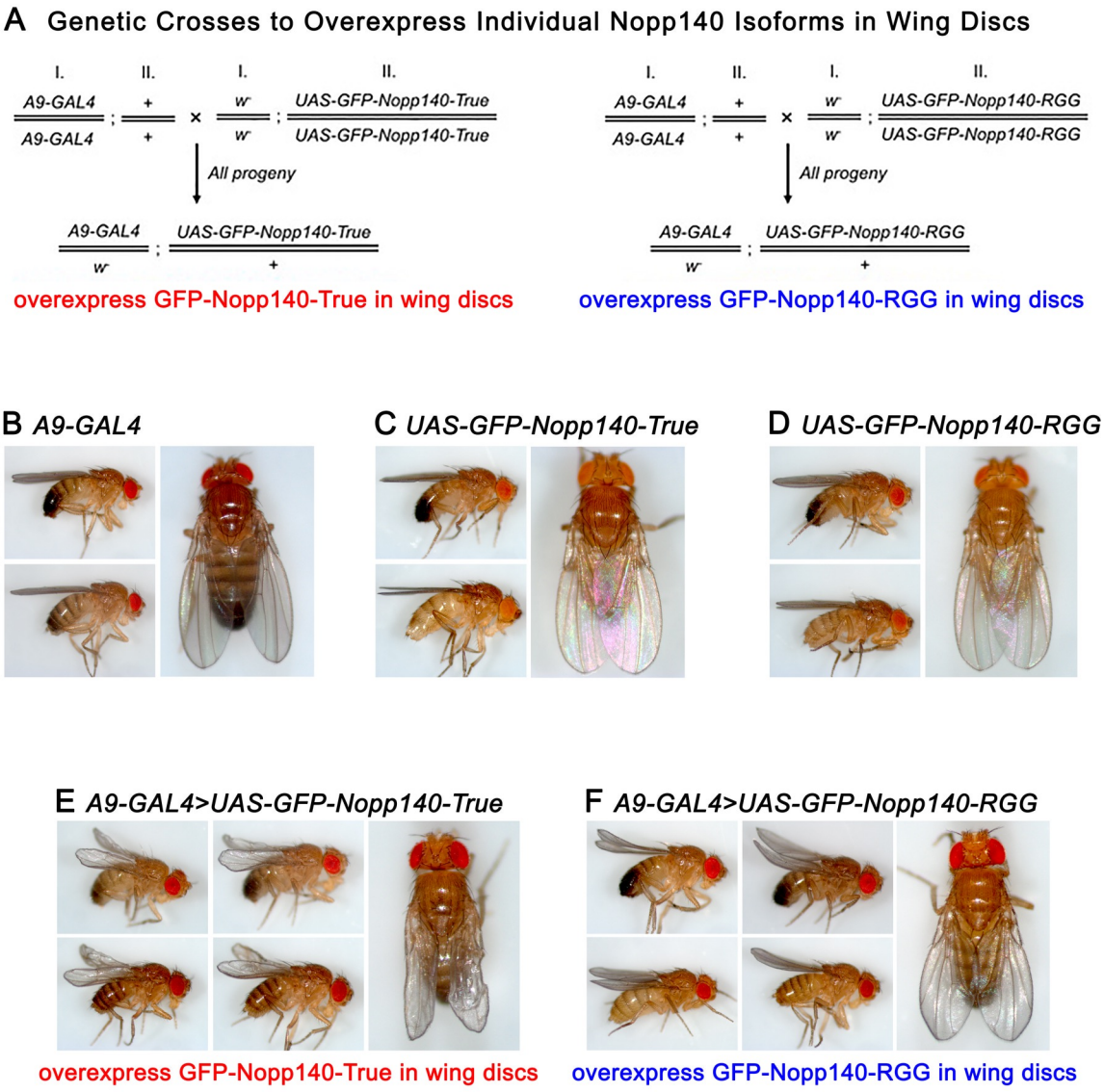

FIGURE 4.4. Over-expression of Nopp140 Isoforms in Wing Discs. (A) Genetic cross diagrams: *A9-GAL4/A9-GAL4; +/+* females were crossed to either *w⁻/w⁻; UAS-GFP-Nopp140-True/"* or *w⁻/w⁻; UAS-GFP-Nopp140-RGG/"* males; all progeny from these crosses express either GFP-Nopp140 isoform selectively in wing discs. Parent flies have a **wild-type** wing phenotype: (B) *A9-GAL4/A9-GAL4* females, *A9-GAL4/w⁻* males, (C) *w-/w-; UAS-GFP-Nopp140-True/"* and (D) *w-/w-; UAS-GFP-Nopp140-RGG/"*. (E) Flies that over-expressed GFP-Nopp140-True in larval wing discs have a **severe** wing phenotype (fragile, severely curled, blistered). (F) Flies that over-expressed GFP-Nopp140-RGG in larval wing discs have a **mild** wing phenotype (smooth, mild to medium curl).

progeny would over-express either Nopp140 isoform and the male progeny would serve as sibling controls (Figure 4.5, white rows). The wing phenotypes of flies over-expressing either GFP-Nopp140-True or GFP-Nopp140-RGG remained consistent, displaying either a severe or mild wing phenotype, respectively (Figure 4.5).

Progeny Genotype	Number of flies scored	Progeny Phenotype
A9-GAL4/w⁻; UAS-GFP-Nopp140-True/+ ♂♂♀♀	232	**severe** wing phenotype 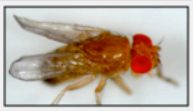
w⁻/Y; UAS-GFP-Nopp140-True/+ ♂♂	59	**wild-type** wing phenotype 
A9-GAL4 w⁻-: UAS-GFP-Nopp140-True/+ ♀♀	34	**severe** wing phenotype 
A9-GAL4/ w⁻; UAS-GFP-Nopp140-RGG/+ ♂♂♀♀	424	**mild** wing phenotype 
w⁻/Y; UAS-GFP-Nopp140-RGG/+ ♂♂	113	**wild-type** wing phenotype 
A9-GAL4/ w⁻: UAS-GFP-Nopp140-RGG/+ ♀♀	97	**mild** wing phenotype 

FIGURE 4.5. Progeny Genotypes and Phenotypes of *A9-GAL4>Nopp140-RNAi* Flies and Controls. Crossing *A9-GAL4* homozygous females to *UAS-GFP-Nopp140-True* or *UAS-GFP-Nopp140-RGG* homozygous males will induce all progeny to over-express either GFP-Nopp140 isoform (grey boxes). Progeny from this cross are also pictured in Figure 4.4. The reciprocal crosses (white boxes), using *UAS-GFP-Nopp140-True* or *UAS-GFP-Nopp140-RGG* homozygous females and *A9-GAL4/w⁻* males produces male progeny, which always display wild type wings, and female progeny, which over-express either GFP-Nopp140 isoform. Results are consistent: over-expression of GFP-Nopp140-True leads to a severely malformed, fragile, often blistered wings (“severe phenotype”); over-expression of GFP-Nopp140-RGG results in smooth, slight to medium-curled wings (“mild phenotype”).

Interestingly, the results described above agree with preliminary observations gained from a separate experiment involving the over-expression of each Nopp140 isoform using the same UAS-GAL4 system. Here, we used a *da-GAL4* driver, that allows expression of each isoform organism-wide, which induces lethality in the third instar. Since loss of Nopp140 resulted in nucleolar stress, decreased 2'-*O*-methylation of pre-rRNA, and a loss of protein synthesis, we wanted to evaluate the consequence of Nopp140 overexpression on ribosome biogenesis. Total RNA was isolated from whole larval lysates and RT-PCR was performed to measure rDNA transcription. The external transcribed spacer (ETS) region of nascent pre-rRNAs is quickly processed, so measuring relative ETS abundance may be used as an approximation of RNA Polymerase I (Pol I) activity (Figure 4.6, A). Larvae over-expressing GFP-Nopp140-RGG showed no change in pre-rRNA production compared to controls (compare Figure 4.6, C to D). On the other hand, larvae over-expressing GFP-Nopp140-True experienced a drastic reduction in rRNA synthesis (Figure 4.6, B). Thus, an imbalance of Nopp140 within the nucleolus, specifically by producing greater amounts of Nopp140-True, hinders Pol I activity and consequently ribosome biogenesis. An intriguing similarity exists between the results reported in Figures 4.4, 4.5, and 4.6: the over-expression of GFP-Nopp140-True induced a more extreme, detrimental phenotype while the consequence of GFP-Nopp140-RGG overexpression is less evident.

More experiments are needed in order to properly understand the consequences of Nopp140 over-expression. First, we must identify the reason

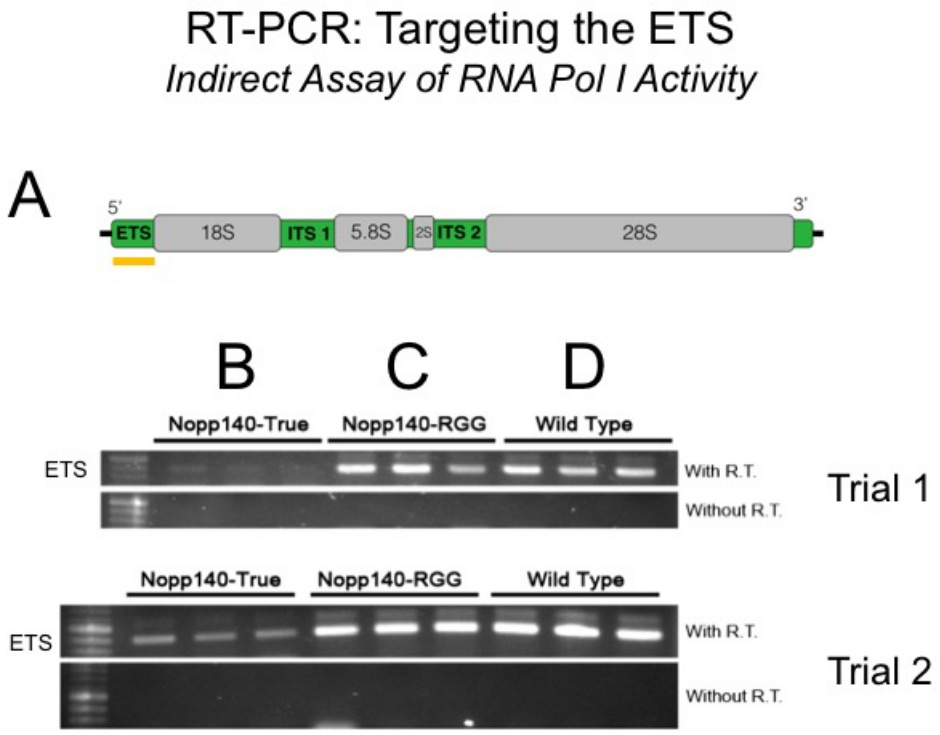

FIGURE 4.6. Over-expression of Nopp140 isoforms and RNA Pol I Activity. The amount of ETS correlates to RNA Polymerase I activity. (A) Diagram of rDNA locus, with ETS region denoted with orange line. (B) Over-expression of GFP-Nopp140-True caused a significant reduction in pre-rRNA synthesis while (C) over-expression of GFP-Nopp140-RGG does not appear to affect RNA Pol I activity compared to (D) wild type controls. Mock reactions performed without RT enzyme (R.T.) are used as negative controls. Two independent RT-PCR experiments with PCR run in triplicate have been performed thus far.

why the adult wing structures seen in Figure 4.4 are malformed: are wing disc cells dying (*e.g.* apoptosis) or are the diploid progenitor tissues incapable of forming new cells? Second, close measurement of the relative expressions of GFP-Nopp140-True and GFP-Nopp140-RGG (both mRNA and protein) will be made, for both organism-wide and wing disc-specific expression. The severe phenotype induced *only* by GFP-Nopp140-True may be because the expression of this isoform is much stronger than that of GFP-Nopp140-RGG. However, the

fact that both GFP-Nopp140 isoforms are expressed under the control of the *A9-GAL4* or *da-GAL4* drivers at 27-28° C suggests that they are indeed expressed at comparable levels for each experiment. Alternatively, the extreme phenotypes (wing formation and reduced Pol I activity) only induced by GFP-Nopp140-True may suggest that Nopp140-True is indispensable for nucleolar function while Nopp140-RGG is less essential.

Still, from these preliminary results, we can deduce that a delicate balance of Nopp140-True and Nopp140-RGG expression must be achieved in order to maintain cell homeostasis.

4.5 Materials and Methods

4.5.1 Fly lines

Lines obtained from Bloomington Stock Center at Indiana University: *w*; P{GAL4-ey.H}4-8 /CyO*, abbreviated here as *ey-gal4/CyO,* which strongly expresses GAL4 in the *eyeless* pattern (stock #5535) and wing disc-specific *P{w[+m*]=GAL4}A9* on the *X* chromosome (stock #8761, referred to here as *A9-GAL4*). *A9-GAL4* expresses GAL4 strongly in larval wing and haltere discs (Haerry et al. 1998). The third chromosome *daughterless-GAL4* (*da-GAL4*) driver line (stock #8461) allows the expression of GAL4 organism-wide. We used the w^{1118} line (stock #3605) to construct our RNAi-expressing transgenic lines (Cui and DiMario 2007), and we use it here as our "wild type" control. Additional lines: *Nopp140-/TM3-GFP*, parental control for *Nopp140-/-* larvae is the *Piggybac* line $P5CDh1^{f04633}/TM6$ containing a *WH- pBac* element, obtained from the Exelixis collection at Harvard University (described in Chapter 3). Overexpression of

Nopp140 isoforms (Cui and DiMario 2007): *pUAST-GFP-Nopp140-RGG* (*RGG-HI* line*)* and *pUAST-GFP-Nopp140-True (True-A9* line*)*; both lines are homozygous viable and fertile with the transgenes on the 2nd chromosome.

4.5.2 RT-PCR

Total RNA was extracted from whole larvae with TRIzol® as recommended by the manufacturer. All samples were treated with DNase I (NEB). RNA concentration was measured by Nanodrop (ThermoScientific) and 2 µg of total RNA was used in each RT reaction using M-MLV reverse transcriptase (Promega) with an oligo-dT to amplify all poly(A+) mRNAs present in the sample. To ensure against any genomic DNA contamination, mock RT-PCR experiments were performed without the RT enzyme. After the RT reaction, all samples were treated with RNase H (NEB) and RNase cocktail (Ambion, Cat.#AM2286). One µL of the RNA-free RT reaction was used as the template for each PCR reaction. PCR reactions were carried out using *Taq* Polymerase (NEB) with ThermoPol Buffer. The number of amplification cycles necessary to produce a measurable product varied between genes: *Actin5C* (25 to 30 cycles), *JNK* (26 to 30 cycles), *puc* (26 cycles), *atg1* and *atg18.2* (27 cycles), and *atg8a* (22 to 24 cycles). *atg1, atg18.2*, and *atg8a* primer sequences were used from Wu et al. (2009). The forward (F) and reverse (R) primer sets were as follows: *atg1* (F) 5'-GAGTATTGCAATGGCGGCGACT-3' and (R) 5'-CAGGAATCGCGCAAACCCAA-3', with an expected product of 243 nt. *atg18.2* (F) 5'-CCGAAAATTCTGCCAAGGAAGC-3' and (R) 5'-AATCCGTCCTCGCACGCAAT-3', with an expected product of 250 nt. *atg8a* (F)

5’-GCAAATATCCAGACCGTGTGCC-3’ and (R) 5’-AGCCCATGGTAGCCGATGTT-3’, with an expected product of 210 nt. *JNK* (F) 5’-CACCATGACGACAGCTCAGCACC-3’ and (R) 5’-CTACCGCGTTCTATTATTTGTATTGTGTGCTTCG-3’, with an expected product of 1,123 nt. *puc* (F) 5’ GATTTCGCGGAGCGCCACCATTGC 3’ and (R) 5’ TCAGTCCCTCGTCAAATTGCTAGCCACATGG 3’, with an expected product of 775 nt. *Actin5C* (F) 5’-CTCACCTATAGAAGACGAAGAAGTTGCTGCTCT-3’ and (R) 5’ CTAACTGTTGAATCCTCGTAGGACTTCTCCAACG-3’, with an expected product of 747 nt. *Note:* for the *Actin5C* primers, only the nucleotides in bold match the cDNA sequence of *Actin5C*. Between 3 and 5 independent experiments were performed for each gene (*jnk, puc, act5C, atg1, atg18.2, atg8a*), with all PCR reactions run in triplicate. Graphed data represent average RT-PCR products of gene-specific primers relative to that of Actin5C, which was measured separately for every RT reaction. The intensities of the PCR bands were measured with ImageJ software; data was analyzed and graphs were assembled using Microsoft Excel.

For ETS rRNA measurements, RT-PCR experiments were performed as described above with minor modifications: third instar larvae were used for RNA preps. One µL of total RNA served as template per RT reaction using the GoScript RT Kit (Promega) and the ETS-reverse primer. PCR reactions were performed in triplicate using Taq polymerase (NEB), ETS For (5’-TGCCGACCTCGCATTGTTCGAAAT-3’) and ETS Rev (5’-ACCGAGCGCACATGATAATTCTTCC-3’) primers. Annealing temperature:

54 °C. Amplification: 26 cycles. The predicted size of ETS RT-PCR product is 378 nt.

4.5.3 Expression of Nopp140-RNAi in Eye

For expression of Nopp140-RNAi in the *eyeless* pattern, parental controls included the *ey-gal4/CyO* line and the *P{w[+mC]=UAS-Nopp140.dsRNA}*$^{C4.2}$ fly line that expresses short hairpin RNA specific for the common 5' end of mRNAs that encode the two Nopp140 isoforms as described previously, abbreviated here as *UAS-C4* (Cui and DiMario 2007). The *UAS-C4* line contains two RNAi-expressing transgenes: one on the second chromosome and the other on the third chromosome and is homozygous and fertile. Crosses were performed at 27-28° C on standard fly medium. F1 progeny were selected based on their wing phenotype: straight-winged progeny were considered to express Nopp140-RNAi while curly-winged progeny were considered sibling controls. Flies were imaged using a Lumar.V12 SteREO (Zeiss) microscope fitted with an Axiocam MRc5 (Zeiss) camera. To measure the eye size, a line was drawn around visible ommatidia using the contour (spline) function on the ZEN 2 Pro Software Blue Edition, Version 2.0.0.0 (Carl Zeiss Microscopy GmbH). Data is represented as average eye size per genotype (measured in μm^2).

4.5.4 Over-Expression of GFP-Nopp140 Isoforms in Wing Discs

Flies were imaged using a Lumar.V12 SteREO (Zeiss) microscope fitted with an Axiocam MRc5 (Zeiss) camera and viewed using the ZEN 2 Pro Software Blue Edition, Version 2.0.0.0 (Carl Zeiss Microscopy GmbH).

4.6 References

Brand A, Perrimon N (1993) Targeted gene expression as a means of altering cell fates and generating dominant phenotypes. Development 118:401-415.

Chang Y-Y, Neufeld TP (2010) Autophagy takes flight in *Drosophila*. FEBS Lett. 584:1342-1349.

Cui Z, DiMario PJ (2007) RNAi knockdown of Nopp140 induces *Minute*-like phenotypes in *Drosophila*. Mol. Biol. Cell 18:2179-2191.

Haerry TE, Khalsa O, O'Connor MB, Wharton KA (1998) Synergistic signaling by two BMP ligands through the SAX and TKV receptors controls wing growth in *Drosophila*. Development 125:3977-3987.

Halder, G, Callaerts, P, Gehring, W (1995) Induction of ectopic eyes by targeted expression of the eyeless gene in Drosophila. Science 267:1788–179.

Juhász G, Puskás LG, Komonyi O, Érdi B, Maróy P, Neufeld TP, et al. (2007) Gene expression profiling identifies FKBP39 as an inhibitor of autophagy in larval *Drosophila* fat body. Cell Death Differ 14:1181-1190.

McNamee LM, Brodsky MH (2009) p53-independent apoptosis limits DNA damage-induced aneuploidy. Genetics 182:423-35. http://dx.doi.org/10.1534/genetics.109.102327.

Nagy P, Varga A, Kovács AL, Takáts S, Juhász G (2014) How and why to study autophagy in Drosophila: It's more than just a garbage chute. Methods 75:151-161.

Noveen A, Daniel A, and Hartenstein V (2000) Early development of the Drosophila mushroom body: the roles of eyeless and dachshund. Development 127:3475-3488.

Quiring R, Walldorf U, Kloter U, Gehring WJ (1994) Homology of the eyeless gene of *Drosophila* to the *Small eye* gene in mice and Aniridia in humans. Science 265:785-789.

Riesgo-Escovar JR, Jenni M, Fritz A, Hafen E (1996) The Drosophila Jun-N-terminal kinase is required for cell morphogenesis but not for DJun-dependent cell fate specification in the eye. Genes Dev 10:2759-2768.

Wang MC, Bohmann D, Jasper H (2005) JNK Extends Life Span and Limits Growth by Antagonizing Cellular and Organism-Wide Responses to Insulin Signaling. Cell 125:115-125. http://dx.doi.org/10.1016/j.cell.2005.02.030.

Wu H, Wang MC, Bohmann D (2009) JNK protects *Drosophila* from oxidative stress by transcriptionally activating autophagy. Mech Dev 126:624-637.

Zars T (2000) Behavioral functions of the insect mushroom bodies. Curr Opin Neurobiol 10:790-795.

CHAPTER 5. CONCLUSIONS AND FUTURE STUDIES

Our studies have focused on Nopp140, a nucleolar and Cajal Body protein that serves as a chaperone for snoRNP complexes responsible for the modification of pre-rRNA. We have developed strategies utilizing protein knockdown (RNAi expression) and gene knockout fly lines. These approaches have produced phenotypes that we can use to elucidate the function of Nopp140. Nopp140 is essential for manufacturing functional ribosomes. Loss of Nopp140 results in nucleolar stress, which is now defined as a disruption of ribosome biogenesis and function that leads to changes in cell homeostasis.

Prior to lethality of third-instar larvae expressing Nopp140-RNAi, depletion of Nopp140 results in a loss of functional cytoplasmic ribosomes (Figure 2.2). Three sets of results provide evidence to support this claim (Figure 2.2). First, a reduction in cytoplasmic ribosomes was visualized in polyploid and diploid cells by electron microscopy. Second, metabolic labeling experiments revealed that larvae expressing Nopp140-RNAi had significantly less protein synthesis organism-wide. Finally, immunoblots using antibodies directed against RpL32 and RpL23a revealed that at least two ribosomal proteins from the large subunit are under-represented during nucleolar stress. Importantly, loss of Nopp140 induced p53-*in*dependent apoptosis in imaginal wing disc cells (Figures 2.4): expression of Nopp140-RNAi in a *Δp53*/*Δp53* background failed to rescue the phenotype (diploid cell apoptosis and vestigial-like wing) observed in the $p53^{+/+}$ background (Figures 2.3 and 2.5). Since >50% of human cancer cell types lack functional p53, understanding p53-independent cell death pathways could

provide clues for cancer therapies that take advantage of the nucleolar stress pathway. Additional phenotypes of Nopp140-RNAi expressing larvae included autophagy in polyploid midgut cells (Figure 2.6), accumulation of phenoloxidase and melanotic masses (Figure 2.7), expression of pro-apoptotic Hid, and activation of JNK (Figure 2.8). These results are summarized in Figure 5.1.

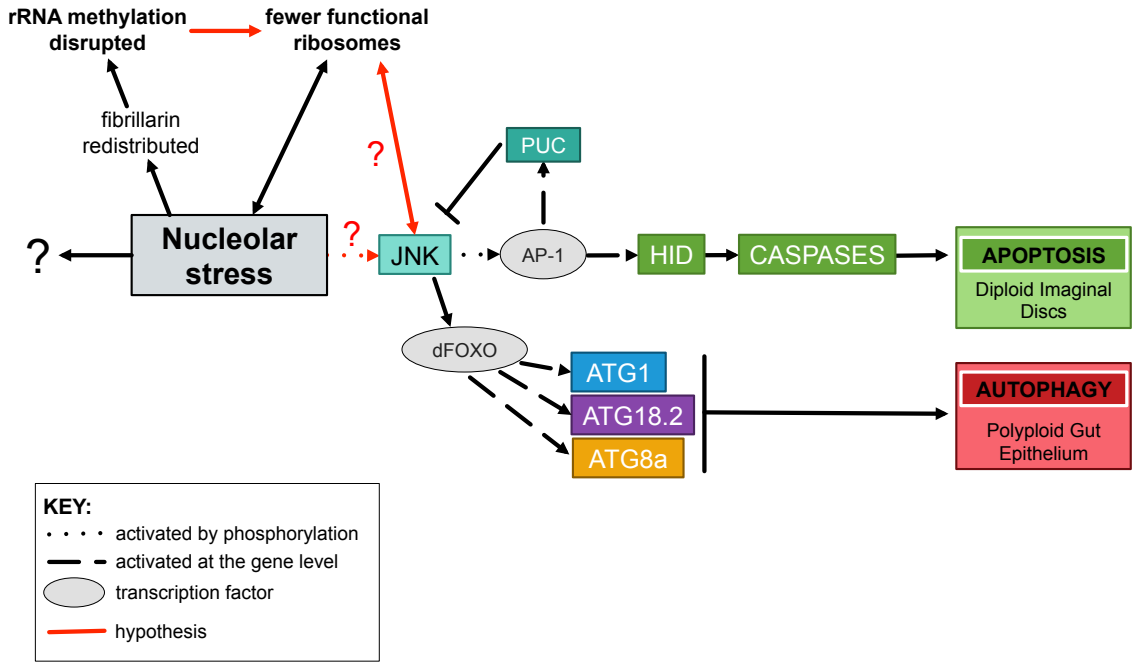

FIGURE 5.1. Overall Model: Nucleolar Stress Responses Induced by the Loss of Nopp140. This figure combines evidence gained from studies involving Nopp140-depletion through RNAi expression (Chapter 2) and gene deletion (Chapter 3). Cell stress responses are tissue-specific: apoptosis was observed in diploid imaginal disc cells and autophagy occurred in polyploid gut cells. We propose that JNK is involved in this p53-independent response pathway; currently, the exact mechanism to activate JNK in this context remains elusive.

Nopp140 expression was knocked down through RNAi only in the imaginal wing discs of larvae, which resulted in severely malformed adult wings (Figure 2.3). Accordingly, selective expression of Nopp140-RNAi in the eye

(*UAS-C4.2/ey-GAL4; UAS-C3/+*) resulted in small, severely malformed eyes compared to control flies (Figure 4.1). These results are complementary: Nopp140 is necessary for the proper development of tissues arising from diploid progenitor discs.

To further elucidate the function of Nopp140, we deleted the *Nopp140* gene using the FLP-FRT system (Figure 3.1 and Figure 3.2) and developed a strategy to select *Nopp140-/-* larvae, using GFP as a marker for the balancer chromosome *TM3-GFP* (Figure 3.1). Compared to knockdown of Nopp140 by RNAi (described in Chapter 2) the total loss of Nopp140 lead to more pronounced phenotypes, including death in the second instar stage (Figure 3.3), loss of 2'-*O*-methylation of certain rRNA bases (Figures 3.4 and 3.5), a severe reduction in functional cytoplasmic ribosomes (Figure 3.6 and 3.7), and the accumulation of electron-dense cytoplasmic granules that appear to be aggregates of non-functional ribosomes (Figure 3.6).

Our hypothesis is that if Nopp140 is not present to properly localize the methyl-transferase enzyme fibrillarin from the Cajal Body to the nucleolus, proper modification (2'-*O*-methylation) of the rRNA cannot occur, which then renders *de novo* ribosomes dysfunctional. Once these improperly assembled, and thus inherently unstable ribosomes are exported to the cytoplasm, some may be degraded and others may aggregate into the electron dense granules seen in Figure 3.6 (solid red arrow in Figure 5.1). The lack of *de novo* protein synthesis and the loss of RpL32 measured in *Nopp140-/-* larvae could be explained by this hypothesis (Figure 3.7).

RT-PCR experiments were performed to expand upon the results described in Chapter 2, which describe JNK activation during nucleolar stress due to loss of Nopp140 (Figure 2.8). JNK is likewise active in *Nopp140-/-* larvae. The results confirmed that JNK is regulated though phosphorylation, as measured by the over-expression of *puc*, rather than gene activation (Figure 4.2).

The RT-PCR results (Figure 4.3) suggest there is at least a transcriptional-activation of autophagy (involving the *atg1, atg18.2,* and *atg8a* genes) in *Nopp140-/-* larvae compared to controls. Since there was no autophagy seen at the EM level during our initial observations, it is possible that the full autophagy pathway (*e.g.* presence of autophagosomes and auto-lysosomes) does not occur before the larvae die in the second instar stage. It is also possible that although the cell attempts an initiation of autophagy at the gene level, there is not a sufficient amount of functional ribosomes to allow synthesis of autophagy-related proteins, so the full autophagy program cannot be achieved.

Figure 5.1 is a summary of our overall hypothesis. Upon nucleolar stress induced by the loss of Nopp140, diploid imaginal disc cells may undergo a p53-*in*dependent apoptosis and polyploid midgut cells undergo autophagy, perhaps dependent on the activation of JNK. Combined experiments (Figures 2.4, 2.8 and 4.2) reveal that the JNK>hid>caspase pathway is active in Nopp140-depleted cells. The induction of autophagy in cells undergoing nucleolar stress due to loss of Nopp140 may involve the transcription factor dFOXO and participation of atg1, atg18.2 and atg8a, at minimum (Figures 2.6 and 4.3) (Juhász et al. 2007; Chang and Neufeld 2010). The *4E-BP1* gene, whose protein product functions as a

translation repressor, is a known target of dFOXO activity during nutrient stress (Jünger et al. 2003, Puig et al. 2003). Therefore, active JNK in cells experiencing nucleolar stress may activate dFOXO, resulting in up-regulation of *4E-BP1*. This interaction, if it occurs could contribute to the observed reduction of protein synthesis in cells experiencing nucleolar stress (red line between 'fewer functional ribosomes' and 'JNK' in Figure 5.1). The story is far from complete: we have yet to uncover how JNK is activated during times of nucleolar stress (red dotted arrow in Figure 5.1). Perhaps there are other consequences of Nopp140 loss and nucleolar stress in *D. melanogaster* that we have yet to identify.

We have not yet tested if the phenotypes described in this thesis are unique to the loss of Nopp140 or if they are a common response to nucleolar stress in *D. melanogaster* (though we are inclined to offer the latter hypothesis). Inducing nucleolar stress in some other way, perhaps through knockdown of other essential ribosome assembly factors, or application of drugs that selectively inhibit RNA Polymerase I such as CX-5461 (Drygin et al., 2011, Xcessbio Biosciences, Inc.) would address this question.

In future efforts to address the hypothesis that the aberrant cytoplasmic granules are aggregates of nonfunctional ribosomes, we plan to express GFP-tagged ribosomal proteins with their endogenous promoter in the *Nopp140-/-* background and perform immuno-EM with antibodies against the GFP protein. CRISPR technology to delete *Nopp140* is currently under way in our lab. We expect to see the same phenotypes with the CRISPR-mediated knockout as we

do with the FLP-FRT knockout lines. The use of CRISPR-mediated *Nopp140* knockout lines will eliminate the need for *WH-/-* parental control larvae from the FLP/FRT recombination, which will simplify our data analysis.

A closer inspection of the cells expressing Nopp140-RNAi in the eyeless pattern (*ey-GAL4>UAS-C4*) is necessary. At this time, we are unsure if the tissues expressing Nopp140-RNAi are unable to form cells during development, or if a cell death program such as apoptosis occurs subsequent to cell formation. Our observations following the expression of Nopp140-RNAi in the *ey* pattern, which includes the embryonic ventral nerve cord and progenitor mushroom body cells, leads us toward a new aspect of studying ribosome biogenesis in stem cells in *Drosophila*. Taking a cue from the human model of Treacher Collins Syndrome, in which neural crest cells are preferentially susceptible to the organism-wide loss of the nucleolar protein treacle, we plan to disrupt Nopp140 function in the developing nervous system and monitor the consequences, behavioral, developmental or otherwise, of such induced nucleolar stress. Experiments are under-way in our lab to knockdown Nopp140 function in embryonic neuroblasts of *D. melanogaster*.

We are very interested in finding the missing link between nucleolar stress and the activation of JNK (Figure 5.1). As a step toward this goal, genetic crosses are being performed to express shRNAs targeting known JNK kinases (ASK1 and TAK1) as well as Nopp140. Rescue of the phenotype induced by Nopp140-RNAi expression in the *ey* pattern (small and malformed eyes) with the simultaneous knockdown of any of these potential effectors will provide a clue as

to which pathway is activated, connecting nucleolar stress and JNK. Additionally, to identify all the genes that are either up- or down-regulated in response to nucleolar stress, RNA-seq experiments will be performed. We expect RNA-seq data to confirm our previous RT-PCR results as well as identify new genes (including those within the JNK pathway) responding the the loss of nucleolar homeostasis.

We know that JNK is involved in the nucleolar stress response during the loss of Nopp140, but yet the question remains: is JNK signaling *necessary* for this response? GAL4-controlled expression of *UAS-Bsk*^{DN} (gift from Dirk Bohmann) would reduce JNK activity, as it encodes a mutant, non-activatable form of JNK (Adachi-Yamada 1999). Again, expression of Nopp140-RNAi in the eye or wing discs induces drastic phenotypes in the adult fly. If JNK activation is required for the response to nucleolar stress in *D. melanogaster*, we expect that abrogating JNK activity and depleting Nopp140 levels concurrently would rescue these phenotypes (*i.e.* adult eye or wing structures would be more similar to wild-type size and morphology).

Lastly, recent experiments involving the over-expression of individual Nopp140 isoforms have brought about a new hypothesis: equimolar amounts of Nopp140 isoforms must be present for nucleolar (cell) homeostasis. Currently, we are attempting to complement the *Nopp140* gene knockout by expressing either Nopp140 isoform under control of their endogenous promoter. Expression of GFP-Nopp140-True alone in the *Nopp140-/-* background was synthetic lethal at the embryonic stage, which we believe is caused by an imbalance of maternal

Nopp140-True to Nopp140-RGG levels. The cross to express GFP-Nopp140-RGG in the *Nopp140-/-* background is still under construction. Additionally, since we have already assayed the phenotypes induced by the over-expression of either Nopp140 isoform selectively in the wing disc cell population, we plan to determine the consequence of Nopp140 over-expression in the *eyeless* pattern, which includes other stem cell populations (described in Chapter 4). If we observe a phenotype reminiscent of that seen in *ey-GAL4>UAS-Nopp140-RNAi* flies, then we will have another piece of the puzzle towards an ultimate goal of determining the function of each Nopp140 isoform in *D. melanogaster* and their unique role(s) in ribosome biogenesis, development, and survival of diploid progenitor cell populations.

5.1 References

Adachi-Yamada T, Nakamura M, Irie K, Tomoyasu Y, Sano Y, Mori E, Goto S, Ueno N, Nishida Y, Matsumoto K (1999) p38 Mitogen-Activated Protein Kinase Can Be Involved in Transforming Growth Factor β Superfamily Signal Transduction in Drosophila Wing Morphogenesis. Mol and Cell Biology 19:2322–2329.

Chang Y-Y, Neufeld TP (2010) Autophagy takes flight in *Drosophila*. FEBS Lett. 584:1342-1349.

Drygin D, Lin A, Bliesath J, Ho CB, O'Brien SE, Proffitt C, et al. (2011) Targeting RNA polymerase I with an oral small molecule CX-5461 inhibits ribosomal RNA synthesis and solid tumor growth. Cancer Res 71:1418-1430. http://dx.doi.org/10.1158/0008-5472.CAN-10-1728.

Juhász G, Puskás LG, Komonyi O, Érdi B, Maróy P, Neufeld TP, et al. (2007) Gene expression profiling identifies FKBP39 as an inhibitor of autophagy in larval *Drosophila* fat body. Cell Death Differ 14:1181-1190.

Jünger MA, Rintelen F, Stocker H, Wasserman JD, Végh M, Radimerski T, Greenberg ME, Hafen E (2003) The Drosophila Forkhead transcription factor FOXO mediates the reduction in cell number associated with reduced insulin signaling. Journal of Biology 2:20.

Puig O, Marr MT, Ruhf L, Tijan R (2003) Control of cell number by *Drosophila* FOXO: downstream and feedback regulation of the insulin receptor pathway. Genes and Development 17:2006-2020.

APPENDIX A: PERMISSION TO REUSE MATERIALS IN DISSERTATION/THESIS

Please see below for permission to reuse materials in Chapter 1 of this thesis.

Volume 5, Issue 5, 2014

Nucleolar stress with and without p53

DOI:
10.4161/nucl.32235

Allison James[a], Yubo Wang[a], Himanshu Raje[a], Raphyel Rosby[a] & Patrick DiMario[*a]

pages 402-426

Publishing models and article dates explained

- Received: 21 Jul 2014
- Accepted: 1 Aug 2014
- Published online: 05 Aug 2014

Abstract

A veritable explosion of primary research papers within the past 10 years focuses on nucleolar and ribosomal stress, and for good reason: with ribosome biosynthesis consuming ~80% of a cell's energy, nearly all metabolic and signaling pathways lead ultimately to or from the nucleolus. We begin by describing p53 activation upon nucleolar stress resulting in cell cycle arrest or apoptosis. The significance of this mechanism cannot be understated, as oncologists are now inducing nucleolar stress strategically in cancer cells as a potential anti-cancer therapy. We also summarize the human ribosomopathies, syndromes in which ribosome biogenesis or function are impaired leading to birth defects or bone narrow failures; the perplexing problem in the ribosomopathies is why only certain cells are affected despite the fact that the causative mutation is systemic. We then describe p53-independent nucleolar stress, first in yeast which lacks p53, and then in other model metazoans that lack MDM2, the critical E3 ubiquitin ligase that normally inactivates p53. Do these presumably ancient p53-independent nucleolar stress pathways remain latent in human cells? If they still exist, can we use them to target >50% of known human cancers that lack functional p53?

Keywords:

- nucleolar stress,
- ribosomal proteins,
- cell cycle,
- p53,
- ribosomopathies

Please see below for permission to re-use materials for Chapter 2 of this thesis.

Taylor & Francis
Taylor & Francis Group

Journal Reprints

Title: Nucleolar stress in Drosophila melanogaster
Author: Allison James, Renford Cindass Jr, Dana Mayer, et al
Publication: Nucleus
Publisher: Taylor & Francis
Date: Mar 1, 2013
Copyright © 2013 Taylor & Francis

Logged in as:
Allison James
Account #:
3000916753
LOGOUT

Thesis/Dissertation Reuse Request

Taylor & Francis is pleased to offer reuses of its content for a thesis or dissertation free of charge contingent on resubmission of permission request if work is published.

BACK CLOSE WINDOW

Copyright © 2015 Copyright Clearance Center, Inc. All Rights Reserved. Privacy statement. Terms and Conditions.
Comments? We would like to hear from you. E-mail us at customercare@copyright.com

Allison James <ajame18@tigers.lsu.edu>

Permission for Thesis

Michael Hellberg <mhellbe@lsu.edu> Fri, May 15, 2015 at 2:06 PM
To: Allison James <ajame18@tigers.lsu.edu>

Dear Candidate James,

You have the department's permission to use your first-authored previously published work in your dissertation.

Michael Hellberg
mhellbe@lsu.edu
Associate Professor
Associate Chair for Graduate Studies
Department of Biological Sciences
202 Life Sciences Building
Baton Rouge, LA 70803 USA
http://www.mhellberg.biology.lsu.edu/index.html

APPENDIX B: LICENSE AGREEMENT TO REUSE MATERIALS IN DISSERTATION/THESIS

Please see below for permission to re-use materials in Chapter 3 of this thesis.

SPRINGER LICENSE
TERMS AND CONDITIONS

May 27, 2015

This is a License Agreement between Allison James ("You") and Springer ("Springer") provided by Copyright Clearance Center ("CCC"). The license consists of your order details, the terms and conditions provided by Springer, and the payment terms and conditions.

All payments must be made in full to CCC. For payment instructions, please see information listed at the bottom of this form.

License Number	3632100607255
License date	May 18, 2015
Licensed content publisher	Springer
Licensed content publication	Chromosoma
Licensed content title	Deletion of Drosophila Nopp140 induces subcellular ribosomopathies
Licensed content author	Fang He
Licensed content date	Jan 1, 2014
Type of Use	Thesis/Dissertation
Portion	Full text
Number of copies	1
Author of this Springer article	Yes and you are the sole author of the new work
Order reference number	None
Title of your thesis / dissertation	Nucleolar Stress due to Depletion of Nopp140 in Drosophila melanogaster
Expected completion date	Aug 2015
Estimated size(pages)	100
Total	0.00 USD
Terms and Conditions	

Introduction
The publisher for this copyrighted material is Springer Science + Business Media. By clicking "accept" in connection with completing this licensing transaction, you agree that the following terms and conditions apply to this transaction (along with the Billing and Payment terms and conditions established by Copyright Clearance Center, Inc. ("CCC"), at the time that you opened your Rightslink account and that are available at any time at http://myaccount.copyright.com).

Limited License
With reference to your request to reprint in your thesis material on which Springer Science

licensing transaction.

Indemnity
You hereby indemnify and agree to hold harmless Springer Science + Business Media and CCC, and their respective officers, directors, employees and agents, from and against any and all claims arising out of your use of the licensed material other than as specifically authorized pursuant to this license.

No Transfer of License
This license is personal to you and may not be sublicensed, assigned, or transferred by you to any other person without Springer Science + Business Media's written permission.

No Amendment Except in Writing
This license may not be amended except in a writing signed by both parties (or, in the case of Springer Science + Business Media, by CCC on Springer Science + Business Media's behalf).

Objection to Contrary Terms
Springer Science + Business Media hereby objects to any terms contained in any purchase order, acknowledgment, check endorsement or other writing prepared by you, which terms are inconsistent with these terms and conditions or CCC's Billing and Payment terms and conditions. These terms and conditions, together with CCC's Billing and Payment terms and conditions (which are incorporated herein), comprise the entire agreement between you and Springer Science + Business Media (and CCC) concerning this licensing transaction. In the event of any conflict between your obligations established by these terms and conditions and those established by CCC's Billing and Payment terms and conditions, these terms and conditions shall control.

Jurisdiction
All disputes that may arise in connection with this present License, or the breach thereof, shall be settled exclusively by arbitration, to be held in The Netherlands, in accordance with Dutch law, and to be conducted under the Rules of the 'Netherlands Arbitrage Instituut' (Netherlands Institute of Arbitration).***OR:***

All disputes that may arise in connection with this present License, or the breach thereof, shall be settled exclusively by arbitration, to be held in the Federal Republic of Germany, in accordance with German law.

Other terms and conditions:

v1.3

Questions? customercare@copyright.com or +1-855-239-3415 (toll free in the US) or +1-978-646-2777.

Gratis licenses (referencing $0 in the Total field) are free. Please retain this printable license for your reference. No payment is required.

VITA

Allison James attended Louisiana State University beginning in the fall of 2007 and graduated in May 2011 with a Bachelor of Sciences degree in Biology. As an undergraduate in her junior year during the fall of 2009, Allison started working in the lab of Dr. Patrick DiMario. She continued her research efforts upon entering graduate school in June 2011. Allison is a candidate for graduation with a Doctor of Philosophy degree in Biological Sciences in December 2015.